AWARD NUMBER: W81XWH-13-1-0146

TITLE:

Broadly Applicable Nanowafer Drug Delivery System for Treating Eye Injuries

PRINCIPAL INVESTIGATOR: Dr. Stephen C. Pflugfelder, M.D.

CONTRACTING ORGANIZATION:

Baylor College of Medicine
Houston, TX 77030

REPORT DATE: August 2017

TYPE OF REPORT: Final

PREPARED FOR: U.S. Army Medical Research and Materiel Command
Fort Detrick, Maryland 21702-5012

REPORT DOCUMENTATION PAGE

Form Approved
OMB No. 0704-0188

1. REPORT DATE	2. REPORT TYPE	3. DATES COVERED
August 2017	Final	1 Sep 2013 - 31 May 2017

4. TITLE AND SUBTITLE

Broadly Applicable Nanowafer Drug Delivery System for Treating Eye Injuries

5a. CONTRACT NUMBER

5b. GRANT NUMBER
W81XWH-13-1-0146

5c. PROGRAM ELEMENT NUMBER

6. AUTHOR(S)
Stephen C. Pflugfelder, M.D.

E-Mail: stevenp@bcm.edu

5d. PROJECT NUMBER

5e. TASK NUMBER

5f. WORK UNIT NUMBER

7. PERFORMING ORGANIZATION NAME(S) AND ADDRESS(ES)

Baylor College of Medicine
One Baylor Plaza, T100
Houston, TX 77030

8. PERFORMING ORGANIZATION REPORT NUMBER

9. SPONSORING / MONITORING AGENCY NAME(S) AND ADDRESS(ES)

U.S. Army Medical Research and Materiel Command
Fort Detrick, Maryland 21702-5012

10. SPONSOR/MONITOR'S ACRONYM(S)

11. SPONSOR/MONITOR'S REPORT NUMBER(S)

12. DISTRIBUTION / AVAILABILITY STATEMENT

Approved for Public Release; Distribution Unlimited

13. SUPPLEMENTARY NOTES

14. ABSTRACT

Eye injuries require immediate and effective treatment to prevent corneal opacification, neovascularization, irregularity and occasionally ulceration of the cornea, which can be potentially blinding. Eye injuries are generally treated with eye drops for 4-8 times per day, which may not be feasible in critically injured patients in intensive care. This research project aims to develop a nanowafer drug delivery system that can deliver the drug to the eye for longer periods of time to treat eye injuries and prevent potential loss of vision. During the third year of this project, dexamethasone loaded nanowafers have been fabricated and evaluated for the in vivo therapeutic efficacy in ocular burn induced mouse model. These studies revealed that the dexamethasone nanowafers are very effective in corneal wound healing and the suppression of corneal neovascularization as revealed by the laser scanning conofocal microscopy. The efficacy of the dexamethasone was also evaluated by PCR analysis. This study also revealed that once a week Dexamethasone nanowafer treatment is as effective as twice a day Dexamethasone eye treatment.

15. SUBJECT TERMS
Nanowafer, fabrication, drug delivery, dexamethasone, pharmacokinetics, ocular burn, confocal microscopy, PCR

16. SECURITY CLASSIFICATION OF:			17. LIMITATION OF ABSTRACT	18. NUMBER OF PAGES	19a. NAME OF RESPONSIBLE PERSON
a. REPORT	b. ABSTRACT	c. THIS PAGE			USAMRMC
U	U	U	UU	79	19b. TELEPHONE NUMBER *(include area code)*

Table of Contents

Page

1. INTRODUCTION

Soldiers affected by eye injuries require immediate and effective treatment. The acute phase occurs at the time of the injury and results in corneal and conjunctival epithelial damage or necrotic death. These events lead to opacification, neovascularization, irregularity and occasionally ulceration of the cornea, which can be potentially blinding. Eye injuries are generally treated by simply introducing drug solution in the form of eye drops; however, achieving sustained therapeutic levels on the ocular surface remains a challenge due to the continuous tear clearance through the lacrimal drainage system. Modulation of the ocular surface response to trauma requires multiple dosing (4-8 times per day) of the eye drops to achieve an effect, which may not be feasible in critically injured patients in intensive care. Hence, there is a strong need for the development of broadly applicable nanowafer drug delivery systems with high drug content and long-term drug release attributes. This research project focuses on the development of a nanowafer drug delivery system that can deliver the drug to the eye in a controlled release fashion for longer periods of time to treat eye injuries and prevent potential loss of vision. In this project, by integrating the nanotechnologies and controlled release drug delivery technology, a nanowafer drug delivery system will be developed that can surmount the limitations of conventional eye drop formulations. The nanowafers will be fabricated *via* the hydrogel template strategy. The nanowafer contains an array of nanoreservoirs loaded with drug matrix. Upon instillation, because the nanowafer is very thin and comprised of mucoadhesive biomaterial, it readily adheres to the conjunctiva and can remain intact for several days without being displaced due to constant blinking. The nanowafer drug delivery system can release the drug in therapeutically effective concentration from a day to a week. The broadly applicable nanowafer drug delivery system upon development can be used for treating ocular surface injuries and also dry eye, corneal ulcers, glaucoma, and infections, and improve the performance efficiency and effectiveness of the soldiers in the warzone.

2. Keywords

nanowafer, fabrication, drug delivery, ocular burn, doxycycline, dexamethasone, cyclosporine-A, pharmacokinetics

3. ACCOMPLISHMENTS:

What were the major goals of the project?

This project focuses on accomplishing the following 5 defined tasks as proposed in the SOW:

Task 1. Regulatory approvals (IACUC/ACURO/HRPO)**.** Duration: 3 months (months 1-3)
Task 2. Fabrication of nanowafer drug delivery systems**.** Duration 18 months (months 1-18)
Task 3. Evaluation of *in vitro* and *in vivo* pharmacokinetics. Duration 24 months (months 6-30)
Task 4. Study of the efficacy of doxycycline-nanowafers, dexamethasone-nanowafers, and cyclosporine-A-nanowafers in an ocular burn mouse model. Duration: 18 months (months 18-36)
Task 5. Data Analysis**.** Duration: 6 months (months 30-36)

What was accomplished under these goals?

This section summarizes the results obtained in our laboratories for the duration of the project. Specifically, we have accomplished: the following objectives defined under each task.

Task 1. Regulatory approvals (IACUC/ACURO/HRPO)

Duration: 3 months (months 1-3)

We have obtained IACUC/ACURO protocol approval from Baylor College of Medicine and DOD. Protocol Title: Broadly applicable nanowafer drug delivery system for treating ocular burn injury Protocol Number: AN-6366.

Task 2. Fabrication of nanowafer drug delivery systems

Duration 18 months (months 1-18)

This task involves the completion of four objectives: **Objective (i)** Nanofabrication of silicon wafer master templates and PDMS imprints with feature dimensions of 100nm, 200nm, 500nm, 1μm, 1.5μm, and 3μm; **Objective (ii)** Fabrication of polyvinylpyrrolidone (PVP), dextran (DTR), carboxymethyl cellulose (CMC), and hydroxypropyl methyl cellulose (HPMC) nanowafers with feature dimensions of 100nm, 200nm, 500nm, 1μm, 1.5μm, and 3μm; and **Objective (iii)** Fabrication of drug-filled nanowafers: doxycycline-nanowafers; dexamethasone-nanowafers; and cyclosporine-A-nanowafers with feature dimensions of 100nm, 200nm, 500nm, 1μm, 1.5μm, and 3μm. **Objective (iv)** Optimization of in vivo compliance after the instillation of nanowafers on cornea and conjunctiva and evaluate their adherence and dissolution by bright field and fluorescence microscopy. Completion of each objective and the outcomes are described below.

Objective (i) Nanofabrication of silicon master templates and PDMS imprints with feature dimensions of 100nm, 200nm, 500nm, 1μm, 1.5μm, and 3μm.

Under this objective, silicon wafer master templates having a series of well diameters were fabricated. The feature patterns to be written on the silicon wafers were designed using AutoCAD program and transferred to the e-beam lithography system. The silicon wafer templates with arrays of wells of 100nm, 200nm, 500nm, and 1μm diameters were fabricated by electron beam lithography, and wells of 1.5μm, and 3μm diameters were fabricated by photolithography. The silicon wafer master templates were examined by scanning electron

microscopy (SEM) for the feature integrity and uniformity. The SEM images revealed the presence of regular arrays of square and circular wells of predefined dimensions (**Figure 1**).

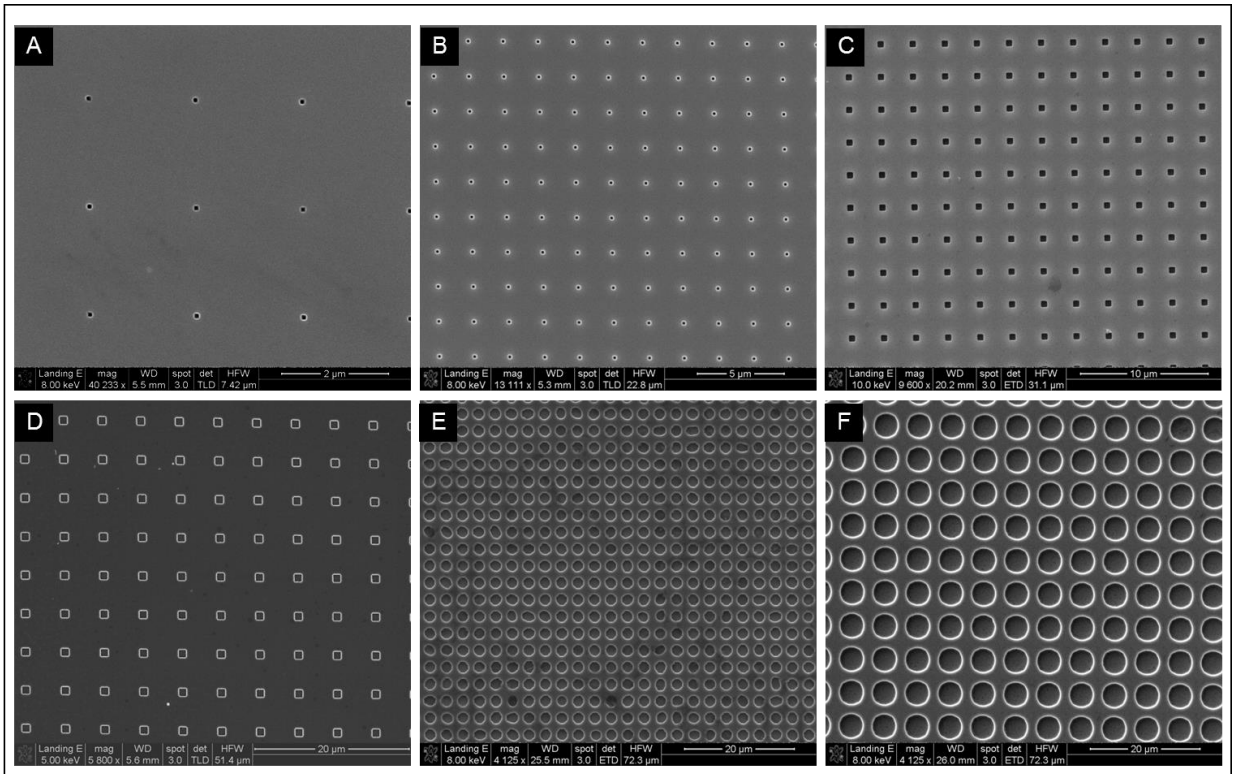

Figure 1. Silicon wafer templates containing wells of a series of dimensions by E-beam and photolithography: (A) 100nm; (B) 200nm; (C) 500nm; (D) 1μm; (E) 1.5μm; and (F) 3μm

Representative experimental procedures for the fabrication of a silicon wafers containing 200nm and 3μm features is described below.

(a) Fabrication of a silicon wafer containing 200nm features by E-beam lithography

Making surface patterns of submicron size features requires e-beam lithography. Circular patterns of 200nm squares were designed using the Auto CAD2007 program. A 6-in. diameter silicon wafer covered with 1 μm thick SiO_2 layer (University Wafer, South Boston, MA) was spin coated with poly(methyl methacrylate) (PMMA, Microchem, Newton, MA) photoresist of 300nm thick layer was spin coated at 3500rpm for 30s (SCS P6708 spin coating system, Indianapolis, IN). The coated PMMA photoresist layer was exposed to e-beam in a pre-programmed pattern using a Leica VB6 High Resolution Ultrawide field e-beam lithography Instrument (Bannockburn, IL) operating at 100KV, transmission rate 25MHz current 5nA. After e-beam lithography, the silicon wafer was developed in 3:1 isopropanol:methyl isobutyl ketone solution to remove exposed regions of the photoresist. A 5nm thick chromium layer and a 20nm thick gold layer were successively deposited on to this pattern followed by liftoff of the residual PMMA film in refluxing acetone. The pattern was transferred to the underlying silicon oxide by deep reactive ion etching with SF_6/O_2 plasma. The silicon master templates having features sizes of 100nm, 200nm, 500nm, 1μm were fabricated by this method.

(b) Fabrication of a silicon wafer containing 3μm wells by UV photolithography

A silicon wafer was spin coated with SU8 2005 photoresist (Microchem, MA) at 3500rpm for 30s followed by baking at 95 °C for 3min. The photoresist coated silicon wafer was exposed to

UV radiation through a mask containing a 3μm diameter circular pattern for 12s. After exposure, the silicon wafer was post baked at 95 °C for 3 min followed by development in SU- 8 developer for 2 min. The silicon wafer was rinsed with isopropanol and dried with nitrogen gas. The wafer thus fabricated contained 3μm diameter wells. Similarly, a silicon wafer template having 1.5μm diameter wells was fabricated following this procedure with minor modifications.

(c) Fabrication of PDMS imprints using the silicon wafer master templates

Using the silicon wafer master templates, polydimethylsiloxane (PDMS) imprints were fabricated. First, a prepolymer solution of Sylgard 184 elastomer (90g) mixed with 9g of the curing agent (10:1 by weight). The prepolymer solution was poured on to the silicon master template and cured at 80 °C for 10h in an oven (Isotemp 500 Series Economy Lab Ovens, Fisher Scientific). At the end of this period, the PDMS template was carefully peeled away from the silicon master template. Using this process, PDMS templates for each feature size (100nm, 200nm, 500nm, 1μm, 1.5μm, and 3μm) were fabricated (**Figure 2**).

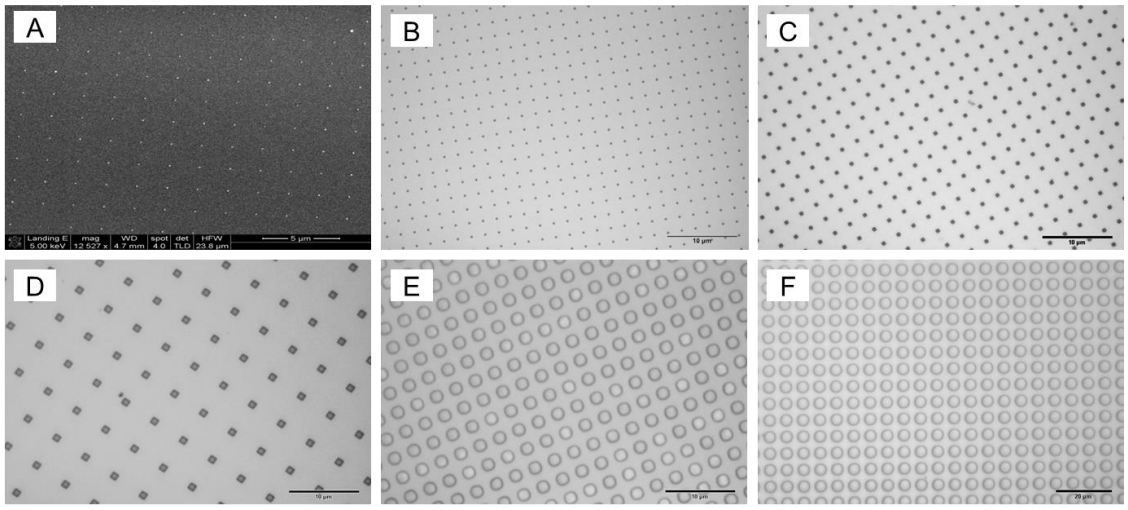

Figure 2. SEM and bright field micrographs of PDMS templates containing vertical posts of: (A) 100 nm; (B) 200 nm; (C) 500 nm; (D) 1 μm; (E) 1.5 μm; and (F) 3 μm. Scale bars: for the micrographs: (A) 5 μm, (B) to (E) is 10 μm, and for (F) 20 μm.

Objective (ii) Fabrication of polyvinylpyrrolidone (PVP), dextran (DTR), carboxymethyl cellulose (CMC), and hydroxypropyl methyl cellulose (HPMC) nanowafers with feature dimensions of 100nm, 200nm, 500nm, 1μm, 1.5μm, and 3μm.

Under this objective, PVP, DTR, CMC, and HPMC nanowafers with well dimensions of 100nm, 200nm, 500nm, 1μm, 1.5μm, and 3μm have been fabricated. These nanowafers were characterized for integrity of the well dimensions and array patterns by atomic force microscopy (AFM). As representative examples, the AFM images of CMC nanowafers are presented in **Figure 3.** The AFM study revealed that all the nanowafers have arrays of wells of predefined dimensions without any defects.

We have fabricated the polymer nanowafers and as a representative example, the fabrication of CMC nanowafers is described here.

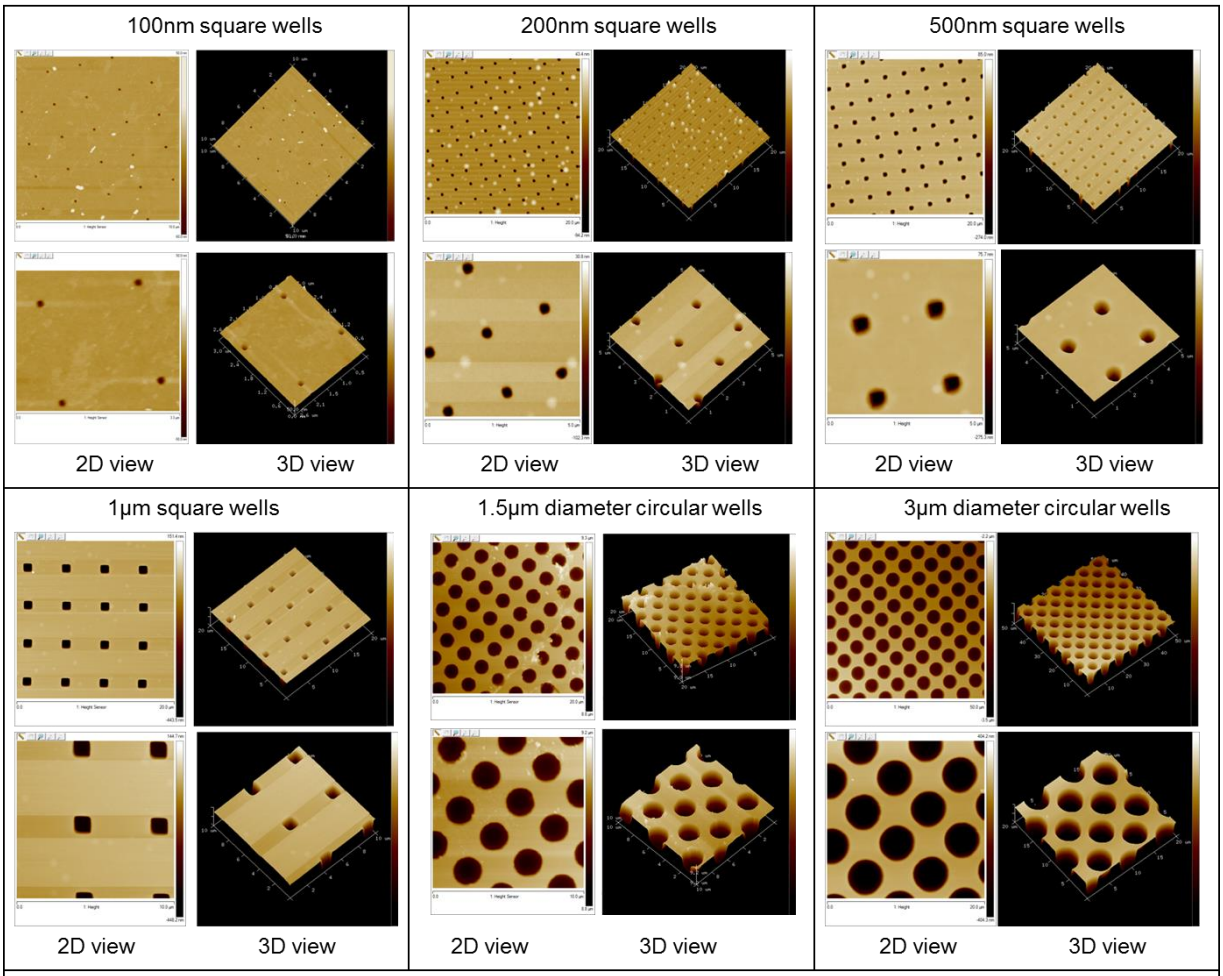

Figure 3. Fabrication of polymer nanowafers. The CMC nanowafers having a series of well dimensions were fabricated and characterized for the feature integrity by atomic force microscopy (AFM): (A) 100nm, (B) 200nm, (C) 500nm, (D) 1µm, (E) 1.5µm, and (F) 3µm .

(a) Fabrication of CMC nanowafers

A clear thick CMC solution (5% w/v) was prepared by dissolving CMC (5g) in 100 ml of ethanol:water mixture (6:4) on a stirring hot plate (RT Elite Stirring Hotplate, Fisher Scientific). This prepared polymer solution (10 ml) was transferred with a pipette onto a PDMS template containing vertical posts placed on a spin coating system. The spin speed was adjusted to 500rpm and spun for 45sec to obtain a100µm thick nanowafer. The concentration of the polymer solution, speed and spinning times were optimized for each polymer to obtain the required thickness of the nanowafer. After spin coating, the wafers were baked in an oven (Isotemp 500 Series Economy Lab Ovens, Fisher Scientific) at 60 ºC for 15min. This procedure resulted in the fabrication of nanowafers having nanoreservoirs of predefined dimensions (e.g. 1µm diameter and 1µm deep). The nanowafer were characterized by AFM (**Figure 3**). By this method, nanowafers of PVP, DTR, CMC, and HPMC for each feature size (100nm, 200nm, 500nm, 1µm, 1.5µm, and 3µm) were fabricated.

(b) Atomic force microscopy (AFM)

A Catalyst Bioscope Atomic Force Microscope (Bruker) combined with a fluorescence microscope (Olympus) was used for testing and imaging the nanowafers. The AFM probe is a Scanasyst-Air (Bruker Nano) with a tip diameter of 2-5nm, cantilever dimensions: 115µm (l), 25 µm (w), and 250nm (thick). The cone shaped probe length is 10 µm with 18º cone. Cantilever spring constant is 0.4Nm. The AFM experiment was conducted under ambient conditions. The scan rate is 1Hz.

Objective (iii) Fabrication of drug-filled nanowafers: doxycycline-nanowafer; dexamethasone-nanowfawers; and cyclosporine-A-nanowaferw with feature dimensions of 100nm, 200nm, 500nm, 1µm, 1.5µm, and 3µm

Under this task, nanowafers filled with doxycycline and dexamethasone were fabricated by microinjection. The following drug filled nanowafer have been fabricated for further study: Dexa-PVP, Doxy-PVP, Dexa-DTR, Doxy-DTR, Dexa-CMC, Doxy-CMC, Dexa-HPMC, Doxy-HPMC, with drug reservoir dimensions of 100nm, 200nm, 500nm, 1µm, 1.5µm, and 3µm. As representative examples, fluorescence micrographs of Doxy-CMC nanowafers are presented in **Figure 4**. Fluorescence imaging study was performed because of the intrinsic fluorescence property of doxycycline. This study revealed the presence of arrays of doxycycline filled drug reservoirs in the Doxy-CMC nanowafers.

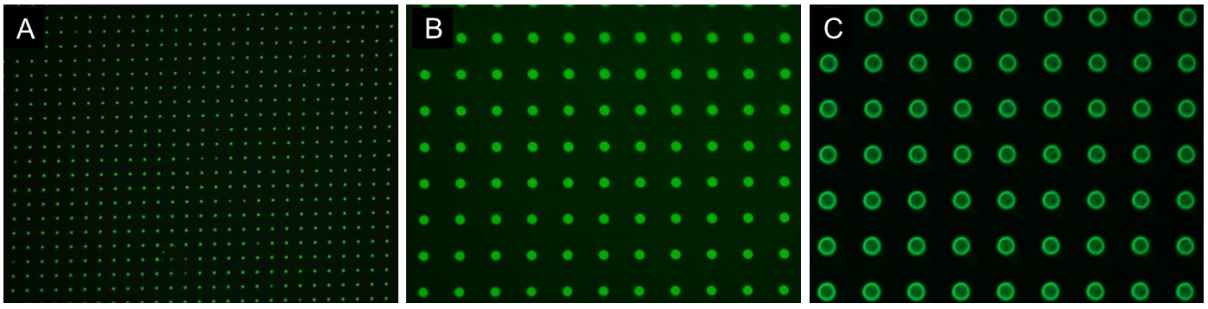

Figure 4. Drug filled nanowafers. Fluorescence micrographs of Doxy-CMC nanowafers: (A) 500nm; (B) 1.5µm; and (C) 3µm

Objective (iv) Optimization of in vivo compliance after the instillation of nanowafers on cornea and conjunctiva and evaluate their adherence and dissolution by bright field and fluorescence microscopy

This project is focused on the development of ocular drug delivery nanowafer, wherein the drug and the drug carrying polymer work synergistically to provide an augmented therapeutic effect compared to conventional eye drop therapy. The nanowafer is a tiny transparent circular disc that can be simply applied on the cornea with a fingertip, like a contact lens and can withstand constant blinking without being displaced (**Figure 5A-B**). It contains arrays of drug-loaded nanoreservoirs from which the drug will be released in a tightly controlled fashion for an extended period of time (**Figure 5C-D**). The slow drug release from the nanowafer increases the drug residence time on the ocular surface and its subsequent absorption into the surrounding ocular tissue. At the end of the stipulated period of drug release, the nanowafer will dissolve and fade away. The nanowafer is highly transparent and when applied, it will have minimal effect on normal vision (**Figure 5E**).

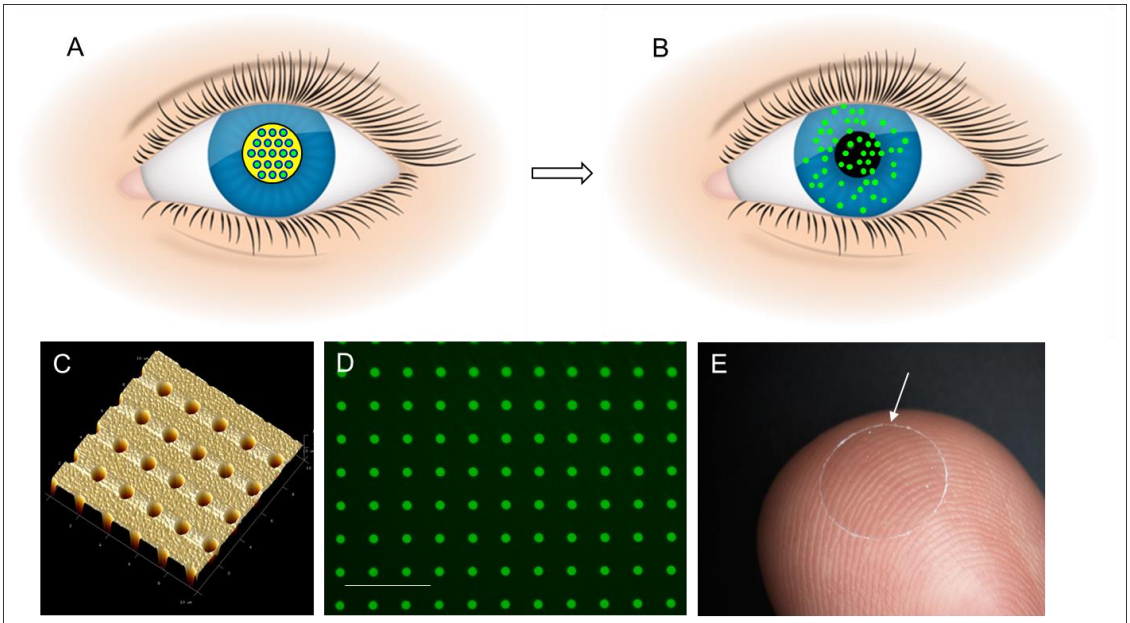

Figure. 5. Ocular drug delivery nanowafer. Schematic of (A) nanowafer instilled on the cornea and (B) diffusion of drug molecules into the corneal tissue. (C) AFM image of a nanowafer demonstrating an array of 500 nm diameter nanoreservoirs. (D) Fluorescence micrograph of a nanowafer filled with doxycycline (scale bar 5 μm). (E) Optical micrograph of a nanowafer on fingertip demonstrating the transparency of the nanowafer: the fingerprint lines are clearly visible through the nanowafer (arrow pointing the nanowafer).

Compliance of nanowafer on the mouse eye

To evaluate the adherence and compliance of the nanowafer on the cornea, a nanowafer was applied on the mouse cornea and examined under a stereoscopic microscope. The nanowafer cleanly adhered to the cornea in compliance with its curvature, and no wrinkling or displacement of the nanowafer was observed (**Figure 6**).

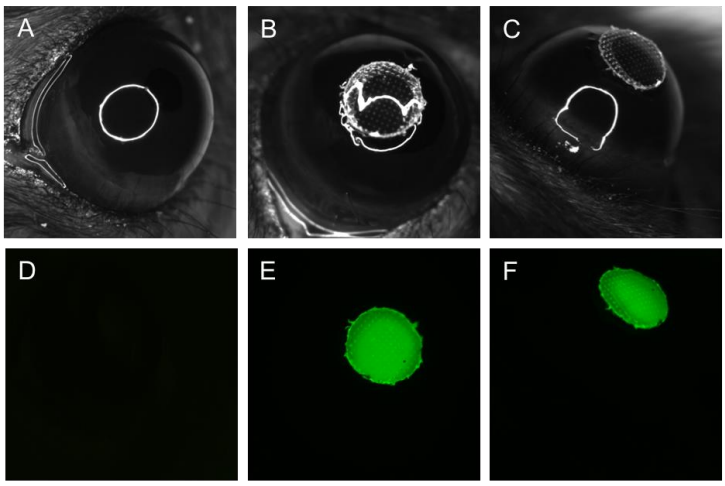

Figure 6. Demonstration of adherence and compliance of nanowafer on the mouse cornea. Optical micrographs of: (A) a mouse eye prior to nanowafer application; nanowafer applied on the mouse eye (B) top view, (C) side view. Fluorescence micrographs of: (D) a mouse eye prior to nanowafer application; doxycycline-nanowafer applied on the mouse eye (E) top view, (F) side view.

Evaluation of dissolution kinetics of the nanowafer on mouse eye

To evaluate the adherence and dissolution of a nanowafer on the cornea, a nanowafer was applied on the mouse cornea and monitored by real-time bright field and fluorescence microscopy. The nanowafer upon application, readily adhered to the cornea. The nanowafer withstood blinking and did not get displaced, thus demonstrating its mucoadhesive nature. The nanowafer dissolved and completely disappeared after 1 h (**Figure 7** Top panel). Real-time fluorescence imaging revealed that, although the nanowafer completely dissolved after 1 h, the cornea was green fluorescent for up to 5 h, confirming the diffusion of fluorescein dye into it (**Figure 7** Bottom panel).

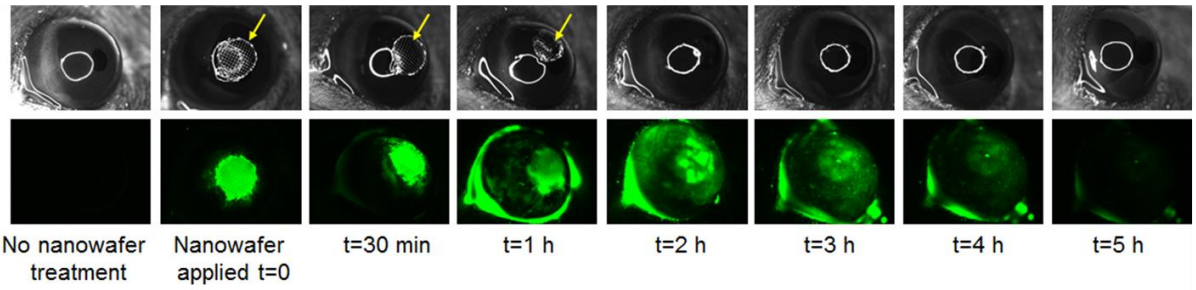

Figure. 7. Demonstration of adherence and dissolution of a nanowafer applied on the cornea. Top panel: Bright field micrographs demonstrating the adherence and dissolution of the nanowafer after 1 hour (please see the arrow pointing the position of the nanowafer). Bottom panel: Fluorescence micrographs demonstrating the presence of fluorescein in the corneal tissue for up to 5 hours.

Task 3. Evaluation of *in vitro* and *in vivo* pharmacokinetics

Duration 24 months (months 6-30)

This task involves the completion of three objectives: **Objective (i)** Study of in vitro drug release and drug concentration in doxycycline-nanowafers, dexamethasone-nanowafers, and cyclosporine-A-nanowafers by fluorescence spectrophotometry and high performance liquid chromatography (HPLC); **Objective (ii)** Study of pharmacokinetics of doxycycline-nanowafers, dexamethasone-nanowafers, and cyclosporine-A-nanowafers in the tear washings of mice; and **Objective (iii)** Study of in vivo pharmacokinetics after the instillation of drug-nanowafers on cornea and conjunctiva, by real-time drug molecular transport, distribution, and residence times in the cornea and conjunctiva by laser scanning confocal fluorescence image analysis in mice for 1-10 days. Completion of each objective and the outcomes are described below.

Objective (i) Study of in vitro drug release and drug concentration in doxycycline-nanowafers, dexamethasone-nanowafers, and cyclosporine-A-nanowafers by fluorescence spectrophotometry and high performance liquid chromatography (HPLC).

The drug-loaded nanowafers were investigated for their drug release kinetics by HPLC analysis and are being optimized for extended drug release. As representative examples, the *in vitro* drug release kinetics of Doxy-CMC and Dexa-CMC nanowafers is described here. The Doxy-CMC and Dexa-CMC nanowafers were evaluated for their total drug content and in vitro drug release kinetics by HPLC. In this study, CMC nanowafers having an array of 1μm diameter reservoirs filled with doxycycline and dexamethasone were used.

Analysis of *in vitro* drug release from the CMC nanowafers

The total drug content in each nanowafer was determined by dissolving accurately weighed nanowafers in 1ml PBS, followed by addition of ethanol (9ml). The precipitated CMC was removed by centrifugation. The clear solution was rotary evaporated and the solid formed was redissolved in the mobile phase (10ml). An aliquot of this solution was filtered through a 0.2µm syringe filter, analyzed by HPLC, and was compared with the standard curve to quantify the content. From this study, (1) the doxycycline content in a 6mm diameter CMC nanowafer was 298µg and is 14% of the total mass of the nanowafer, and (2) the dexamethasone content in a 6mm diameter CMC nanowafer was 433µg and is 16% of the total mass of the nanowafer.

The drug release from the CMC nanowafers was studied by HPLC analysis. Accurately weighed Doxy-CMC nanowafers were placed in 5 separate 1ml dialysis tubes filled with PBS buffer as release medium. Each dialysis tube was placed in 5ml conical tube filled with 5ml of the release medium. The conical tubes were kept in an orbital shaker maintained at 37 °C with constant agitation. At predefined time intervals 1ml of the release medium was withdrawn from each tube and replaced with the same amount of the fresh medium. Thus collected samples were transferred into glass vials and stored in the refrigerator. Sampling of the release medium was continued for 24h. The samples thus collected were subjected to HPLC analysis. Exactly the same procedure was followed for the dexamethasone release study from Dexa-CMC nanowafers.

The HPLC analysis of the drug release study revealed that the Doxy-CMC nanowafers released ~18% (150 µg) of doxycycline after 6h and it was ~39% (340µg) after 24h (**Figure 8**). In the case of Dexa-CMC nanowafer, the dexamethasone released was ~17% (215µg) after 6h and ~39% (490µg) after 24h (**Figure 9**). Taken together, the in vitro drug release study confirmed that, both doxycycline and dexamethsone release from the CMC nanowafers was slow and there was no initial burst release, and followed a zero order release kinetics. Presently, work is in progress to optimize the fabrication, well diameters, and drug loading parameters for the nanowafer to accomplish drug release for up to 5 days.

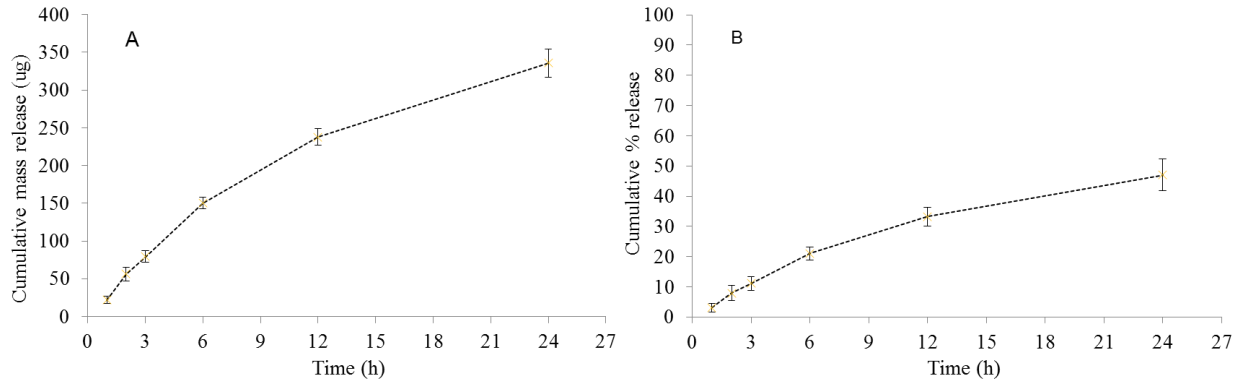

Figure 8. *In vitro* doxycycline release from the CMC-Doxy nanowafer analyzed by HPLC: (A) cumulative amount of drug released and (B) cumulative percentage drug released in a 24 hour time period.

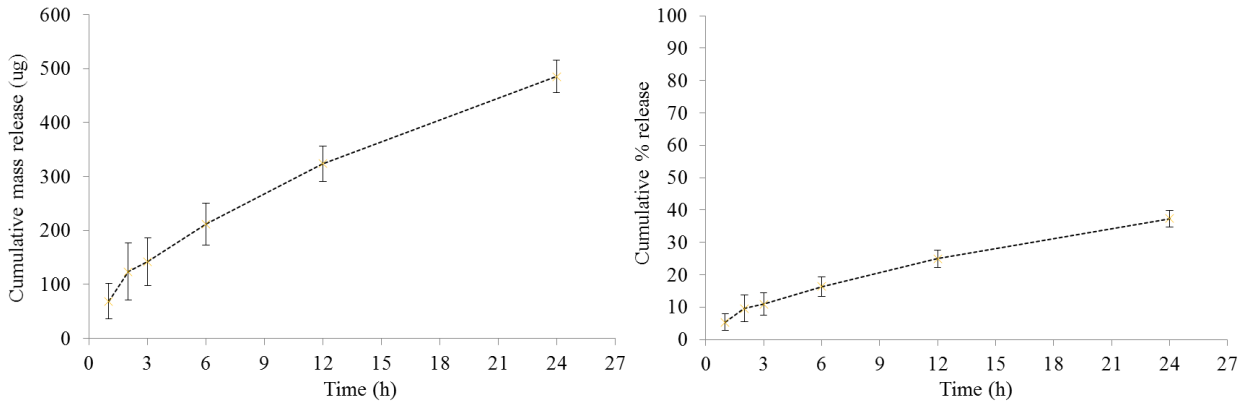

Figure 9. *In vitro* dexamethasone release from the CMC-Dexa nanowafer analyzed by HPLC: (A) cumulative amount of drug released and (B) cumulative percentage drug released in a 24 hour time period.

The experimental procedures for the HPLC analysis are presented below.

(a) Determination of total drug content in a nanowafer

The total amount of a drug loaded in the nanowafer was be determined by dissolving an accurately weighed nanowafer in 5 ml PBS solution, followed by addition of ethanol (5 ml). The precipitated polymer was removed by centrifugation. The clear solution was rotary evaporated to separate the solid drug. The solid drug was re-dissolved in 10 ml of the mobile phase (90% methanol and 10% ammonium acetate, pH 7). An aliquot of this solution was filtered through a 0.2µm syringe filter, analyzed by HPLC, and compared with the standard curve to quantify the total drug content in the nanowafer. This experiment was performed in triplicate.

(b) Study of drug release kinetics of the nanowafers by HPLC analysis

HPLC experiments were performed on a Shimadzu Prominence HPLC. The analytical column was Kinetex 5uXB-C18 100A (150 mm x 4.6 mm) from Phenomenex. The system was equipped with autosampler, in line degasser, and column oven set at room temperature. The mobile phase for doxycycline analysis was a mixture of 5% acetic acid (55%) and methanol (45%) ammonium acetate (10%, pH 7), and for dexamethasone it was mono phosphate buffer ($NaHPO_4$, 100mM, pH 4.6) and acetonitrile used in gradient mode (monophosphate buffer 90%-65% and acetonitrile 10%-35%). Injection volume was 65 µl, the flow rate was 1.0 ml/min and the pressure was 1200 mm. Each sample was filtered through a 0.22µm syringe filter and subjected to HPLC analysis. The UV detection wavelength for doxycycline was 274nm and for dexamethasone it was 240nm. The drug concentration was calculated by comparing the peak area of standards and sample. Exactly the same procedure was followed for the dexamethasone release study from Dexa-CMC nanowafers.

Objective (ii) Study of pharmacokinetics of doxycycline-nanowafers, dexamethasone-nanowafers, and cyclosporine-A-nanowafers in the tear washings of mice

The nanowafers were tested for their *in vivo* drug release in healthy mice. In healthy mice, the drug released can be accurately measured compared to ocular burn induced mice because, the drug will not be immediately consumed for therapeutic activity. For this study, 2 mm diameter nanowafers were used. Doxycycline loaded nanowafers (Doxy-NW) and Dexamethasone loaded nanowafers (Dex-NW) were fabricated for this study. A nanowafer was placed on the cornea and the drug release was monitored every hour by collecting the tear washings followed by HPLC analysis.

Collection of mouse tear fluid washings: A drug nanowafer was applied on the corneas of healthy mice and the tear fluid washings were collected by first instilling 1.5 μL of PBS containing 0.1% bovine serum albumin (BSA) in the conjunctival sac. The tear fluid was collected with a 1 μL volume glass capillary at hourly time intervals for 5 h. The tear washings were stored at -80 ºC until all the tear samples were collected. The drug concentration in tear washings was determined by HPLC method.

Drug release from the nanowafers in mouse tear samples

To monitor the drug concentration on the ocular surface as a measure of drug release from the nanowafer, tear samples were collected hourly for 5 h, and the doxycycline content was analyzed by HPLC. After placement of a doxycycline nanowafer on the cornea, the drug concentration in the tears slowly decreased with time, and after 4 h, no detectable doxycycline concentration was present (**Figure 10**).

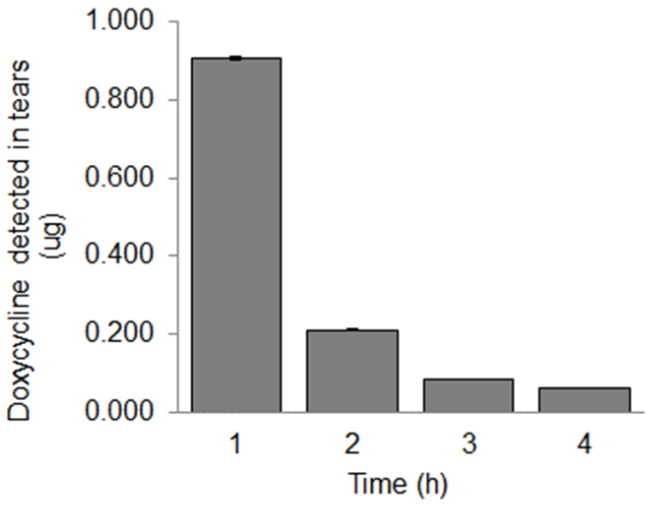

Figure 10. In vivo drug release from Doxy-nanowafer on the mouse ocular surface.

To assess the drug release from the Dex-NW after its instillation on the conjunctiva, tear samples were collected at hourly intervals and analyzed for Dex concentration by HPLC. This study revealed the presence of Dex in tear samples for up to 2 h, at significantly greater concentrations than eyes treated with Dex eye drops containing the same amount (10 μg in 2 μl) of the drug (**Figure 11**). Also, in the case of Dex release from the nanowafer, more drug was present in the first hour tear samples compared to the second hour samples. Because of the ocular surface barriers, such as reflex tearing and tight epithelial junctions, the drug diffusion into the cornea is very slow in the beginning, hence more drug was present in the first hour tear samples. However, with longer drug residence time provided by the nanowafer, more drug penetrates into the cornea. This results in a decrease in drug concentration in the tear samples collected at later time points.

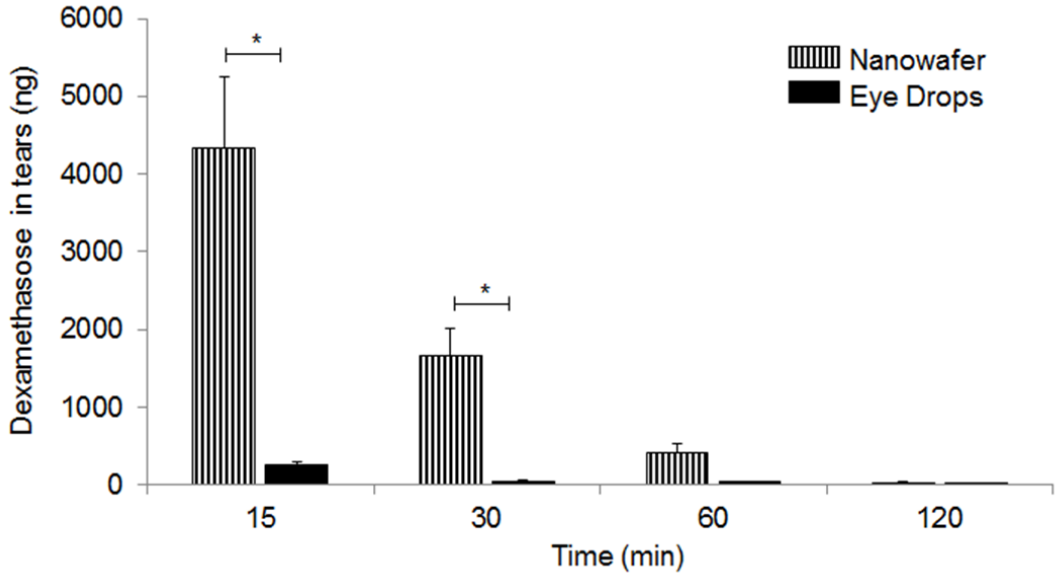

Figure 11. In vivo drug release from the Dex-NW on the ocular surface**.** Dex concentration measured in tear samples collected from eyes treated with Dex-NW.

Objective (iii) Study of in vivo pharmacokinetics after the instillation of drug-nanowafers on cornea and conjunctiva, by real-time drug molecular transport, distribution, and residence times in the cornea and conjunctiva by laser scanning confocal fluorescence image analysis in mice for 1-10 days.

To demonstrate the controlled drug release from the nanowafer, diffusion of drug molecules and their increased residence times in the cornea, *in vivo* drug release studies were conducted in a healthy mouse model. In this study, doxycycline loaded nanowafers were fabricated. Doxycycline was chosen as a model drug because of its green fluorescence, which will be very useful in monitoring the drug diffusion and residence times in the cornea by real-time confocal fluorescence imaging. After the instillation of a doxycycline-nanowafer on a mouse cornea, the drug slowly diffused into the cornea and corresponding increase in fluorescence intensity was monitored for 5h (**Figure 12**).

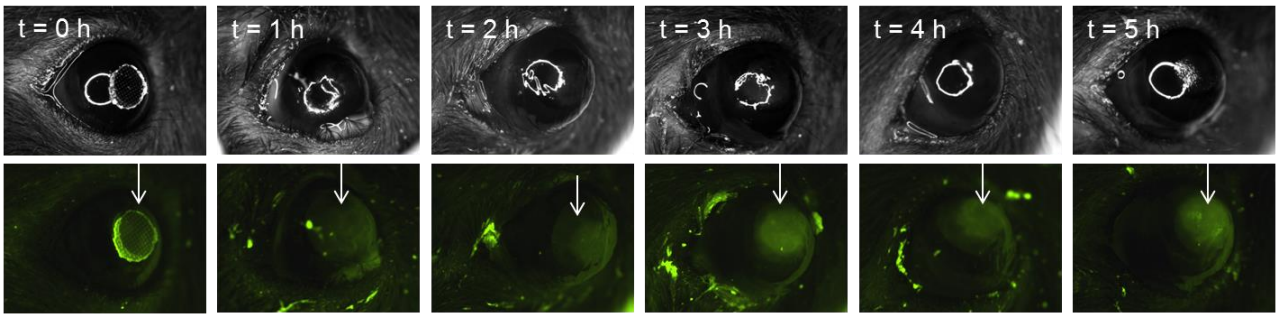

Figure 12. *In vivo* drug release from the nanowafer in mouse eyes. The bright field (top row) and fluorescence images (bottom row) demonstrating the controlled release of doxycycline from the nanowafer into the cornea for up to 5 h. The nanowafer was instilled at t=0.

The doxycycline-nanowafer treated mice were further subjected to intravital confocal imaging to investigate the presence of doxycycline molecules in the cornea. This study revealed that the green fluorescent doxycycline molecules were present in the cornea for up to 48h (**Figure 13**).

At this point, to compare the drug diffusion into the cornea by eye drop administration with that of nanowafer delivery, healthy mice were treated with doxycycline eye drops. As can be seen from the **Figure 14**, mild green fluorescence was observed within a minute after the eye drops administration, however there was no observable fluorescence was detected after 15min, thus confirming that the doxycycline eye drops were completely wiped out from the ocular surface. Because of the very short drug residence times on the cornea, eye drops need to be administered several times in a day for an observable therapeutic efficacy.

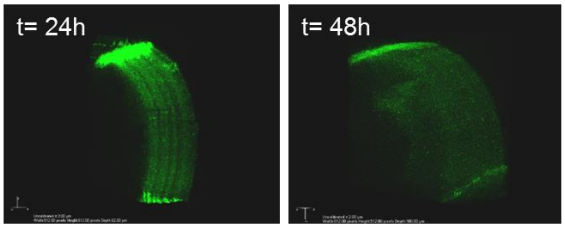

Figure 13. Nanowafer drug delivery enhances the drug molecular transport into the cornea. Intravital laser confocal imaging of the live mouse cornea demonstrating the presence of drug in the cornea for up to 48 hours.

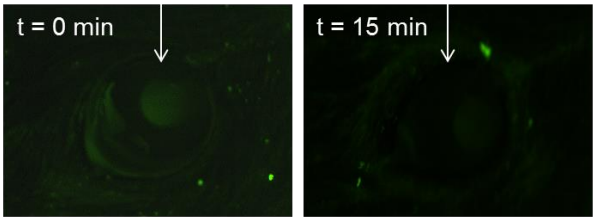

Figure 14. Rapid clearance of doxycycline delivered as topical eye drop formulation in mice. The nanowafer was instilled at t=0.

To study the ability of the nanowafer in improving the drug molecular residence time on the ocular surface and its subsequent diffusion into it, fluorescein (a green fluorescent dye, MW = 332 g/mol) loaded nanowafers (Flo-NW) were fabricated. The Flo-NWs were instilled on the corneas of healthy mice and were examined by fluorescence imaging at every hour for 5 h. The ocular surface was initially non-fluorescent (**Figure 15A**). After the placement of a nanowafer, the fluorescein molecules were slowly released on the cornea and green fluorescence was observed. Since, the fluorescein released from the nanowafer is in direct contact with the cornea, most of the drug will be able to penetrate into it. After 4 h, the green fluorescence of the cornea started to fade because of the diffusion of fluorescein molecules into the anterior

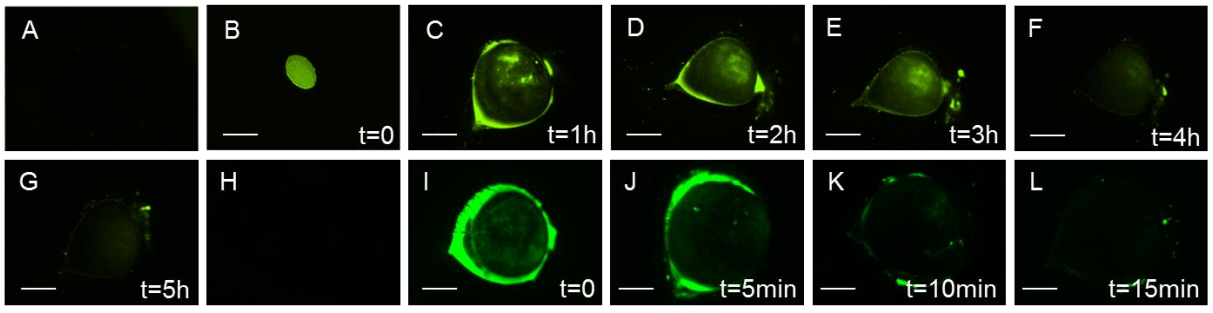

Figure 15. Nanowafer improves the drug residence time on the cornea. (A) Fluorescence micrograph of the eye prior to fluorescein nanowafer (Flo-NW) instillation; (B–G) fluorescence micrographs depicting the presence of fluorescein dye at the specified time points in the corneal tissue after Flo-NW instillation. (H) Fluorescence micrograph of the eye prior to fluorescein eye drops instillation; (I-L) Rapid clearance of fluorescein dye drops within 5 min.

chamber and its clearance by tear secretion (**Figure 15B-G**). Once the fluorescein molecules pass through the cornea and reach the aqueous humor in the anterior chamber, they are cleared through the trabecular meshwork.

In comparison, eyes treated with fluorescein eye drops were non-fluorescent after 5 min, indicating its rapid clearance from the ocular surface (**Figure 15I-L**). Also, after instillation of the fluorescein drops on the eye, within a few minutes, most of it is concentrated on the eye lids, indicating its clearance from the ocular surface, compared to the nanowafer drug release, wherein only a small amount of fluorescein concentrated around the eyelids and most of it in the eye. This study has qualitatively demonstrated the ability of nanowafer to release the drug for a few hours thus improving the drug residence time on the cornea. To quantify the amount fluorescein present at each time point, the fluorescence intensities were plotted in **Figure 16**.

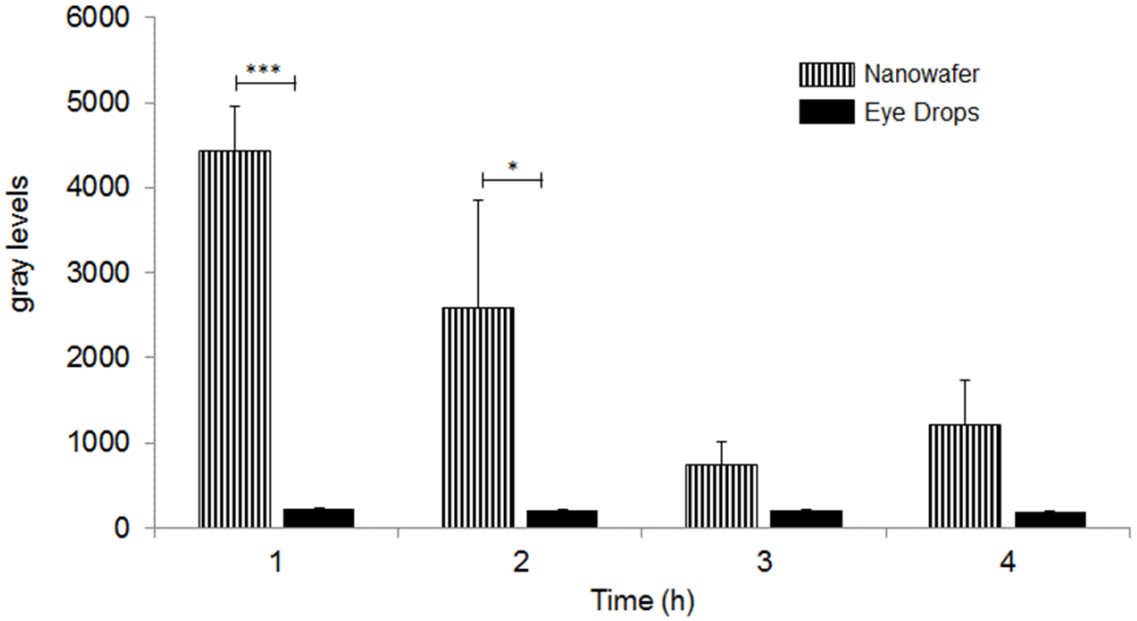

Figure. 16. Nanowafer improves the drug residence time on the cornea. A plot depicting the fluorescence intensities (n=3).*P <0.05, ***P <0.001. All error bars represent standard error of the mean. Scale bar: 1 mm

Taken together, these results confirm that the nanowafer releases the drug in a tightly controlled fashion and the released drug remains in the cornea for a longer duration of time. The controlled drug release from the nanowafer will facilitate the drug molecules to effectively diffuse into the corneal and improve the bioavailability of the drug, consequently enhancing the drug efficacy. Presently, studies are underway to optimize the drug retention times and therapeutic concentrations in the cornea with nanowafer drug delivery for an enhanced efficacy.

Nanowafer Enhances Drug Diffusion into the Cornea.

To demonstrate the ability of the nanowafers to release the drug for an extended period of time, PVA nanowafers loaded with doxycycline were fabricated. Doxycycline (antibiotic drug) was chosen for this study because of its green fluorescence, which allowed us to monitor the precorneal drug residence time and its subsequent diffusion into the cornea by real-time fluorescence imaging.

To monitor the drug diffusion into the mouse cornea a doxycycline nanowafer was applied on a mouse cornea (**Figure 17A**). The mouse eye was subjected to fluorescence imaging at hourly intervals while the mouse was under general anesthesia. The corneas were green fluorescent even after 5 h when viewed under a stereomicroscope with 488 nm illumination, indicating the presence of drug in the cornea (**Figure 17B-F**). The corneas exhibited a strong green fluorescence for up to 48 h, when subjected to intravital laser scanning confocal imaging, indicating the presence of doxycycline in the corneal tissue (**Figure 17G-H**). To compare the efficacy of the doxycycline delivery by nanowafer with topical eye drop treatment, another group of mice were treated with doxycycline eye drops. Upon examination under a fluorescence microscope, the corneas did not exhibit a measurable green fluorescence, indicating the complete clearance of the drug within 15 minutes (**Figure 17I-J**).

Although, doxycycline concentration was undetectable in tears after 1h (**Figure 10**), the fluorescence and intravital confocal imaging studies have confirmed the presence of the drug in the corneal tissue for up to 48 h (**Figure 17**). Taken together, this study clearly demonstrated the ability of the nanowafer to release doxycycline for an extended period of time, thus enhancing the precorneal drug residence time and subsequent diffusion of drug molecules into the cornea.

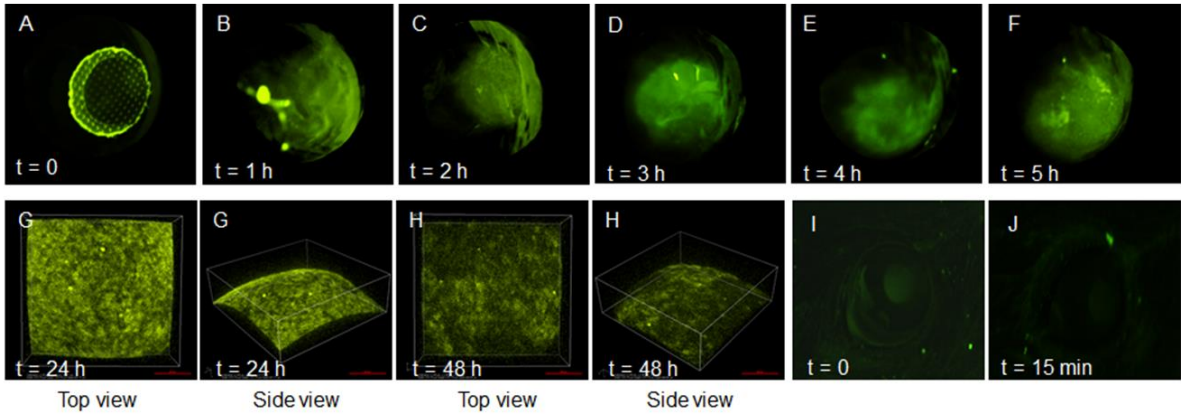

Figure 17. Nanowafer drug delivery enhances drug molecular transport into the cornea. (A-F) Real-time in vivo fluorescence imaging of the mouse cornea at regular time intervals demonstrating the doxycycline release from the nanowafer into the cornea. (G-H) Intravital confocal fluorescence image of the mouse eye showing the presence of doxycycline for up to 48 hours. (I-J) Rapid clearance of doxycycline eye drops in 15 min in mice.

To further evaluate the ability of a nanowafer to increase the drug molecular residence time on the cornea and its subsequent diffusion into the corneal tissue, a red QD-NW was fabricated and tested on a healthy mouse cornea. Because Dexamethasone drug is nonfluorescent, it cannot be monitored by fluorescence microscopy. Hence, a QD-NW was fabricated to monitor QD diffusion and residence times in the cornea by fluorescence microscopy. The QD-NW were fabricated using hydrophobic CdSe/ZnS core−shell-type quantum dots stabilized with octadecylamine ligands (**Figure 18A**). The fluorescence emission wavelength of the QD-NW is λem 580 nm. Although, this is not an exact replication of drug diffusion into the cornea, this study provides evidence for the drug diffusion into the cornea.

The mouse cornea is ~3.2 mm in diameter and for the in vivo experiments in mice, nanowafers of 2 mm diameter and 80 μm thick were fabricated, so as to exactly fit within the cornea. Since, the nanowafers are fabricated with a mucoadhesive polymer, they readily adhere to the corneal surface. The nanowafer is soft and stretchable in dry state. The nanowafer, upon application, adheres and conforms to the curvature of the cornea. Also, after application of a nanowafer on the mouse cornea, 5 μL of balanced salt solution (BSS) was added to wet the cornea and further improve the nanowafer adhesion. During the application of the nanowafer, no pressure or bending is required. Furthermore, PVA nanowafer is known to elicit negligible inflammatory responses when applied on the eye. The nanowafer was applied on the mouse cornea with forceps followed by the instillation of 5 μL of BSS to wet the surface (**Figure 18B-C**).

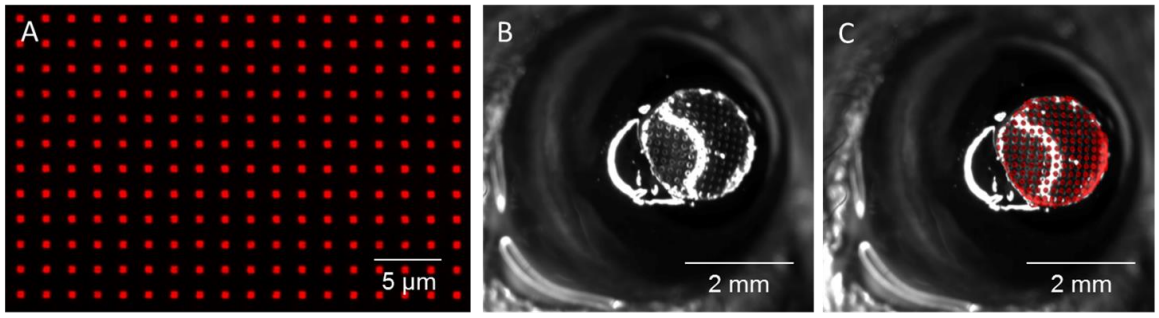

Figure 18. Ocular drug delivery nanowafer. (A) Fluorescence image of a red quantum dot-filled nanowafer. (D) Nanowafer applied on a mouse eye.

Upon placement of the QD-NW on the mouse cornea, the QDs began to diffuse into the corneal tissue, and it was observed for up to 48 h (**Figure 19**). At this point, the fluorescence intensity of the QDs in the corneal tissue began decreasing as the QDs diffuse through the cornea and reach the aqueous humor in the anterior chamber and cleared through the trabecular meshwork.

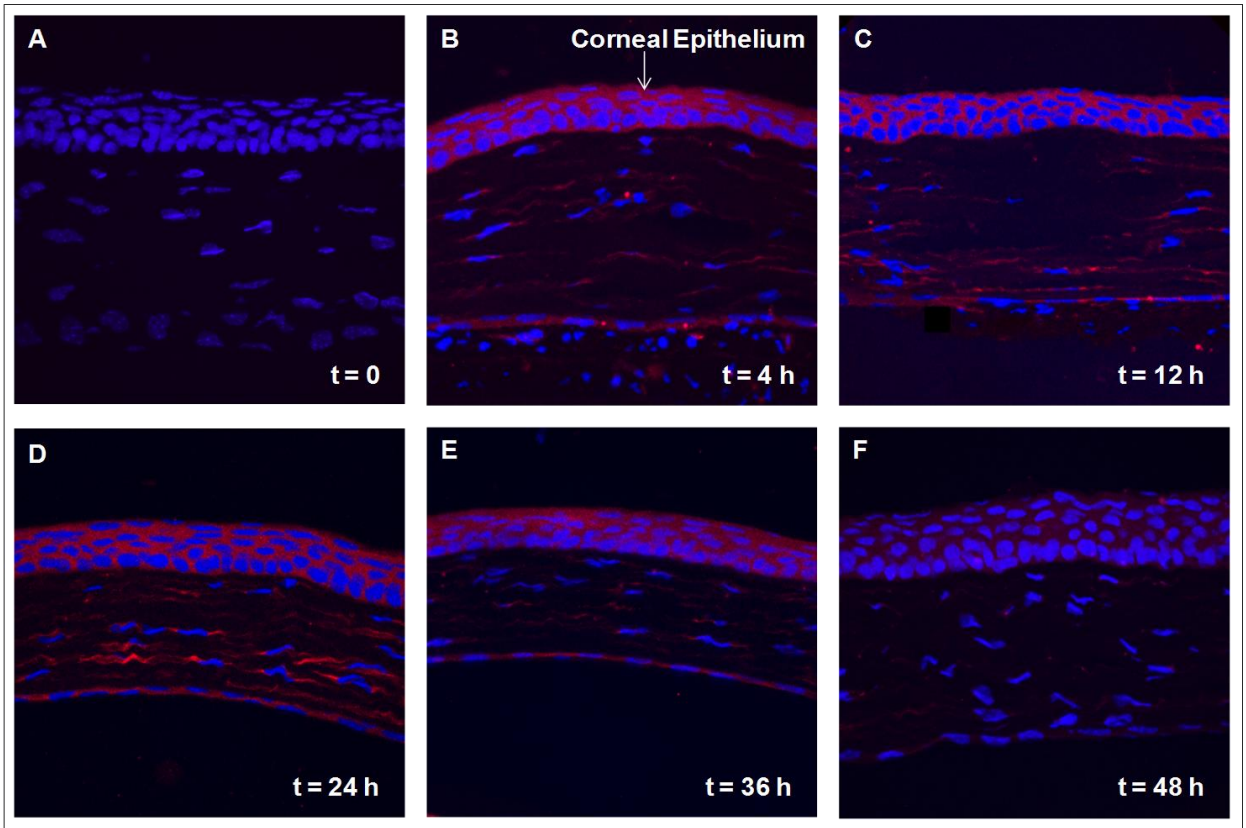

Figure 19. Nanowafer drug delivery enhances the drug diffusion into the cornea. Confocal laser scanning microscopic images of (**A**) Untreated cornea (control). (**B-F**) QD-NW treated corneal sections obtained at regular time intervals demonstrating the QD diffusion and retention in the corneas for up to 48 h.

Nanowafer can release the drug for up to 14 days

To demonstrate the ability of the nanowafer to release the drug for an extended period of time, increase drug residence time and its diffusion into the cornea, real-time *in vivo* corneal imaging experiments were performed in an ocular burn induced (OB) mouse model [20]. For this study, Dextran nanowafers filled with fluorescein coupled dextran (FITC-Dextran) were fabricated. After the instillation of this nanowafer on a mouse eye, the cornea was subjected to

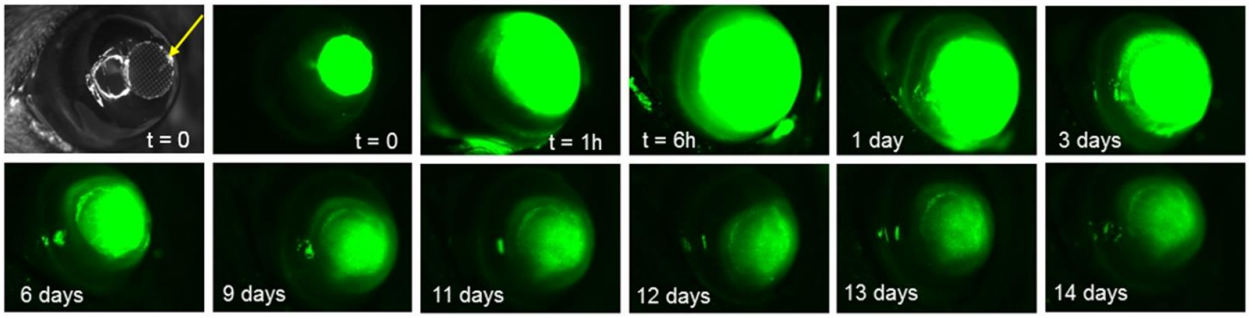

Figure 20. Nanowafer drug delivery enhances the drug residence time on the cornea for up to 2 weeks. (A) Bright field micrograph demonstrating the application of a nanowafer on an ocular burn induced mouse cornea. (B-L) Fluorescence micrographs demonstrating FITC-Dextran release from the nanowafer for 2 weeks.

real-time fluorescence imaging to monitor the presence of FITC-Dextran (**Figure 20**). This study revealed that the green fluorescent FITC-Dextran molecules were present in the cornea for up to 14 days (**Figure 20**). This study also confirmed that a longer drug residence time on the cornea will allow the drug molecules to effectively diffuse into the cornea and improve the bioavailability of the drug molecules. By optimizing the drug retention time in the cornea, a therapeutic concentration of the drug can be maintained in the cornea thus enhancing the drug efficacy.

In comparison, ocular burn induced eyes treated with FITC-Dextran eye drops became non-fluorescent within 4h, indicating its rapid clearance from the ocular surface (**Figure 21**). Also, after instillation of the FITC-Dextran drops on the eye, most of it is concentrated on the eye lids in addition to the cornea, indicating its clearance from the ocular surface (**Figure 21B**), compared to the nanowafer drug release, wherein little fluorescence intensity was observed around the eyelids and most of it in the eye. Because of the very short drug residence time on the cornea, eye drops need to be administered several times in a day for an observable therapeutic efficacy. This study has qualitatively demonstrated the ability of nanowafer to release the drug for an extended period of time and improve the drug diffusion into the corneal tissue for up to 14 days.

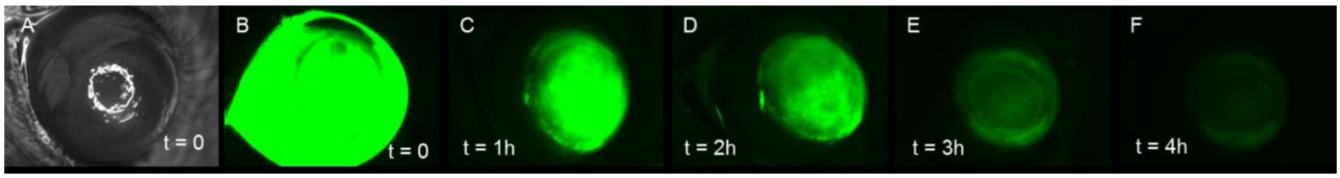

Figure 21. Rapid clearance of topically applied FITC-Dextran eye drops from the ocular surface in ocular burn mouse eye.

<u>Task 4. Study of the efficacy of doxycycline-nanowafers, dexamethasone-nanowafers, and cyclosporine-A-nanowafers in ocular burn mouse model</u>

Duration: 18 months (months 18-36)

This task involves the completion of two objectives: **Objective (i)** Quantification of the drug-nanowafer efficacy by time to epithelial healing using confocal fluorescence imaging; and **Objective (ii)** Measurement of expression of relevant inflammatory mediator genes by real-time PCR in an ocular burn mouse model. Completion of each objective and the outcomes are described below.

Objective (i) Quantification of the drug-nanowafer efficacy by time to epithelial healing using confocal fluorescence imaging

Corneal blindness is caused by corneal scarring and vascularization after injury. In mouse ocular burn model, corneal epithelium generally heals in two weeks with very loosely packed corneal stroma and neovascularization. The efficacy of nanowafer treatment in ocular burn mouse model was evaluated as a measure of corneal wound healing after a two-week treatment period.

To evaluate the therapeutic efficacy of the nanowafer on wound healing, ocular burn (OB) induced mice were treated once a week with dexamethasone nanowafers (Dex-NW) and compared with twice a day topical Dex eye drop treatment for two weeks and cornea wound healing was evaluated by histopathology at 2 weeks. In a healthy cornea, epithelium and the

collagen fibers in the stroma are tightly packed (**Figure 22A**). In OB induced corneas, the epithelium was healed in most eyes, but stromal swelling (edema), fibrosis, and invasion of inflammatory cells (non-bacterial keratitis) was observed (**Figure 22B**). Once a week Dex-NW treatment was very effective in wound healing with complete epithelial healing, minimal stromal edema and fibrosis, and the stromal collagen fibers were tightly packed (**Figure 22D**). In comparison, twice a day topical Dex eye drop (0.1%) treatment was able to minimize fibrosis; however, the stromal collagen was very loosely packed with several empty spaces (**Figure 22C**). These studies have clearly demonstrated an enhanced efficacy of Dex-NW in two weeks compared to topical Dex eye drop treatment on corneal wound healing.

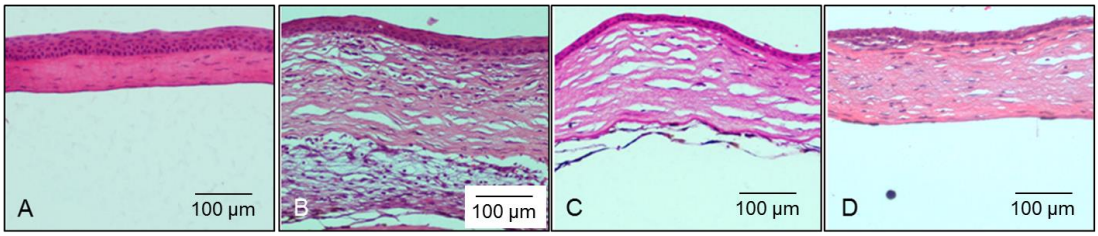

Figure 22. Nanowafer drug delivery is more effective in corneal wound healing and preventing fibrosis. (A) healthy cornea, (B) ocular burn (OB) induced cornea, (C) OB induced cornea treated twice a day with dexamethasone eye drops. (D) OB induced cornea treated with Dex-NW once a week.

The therapeutic efficacy of doxycycline nanowafers (Doxy-NW) and cyclosporine-A nanowafers (CyA-NW) were also evaluated on corneal wound healing. Four groups of OB induced mice were treated with Doxy-NW, Doxy eye drops, CyA-NW, and Cya-eye drops. Corneal wound healing in the CyA-NW and CyA eye drop treated corneas showed no difference compared to untreated OB induced corneas. Doxycyline treatment of the OB was evaluated, but the drug molecule was highly unstable and we experienced variability between the experiments. Based on these results, Dex-NW was selected for further evaluation.

Efficacy of Dexamethasone Nanowafer on Suppressing Corneal Neovascularization

Because of the physiological barriers of the ocular surface, topical eye drops must be applied several times a day for a therapeutic effect, thus increasing the potential for toxic side effects. Excessive use of Dex eye drops are known to cause side effects such as, cataract formation and increased intraocular pressure leading to glaucoma.

In this study, once a week Dex-NW treatment was compared with twice a day topical Dex eye drops (0.1%) treatment on inhibiting corneal neovascularization (CNV) in an ocular burn (OB) induced mouse model. A circular Dex-NW was placed on the injured cornea under general anesthesia, once in a week. On the 7th day, the corneas were collected, processed, and subjected to laser scanning fluorescence confocal microscopy.

The images of whole mount corneas clearly demonstrated a strong therapeutic effect of the Dex-NW treatment compared to the untreated OB control group (**Figure 23**). The Dex-NW treatment has restricted the proliferation of blood vessels to the limbal area and very closely resembled the healthy uninjured cornea. However, the OB control, PVA-NW, and Dex eye drop treated corneas exhibited an extensive neovascularization. The new blood vessels were highly branched and extended from the limbal area toward the center of the cornea. In the case of Dex-NW treatment, the amount of drug delivered to the cornea was 10 µg per week, and for Dex eye drop treatment it was 10 µg per day, i.e., 70 µg per week). Although, eye drop treated mice received a lot more drug than the Dex-NW treated group, still the nanowafer was more

effective than the topical eye drop treatment. These results also confirmed that the controlled drug release from Dex-NW is more effective in inhibiting CNV compared to the eye drop treatment even at a substantially lower dosing frequency.

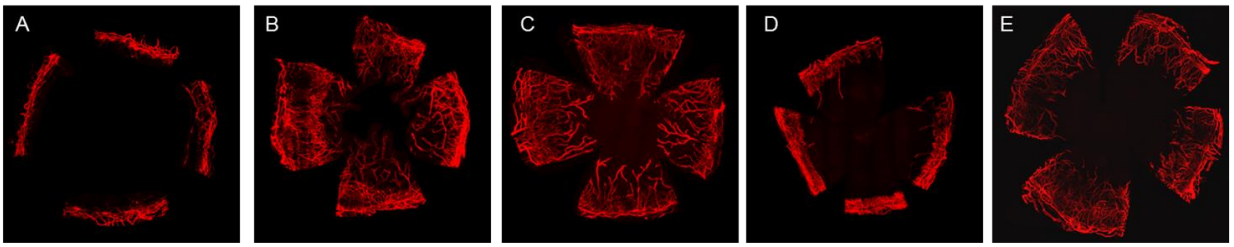

Figure 23. Efficacy of Dexamethasone nanowafer on inhibiting corneal neovascularization. Representative 3D reconstructed laser scanning confocal fluorescence images of the cornea demonstrating the enhanced therapeutic efficacy of Dex-NW compared to the Dex eye drop treatment. (a) Healthy cornea. (b) OB-induced cornea. (c) PVA-NW. (d) Dex-NW. (e) Twice a day Dex-eye drop (0.1%) treatment.

Objective (ii) Measurement of expression of relevant inflammatory mediator genes by real-time PCR in an ocular burn mouse model

The inflammatory response to injury is important to recovery, but if dysregulated can enhance tissue damage, stimulate angiogenesis, disrupt healing, and cause corneal opacity. Since the cornea is optically clear and avascular, its neovascularization and opacification result in eventual loss of vision. The biopolymers used in the nanowafer fabrication is crucial, as they can be immunostimulatory, i.e., can induce inflammation and exacerbate the condition, leading to delayed wound healing and incomplete recovery. Choosing the right biopolymer that is nonstimulatory to the cornea's immunological and inflammatory responses and that improves the tolerability, stability, and therapeutic effect of the drug with minimal side effects is vital for the success of the ocular drug delivery nanowafer.

As a first step, a quantitative analysis of the ability of the polymers to elicit proinflammatory and proangiogenic responses in an ocular burn (OB) induced mouse model was developed. The polymer nanowafers (tiny circular discs of 2 mm diameter and 100 μm thickness) were instilled on the corneas of OB-induced mice, daily for 5 days. At the end of the treatment period, the corneas were collected and processed for evaluating proinflammatory and proangiogenic genes by reverse transcription polymerase chain reaction (RT-PCR) analysis.

During the wound-healing process, the expression levels of several proinflammatory cytokines and their receptors, IL-1R, IL-1β, and IL-6, tumor necrosis factor TNF-R, and proangiogenic matrix metalloproteinases MMP-2, MMP-8, MMP-9, and MMP-13, and transforming growth factor TGF-β1 will be upregulated. Quantification of the expression levels of these factors gives insights into the effect of polymer materials on inflammation and angiogenesis. In this study, proinflammatory and proangiogenic attributes of Poly (vinyl alcohol) (PVA), Polyvinylpyrrolidone (PVP), (Hydroxypropyl)methyl cellulose (HPMC), and Carboxymethyl cellulose (CMC) nanowafers were evaluated in the corneas after injury by RT-PCR analysis (**Figure 24**). The PVA nanowafers were nonstimulatory, and the expression levels of proinflammatory factors were almost equal to the OB control group, while the PVP, HPMC, and CMC nanowafers significantly upregulated the expression of one or more inflammatory cytokines (IL-1R, IL-1β, and TNF-R) compared to the OB control group. The PVP, HPMC, and CMC nanowafers stimulated the expression levels of MMP-8, MMP-9, and TGF-β1, while the

PVA nanowafers were nonstimulatory, and the expression levels of these factors were very close to the OB control group.

The polymer nanowafers were further investigated for their effect on the expression levels of proangiogenic vascular endothelial growth factor A (VEGF-A), tyrosine kinase receptors VEGF-R1 and VEGF-R2, and platelet-derived growth factor receptors (PDGFR-A and PDGFR-B). The PVA nanowafer has a nonstimulatory effect on the expression levels of these factors, and they remain very close to the OB control group. However, all other polymer nanowafers have upregulated VEGF-R1, VEGF-R2, and PDGFR-B expression levels.

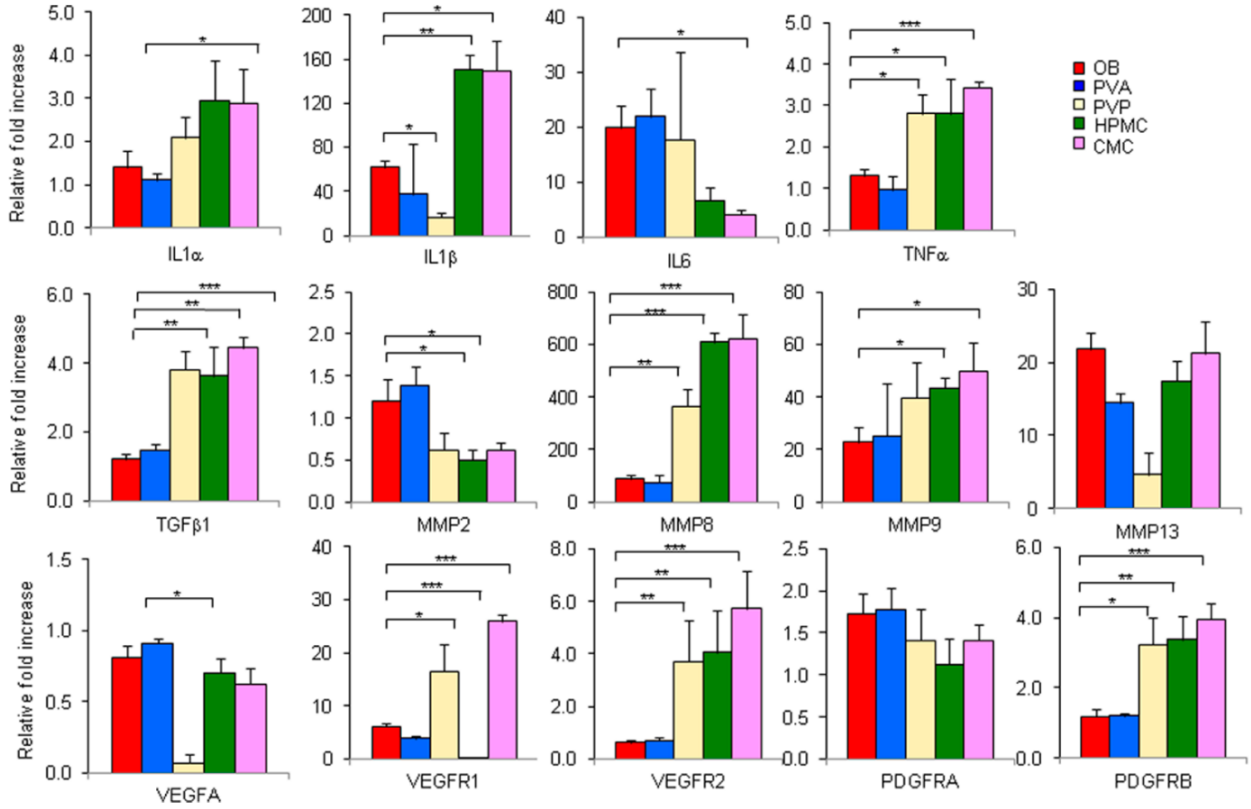

Figure 24. Analysis of inflammatory properties of biopolymers used in the nanwoafer fabrication. RT-PCR analysis confirming that PVA nanowafers do not induce upregulation of pro-inflammatory and proangiogenic factors. n = 3 (5 animals per group), *P < 0.05, **P < 0.01, ***P < 0.001). All error bars represent standard deviation from the mean.

Therapeutic efficacy of the of nanowafer drug delivery was quantified by the measurement of the expression levels of proinflammatory cytokines and proangiogenic factors by reverse transcription polymerase chain reaction (RT-PCR) analysis in ocular burn (OB) induced mouse model. In this study, the therapeutic efficacy of once a week dexamethasone nanowafer (Dex-NW) treatment was compared with twice a day topical dexamethasone eye drop (Dex-eye drops) treatment by PCR analysis. The nanowafers (tiny circular discs of 2 mm diameter and 100 μm thickness) were applied once a week on the corneas of OB-induced mice. Another group of OB-induced mice were subjected to topical Dex eye drop treatment twice a day for a week. After one week, the mice were sacrificed. The corneas were collected and processed for evaluating proinflammatory and proangiogenic genes by RT-PCR analysis.

During the wound-healing process, the expression levels of proinflammatory cytokines, IL-1β, and IL-6 and proangiogenic factors IL-8, VEGF-A, and MMP-12, tumor necrosis factor TNF, and transforming growth factor TGF-β1 will be upregulated. Quantification of the expression levels of these factors gives insights into the efficacy of Dex-NW on the regulation of inflammation and angiogenesis. Once a week Dex-NW was as effective as twice a day Dex-eye drop treatment for a week in suppressing the expression levels of proinflammatory cytokines, IL-1β, and IL-6, and proangiogenic factors IL-8, VEGF-A, and MMP-12, tumor necrosis factor TNF, and transforming growth factor TGF-β1 (**Figure 25**). Most importantly, the amount of Dex delivered by the Dex-NW was 10 µg per week, compared to 70 µg of Dex delivered as a topical eye drops twice a day for a week. These results reaffirmed the enhanced efficacy of Dex-NW once a week compared to the twice a day Dex eye drop treatment for the same period of time.

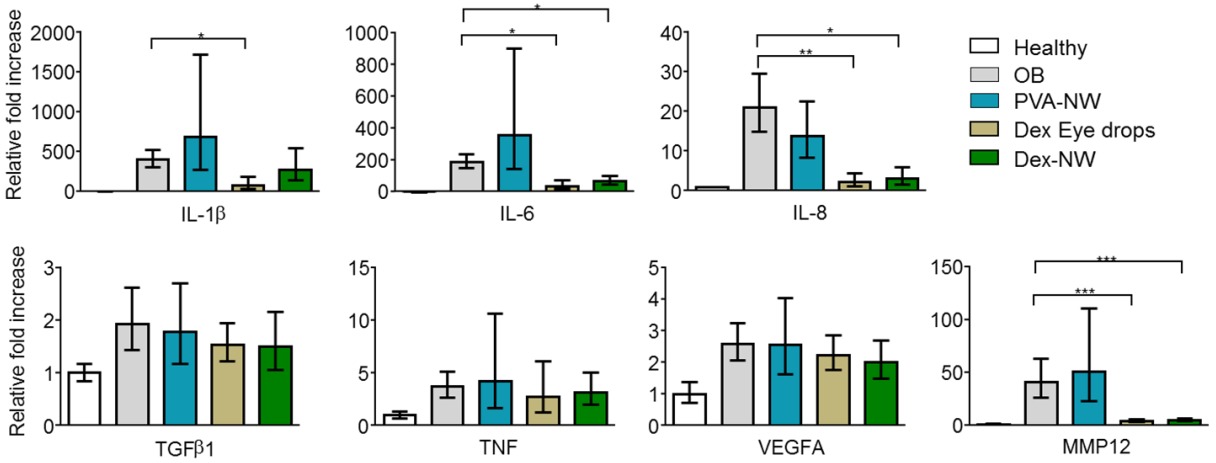

Figure 25. Enhanced therapeutic effect of Dexamethasone nanowafer. RT-PCR analysis revealing the suppression of the expression levels of proinflammatory and proangiogenic factors by Dex-NW. n = 3 (5 animals per group). *P < 0.05, **P < 0.01, ***P < 0.001. All error bars represent standard deviation from the mean.

To further optimize the efficacy of Dex-NW, we have fabricated Dex-NW containing 15 µg of Dex. The Dex-NWs were applied once a week and compared with twice a day topical Dex eye drop treatment for a week in two groups of ocular burn induced mice. At the end of the treatment period, the mice were sacrificed and the corneas were collected. The corneas were processed for RT-PCR analysis.

To compare the efficacy of Dex-NW and Dex eye drops, expression levels of proinflammatory and proangiogenic factors: IL-6, bFGF, PDGFR-A, PDGFR-B, TNF-α, and TGF-β, in addition to proangiogenic matrix metalloproteinases were measured. The Dex-NW was as effective as Dex eye drop treatment in suppressing the expression levels of proinflammatory and proangiogenic factors, and MMPs. (**Figure 26**). Once a week Dex-NW treatment delivered 15µg of Dex compared to 70 µg of Dex delivered as topical eye drops during the same treatment period. The Dex-NW was effective even at a very low drug concentration delivered by the Dex-NW compared to the topical eye drop treatment. In summary, these results have established the enhanced efficacy of Dex-NW when applied once a week compared to the twice a day topical eye drop treatment.

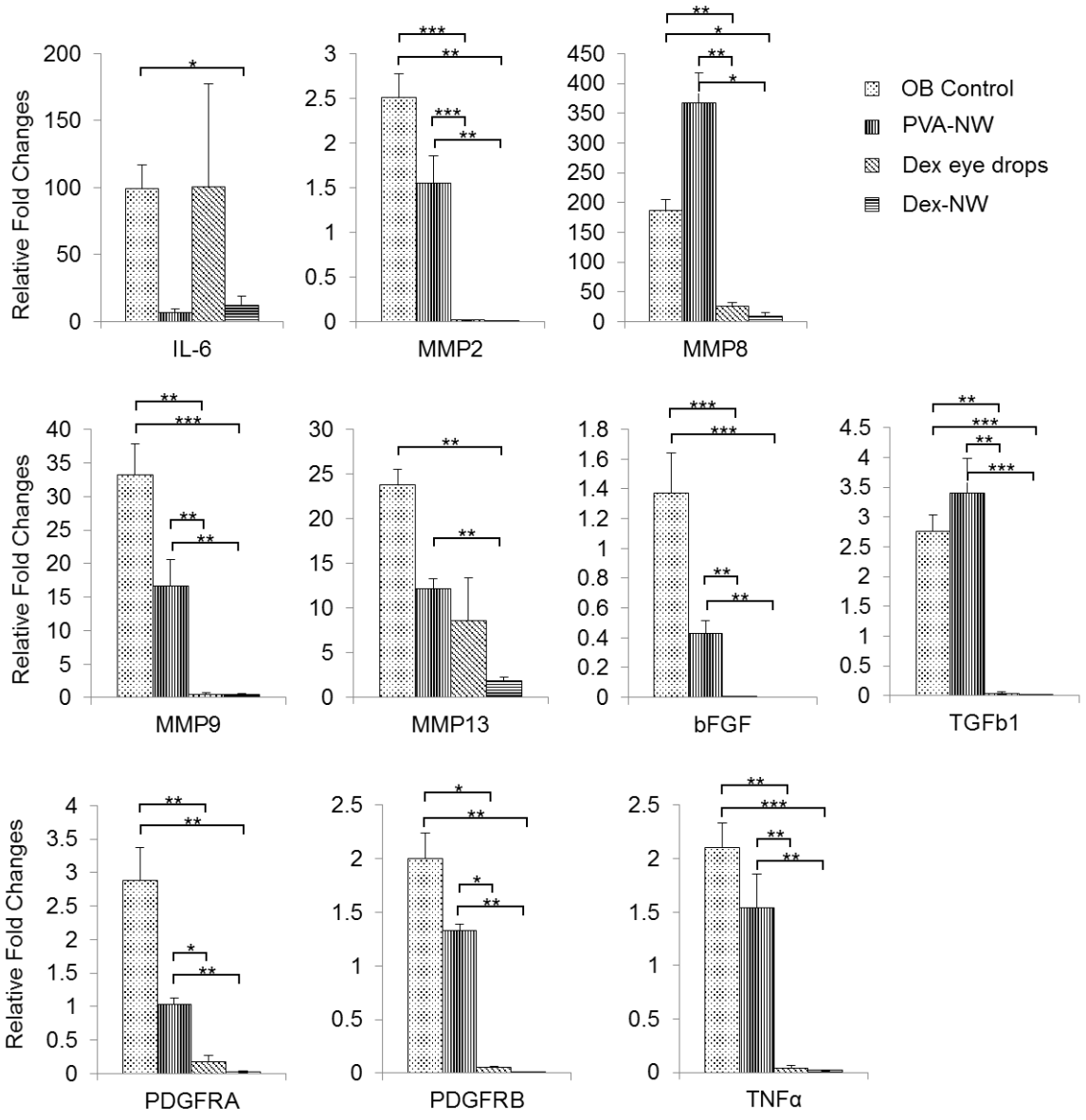

Figure 27. Therapeutic effect of Dexamethasone nanowafer. RT-PCR analysis revealing the suppression of the expression levels of proinflammatory and proangiogenic factors by Dex-NW. n = 3 (5 animals per group). *P < 0.05, **P < 0.01, ***P < 0.001. All error bars represent standard deviation from the mean.

What opportunities for training and professional development has the project provided?

1. **Dr. Daniela Marcano, Ph.D.** a postdoctoral research associate working on this project was provided necessary training and professional development opportunities. Specifically, Dr. Marcano was trained: (i) in the fabrication of nanowafer drug delivery systems, (ii) use of Nikon laser confocal fluorescence microscope and image analysis, (iii) pharmacokinetic analysis by HPLC, and (iv) preparation of animal protocols. As part of professional development, Dr. Marcano actively participated in the lab meetings, attended BCM seminars, and ARVO meeting held in Denver, CO. In addition, during one-on-one meetings, we have systematically reviewed and analyzed Dr. Marcano's experimental protocols and results. All these activities have helped Dr. Marcano accomplish the defined objectives of the project and develop into a trained scientist.

2. **Dr. Crystal S. Shin, Ph.D.** a postdoctoral research associate working on this project was provided necessary training and professional development opportunities. Specifically, Dr. Shin was trained: (i) in the fabrication and optimization of nanowafer drug delivery systems, (ii) use of Nikon laser confocal fluorescence microscope and image analysis, (iii) in vitro pharmacokinetic analysis by HPLC. For professional development, Dr. Shin actively participated in the lab meetings, attended seminars and symposiums hosted by BCM, Rice University, and Texas Medical Center, and attended ARVO meeting held in Denver, CO. During one-on-one meetings, we have reviewed and analyzed Dr. Shin's experimental progress and results. Dr. Shin was awarded the NIH-NEI travel grant to attend ARVO 2016 conference at Seattle, WA, and present this research work. With all these activities Dr. Shin was able to achieve the defined objectives of the project and develop into an independent scientist.

How were the results disseminated to communities of interest?
"Nothing to Report"

What do you plan to do during the next reporting period to accomplish the goals?
The project has been successfully completed.

4. **IMPACT**

What was the impact on the development of the principal discipline(s) of the project?
"Nothing to Report"

What was the impact on other disciplines?
"Nothing to Report"

What was the impact on technology transfer?
"Nothing to Report"

What was the impact on society beyond science and technology?
"Nothing to Report"

5. **CHANGES/PROBLEMS:**
The progress of the project was delayed due to unexpected delays in procuring mice and PCR reagents. Because of this a no cost extension of the project approval has been obtained from DOD.

6. **PRODUCTS:**

Journal publications.

1. X Yuan, DC Marcano, CS Shin, X Hua, LC Isenhart, SC Pflugfelder, G Acharya. Ocular drug delivery nanowafer with enhanced therapeutic efficacy, *ACS Nano* **9**, 1749–1758 (2015).

2. TG Coursey, JT Henriksson, DC Marcano, CS Shin, LC Isenhart, F Ahmad, CS De Paiva, S C Pflugfelder, G Acharya. Dexamethasone nanowafer as an effective therapy for dry eye disease, *J. Control Release*. **213**, 168–174 (2015).

3. DC Marcano, CS Shin, B Lee, LC Isenhart, X Liu, F Li, JV Jester, SC Pflugfelder, J Simpson, G Acharya. Synergistic cysteamine delivery nanowafer as an efficacious treatment modality for corneal cystinosis. *Mol Pharm*. **13**, 3468-3477 (2016).

Conference papers

1. G Acharya, X Yuan, D Marcano, C Shin, X Hua, L Isenhart, SC Pflugfelder. Nanowafer Drug Delivery to Treat Corneal Neovascularization. *Invest. Ophthalmol. Vis. Sci.* 2015; 56(7):5032

2. CS Shin, DC Marcano, JT Henriksson, G Acharya, SC Pflugfelder. Nanowafer Drug Delivery for Restoration of Healthy Ocular Surface in Dry Eye Condition. *Invest. Ophthalmol. Vis. Sci.* 2015; 56(7):321.

3. CS Shin, X Yuan, DC Marcano, LC Isenhart, K Simmons, SC Pflugfelder, G Acharya.
   Anti-angiogenic polymer therapeutic for corneal neovascularization. *Invest. Ophthalmol. Vis. Sci.* 2016; 57:3516

4. DC Marcano, CS, Shin, B Lee, LC Isenhart, X Liu, F Li, JV Jester, SC Pflugfelder; J Simpson, G Acharya. Extended release cysteamine nanowafer as an efficacious treatment modality for corneal cystinosis. Controlled Release Society Meeting 2016, July 17-20, Seattle, WA.

5. CS Shin, X Yuan, DC Marcano, LC Isenhart, K Simmons, SC Pflugfelder, G Acharya. Dextran sulfate wafer as an anti-angiogenic polymer therapeutic. Controlled Release Society Meeting 2016, July 17-20, Seattle, WA.

Presentations

1. Ghanashyam Acharya: Invited seminar: “Ocular Drug Delivery Nanowafer” at Texas Tech University, Lubbock, TX. Date: 10-20-2014.
2. Ghanashyam Acharya: Invited seminar: “Ocular Drug Delivery Nanowafer: Design and Development,” Bench to Bedside Symposium, Gavin Herbert Eye Institute, University of California, Irvine, CA. Date: 06-19-2015
3. Ghanashyam Acharya: Invited seminar: “Ocular Drug Delivery Nanowafer: Design and Applications,” Houston Methodist Research Institute, Houston, TX. Date: 08-08-2016.

Press Releases of Nanowafer publication

1. **American Chemical Society Press release: “An end to the medicine dropper for eye injuries”**
   02-04-2015
   http://www.acs.org/content/acs/en/pressroom/presspacs/2015/acs-presspac-february-4-2015/an-end-to-the-medicine-dropper-for-eye-injuries.html

2. Chemical & Engineering News: “Dissolving Disks Deliver Drugs To The Eye” 02-05-2015
   http://cen.acs.org/articles/93/web/2015/02/Dissolving-Disks-Deliver-Drugs-Eye.html

3. National Public Radio (NPR): “Dissolving Contact Lenses Could Make Eye Drops Disappear” 02-20-2015
   http://www.npr.org/sections/health-shots/2015/02/20/387301576/dissolving-contact-lenses-could-make-eye-drops-disappear

Books or other non-periodical, one-time publications.
"Nothing to Report"

Website(s) or other Internet site(s)
"Nothing to Report"
Technologies or techniques
"Nothing to Report"

Inventions, patent applications, and/or licenses
"Nothing to Report"
Other Products
"Nothing to Report

7. **PARTICIPANTS & OTHER COLLABORATING ORGANIZATIONS**

What individuals have worked on the project?

Name	**Stephen C. Pflugfelder, M.D.**
Project Role	Principal Investigator
Researcher Identifier	
Nearest person month worked	1
Contribution to the Project	Directed and oversaw the project performance of all experiments defined under Tasks 1, 2, and 3. Reviewed and analyzed the experimental results. Reviewed the animal protocol for IACUC/ACURO approval
Funding Support	(Complete only if the funding support is provided from other than this award).
Name	**Ghanashyam Acharya, Ph.D.**
Project Role	Co-Principal Investigator
Researcher Identifier	
Nearest person month worked	4
Contribution to the Project	Directed Tasks 2 & 3. Fabricated the silicon wafer master templates, by e-beam lithography and photolithography. Fabricated PDMS imprints. Fabricated doxycycline and dexamethasone nanowafers. Developed HPLC methods for in vitro and in vivo drug release study of doxycycline and dexamethasone from the nanowafers. Designed the experiments, reviewed and analyzed the experimental results.
Funding Support	Cystinosis Research Foundation, DOD
Name	**Daniela Marcano, Ph.D.**
Project Role	Postdoctoral Research Associate
Researcher Identifier	
Nearest person month worked	12
Contribution to the Project	Prepared the animal protocol for IACUC/ACURO submission. Fabricated the PDMS imprints. Fabricated doxycycline and dexamethasone loaded nanowafers. Performed in vitro drug release study of the nanowafers. Performed the fluorescence confocal imaging to monitor the in vivo doxycycline release in mouse eye. Performed the animal studies to evaluate the therapeutic efficacy of nanowafer drug delivery and compared it with topical eye drop treatment in ocular burn induced mice
Funding Support	

Name	**Crystal S. Shin, Ph.D.**
Project Role	Postdoctoral Research Associate
Researcher Identifier	
Nearest person month worked	12
Contribution to the Project	Performed and optimized the nanowafer compliance experiments on mouse eyes. Performed in vivo drug release experiments. Performed laser confocal imaging experiments and quantified the epithelial recover and corneal neovascularization using IMARIS data analysis software.
Funding Support	

Has there been a change in the active other support of the PD/PI(s) or senior/key personnel since the last reporting period?
"Nothing to Report"

What other organizations were involved as partners?
"Nothing to Report"

8. SPECIAL REPORTING REQUIREMENTS

COLLABORATIVE AWARDS:
"Not Applicable"

9. APPENDICES

Appendix 1: Journal publication
Yuan et al, Ocular drug delivery nanowafer with enhanced therapeutic efficacy, *ACS Nano* **9**, 1749–1758 (2015).

Appendix 2: Journal publication
Coursey et al, Dexamethasone nanowafer as an effective therapy for dry eye disease, *J. Control Release*. **213**, 168–174 (2015).

Appendix 3: Journal publication
Marcano et al. Synergistic cysteamine delivery nanowafer as an efficacious treatment modality for corneal cystinosis. *Mol Pharm.* **13**, 3468-3477 (2016).

Appendix 4: Conference paper
Acharya et al, Nanowafer Drug Delivery to Treat Corneal Neovascularization. *Invest. Ophthalmol. Vis. Sci.* 2015; 56(7):5032

Appendix 5: Conference paper
Shin et al, Nanowafer Drug Delivery for Restoration of Healthy Ocular Surface in Dry Eye Condition. *Invest. Ophthalmol. Vis. Sci.* 2015; 56(7):321.

Appendix 6: Conference paper
Shin et al. Anti-angiogenic polymer therapeutic for corneal neovascularization. Invest. Ophthalmol. Vis. Sci. 2016; 57:3516.

Appendix 7: Conference abstract
Marcano et al. Extended release cysteamine nanowafer as an efficacious treatment modality for corneal cystinosis. Controlled Release Society Meeting 2016, July 17-20, Seattle, WA.

Appendix 8: Conference abstract
Shin et al. Dextran sulfate wafer as an anti-angiogenic polymer therapeutic. Controlled Release Society Meeting 2016, July 17-20, Seattle, WA.

Appendix 1: Journal publication

Yuan et al, Ocular drug delivery nanowafer with enhanced therapeutic efficacy, *ACS Nano* **9**, 1749–1758 (2015).

Ocular Drug Delivery Nanowafer with Enhanced Therapeutic Efficacy

Xiaoyong Yuan,[†] Daniela C. Marcano, Crystal S. Shin, Xia Hua,[†] Lucas C. Isenhart, Stephen C. Pflugfelder,[*] and Ghanashyam Acharya[*]

Ocular Surface Center, Cullen Eye Institute, Department of Ophthalmology, Baylor College of Medicine, One Baylor Plaza, Houston, Texas 77030, United States.
[†]Present address: Tianjin Eye Hospital, Clinical College of Ophthalmology, Tianjin Medical University, Tianjin, China 300020.

ABSTRACT Presently, eye injuries are treated by topical eye drop therapy. Because of the ocular surface barriers, topical eye drops must be applied several times in a day, causing side effects such as glaucoma, cataract, and poor patient compliance. This article presents the development of a nanowafer drug delivery system in which the polymer and the drug work synergistically to elicit an enhanced therapeutic efficacy with negligible adverse immune responses. The nanowafer is a small transparent circular disc that contains arrays of drug-loaded nanoreservoirs. The slow drug release from the nanowafer increases the drug residence time on the ocular surface and its subsequent absorption into the surrounding ocular tissue. At the end of the stipulated period of drug release, the nanowafer will dissolve and fade away. The *in vivo* efficacy of the axitinib-loaded nanowafer was demonstrated in treating corneal neovascularization (CNV) in a murine ocular burn model. The laser scanning confocal imaging and RT-PCR study revealed that once a day administered axitinib nanowafer was therapeutically twice as effective, compared to axitinib delivered twice a day by topical eye drop therapy. The axitinib nanowafer is nontoxic and did not affect the wound healing and epithelial recovery of the ocular burn induced corneas. These results confirmed that drug release from the axitinib nanowafer is more effective in inhibiting CNV compared to the topical eye drop treatment even at a lower dosing frequency.

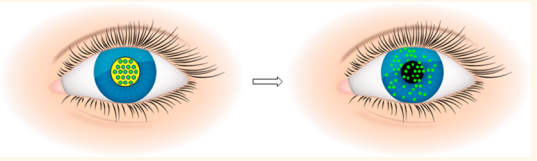

KEYWORDS: nanowafer · drug delivery · inflammation · corneal neovascularization · therapeutic efficacy

Eye injuries are one of the major causes of blindness worldwide, and in the United States alone 2.5 million eye injuries occur every year.[1] Ocular surface injuries disrupt corneal angiogenic privilege and trigger corneal neovascularization (CNV), eventually leading to loss of vision.[2] Ocular drug delivery, although it may seem to be deceptively simple, is a challenging task mainly because of the unique barriers associated with the ocular surface that impede adequate drug delivery and therapeutic efficacy.[3] Topical drug therapy with eye drop formulations is the most accessible and noninvasive. However, its potential is limited by the ocular surface protective barriers, such as reflex tearing, constant blinking, impervious nature of the ocular surface due to tight epithelial junctions, and nasolacrimal drainage that can rapidly clear the eye drops from the ocular surface in a few minutes.[4,5] In addition, drug clearance due to systemic absorption through blood capillaries in the conjunctival sac can further reduce the amount of drug available for effective ocular absorption.[6,7] These physiological barriers contribute to inadequate drug delivery and reduced bioavailability of the drug to the eye. Hence, topical eye drops must be applied several times a day, thus increasing the potential for toxic side effects such as cellular damage, inflammation of the ocular surface, and temporary blurred vision, leading to discomfort and poor patient compliance.[8,9] Topical eye drop therapies that target CNV often produce side effects such glaucoma and cataract formation.[10,11]

To improve treatment efficacy, emulsions, liposomes, micelles, and nanoparticle suspensions have been used in ocular drug delivery. However, these formulations were also rapidly cleared from the eye.[12−15] *In situ* gel-forming systems have been developed for ocular drug delivery.[16] A hydrogel-forming solution containing drug upon instillation as eye drops undergoes sol-to-gel phase transition on the eye surface. The *in situ*-formed gels are expected to hold the drug for a longer period of time, thus enhancing its bioavailability. However, these formulations are also quickly cleared

* Address correspondence to gacharya@bcm.edu, stevenp@bcm.edu.

Received for review November 19, 2014 and accepted January 13, 2015.

Published online January 13, 2015
10.1021/nn506599f

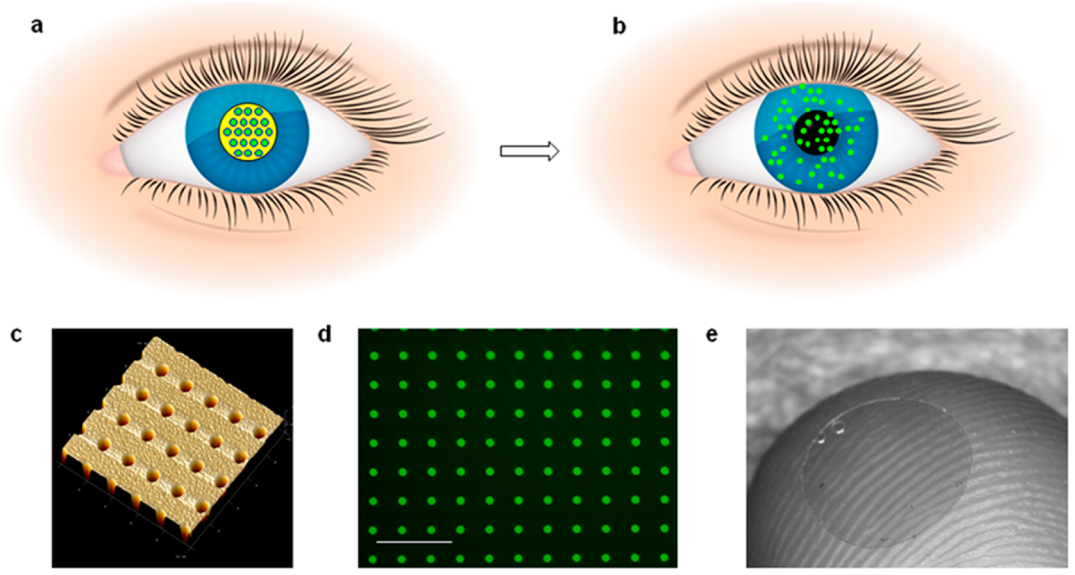

Figure 1. Ocular drug delivery nanowafer. (a) Schematic of the nanowafer instilled on the cornea. (b) Diffusion of drug molecules into the corneal tissue. (c) AFM image of a nanowafer demonstrating an array of 500 nm diameter nanoreservoirs. (d) Fluorescence micrograph of a nanowafer filled with doxycycline (scale bar 5 μm). (e) Nanowafer on a fingertip.

from the ocular surface, resulting in limited therapeutic efficacy. Drug-loaded contact lenses have been developed to improve the drug retention time in the eye.[17,18] All these systems could not release the drug for extended periods of time, leading to limited drug efficacy, thus requiring multiple administrations.

In this context, development of a novel nano drug delivery system that can surmount the ocular surface barriers and release the drug for extended periods of time, thus enhancing therapeutic efficacy and improving patient compliance, is vitally important to treat ocular injuries, infections, and inflammatory conditions and restore normal physiological functions of the eye.

RESULTS AND DISCUSSION

This article presents the development of an ocular drug delivery nanowafer, wherein the drug carrying polymer and the drug work synergistically to provide an augmented therapeutic effect compared to conventional eye drop therapy. The nanowafer is a tiny transparent circular disc that can be applied on the ocular surface with a fingertip and can withstand constant blinking without being displaced (Figure 1). It contains arrays of drug-loaded nanoreservoirs from which the drug will be released in a tightly controlled fashion for a few hours to days. The slow drug release from the nanowafer increases the drug residence time on the ocular surface and its subsequent absorption into the surrounding ocular tissue. At the end of the stipulated period of drug release, the nanowafer will dissolve and fade away. The development of an ocular drug delivery nanowafer and its enhanced *in vivo* therapeutic efficacy is herein demonstrated by treating corneal neovascularization in a murine ocular burn (OB) model.[19]

Nanowafer Fabrication. In this study, four different polymers, poly(vinyl alcohol) (PVA), polyvinylpyrrolidone (PVP), (hydroxypropyl)methyl cellulose (HPMC), and carboxymethyl cellulose (CMC), were used for nanowafer fabrication. These polymers were selected for their water solubility, biocompatibility, mucoadhesivity, transparency, and film-forming properties so as to readily adhere to a wet mucosal surface and conform to the curvature of the eye.[20] Aqueous solutions of these polymers are currently in clinical use as artificial tears, and therefore nanowafers fabricated with these polymers can function both as a drug delivery system and also as lubricant.[21,22] The nanowafers were fabricated *via* the hydrogel template strategy with a few modifications (Figure 2).[23,24] The first step involves the fabrication of arrays of wells (500 nm diameter and 500 nm depth) on a silicon wafer by e-beam lithography followed by preparation of its poly(dimethylsiloxane) (PDMS) imprint. In the second step, a polymer solution will be poured on the PDMS template followed by baking. The polymer wafer containing 500 nm diameter wells was peeled off and placed on the flat surface to expose the wells. The wells in the polymer wafer were filled with a solution of drug/polymer mixture. In this study, blank nanowafers (without the drug) of PVA, PVP, HPMC, and CMC and PVA nanowafers loaded with sunitinib, sorafenib, axitinib, and doxycycline were fabricated.

Immunostimulatory Properties of Nanowafers. The inflammatory response to injury is important to recovery, but if dysregulated can enhance tissue damage, stimulate angiogenesis, disrupt healing, and cause corneal opacity.[25,26] Since the cornea is optically clear and avascular, its neovascularization and opacification result in eventual loss of vision. The biopolymers

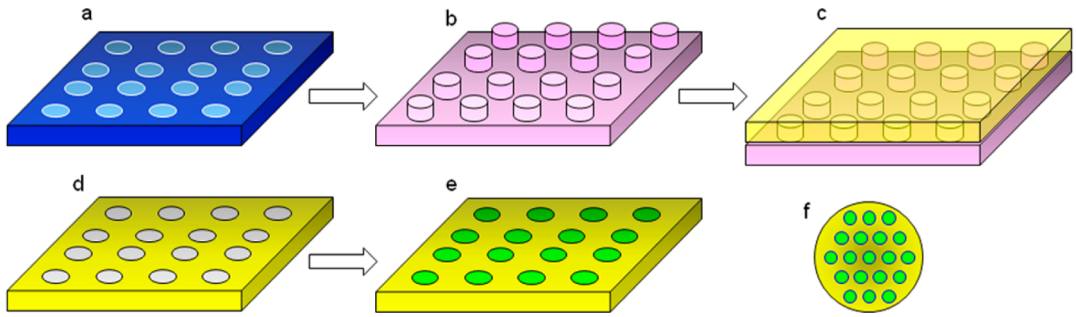

Figure 2. Schematic of nanowafer fabrication. (a) Silicon wafer master template having 500 nm wells fabricated by e-beam lithography. (b) PDMS imprint containing vertical posts. (c) Fabrication of a PVA template. (d) PVA template. (e) PVA template filled with drug. (f) Drug-filled nanowafer.

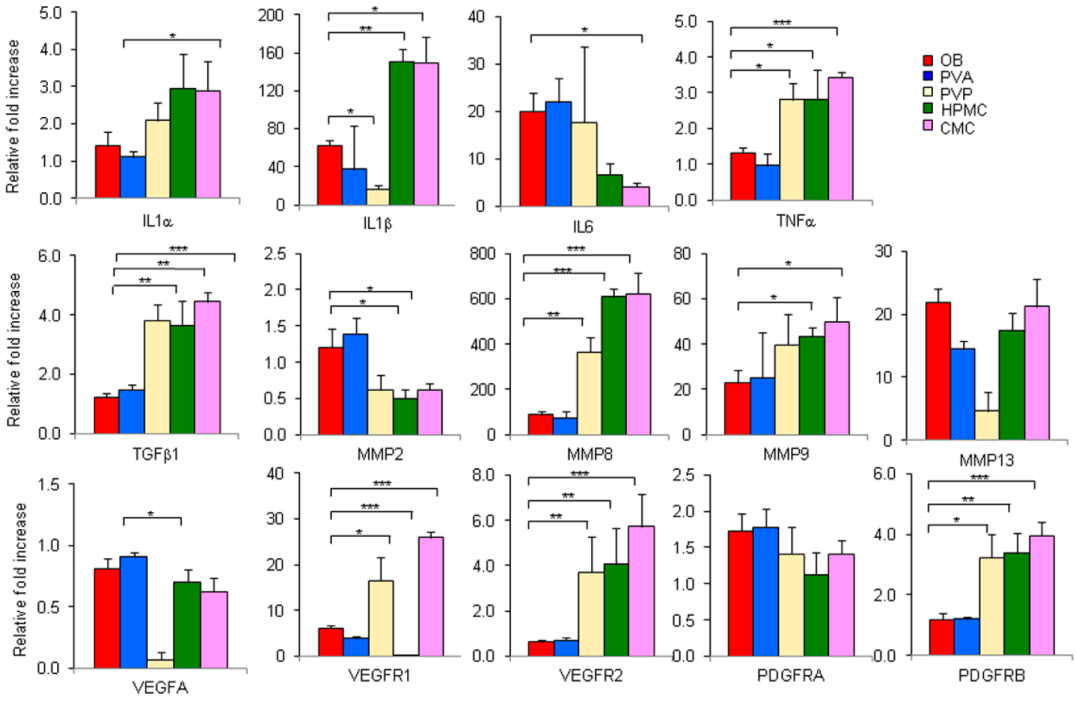

Figure 3. Poly(vinyl alcohol) nanowafer is nonimmunogenic. RT-PCR analysis confirming that PVA nanowafers do not induce upregulation of proinflammatory and proangiogenic factors. $n = 3$ (5 animals per group), $^{*}P < 0.05$, $^{**}P < 0.01$, $^{***}P < 0.001$). All error bars represent standard deviation from the mean.

used in the nanowafer fabrication is crucial, as they can be immunostimulatory, *i.e.*, can induce inflammation and exacerbate the condition, leading to delayed wound healing and incomplete recovery.[27−29] Choosing the right biopolymer that is nonstimulatory to the cornea's immunological and inflammatory responses and that improves the tolerability, stability, and therapeutic effect of the drug with minimal side effects is vital for the success of the ocular drug delivery nanowafer.

As a first step, a quantitative analysis of the ability of the polymers to elicit proinflammatory and proangiogenic responses in an OB mouse model was developed. The polymer nanowafers (tiny circular discs of 2 mm diameter and 100 μm thickness) were instilled on the corneas of OB-induced mice, daily for 5 days. At the end of the treatment period, the corneas were collected and processed for evaluating proinflammatory and proangiogenic genes by reverse transcription polymerase chain reaction (RT-PCR) analysis.

During the wound-healing process, the expression levels of several proinflammatory interleukins, IL-1α, IL-1β, and IL-6, tumor necrosis factor TNF-α, and proangiogenic matrix metalloproteinases MMP-2, MMP-8, MMP-9, and MMP-13, and transforming growth factor TGF-β1 will be upregulated.[30−33] Quantification of the expression levels of these factors gives insights into the effect of polymer materials on inflammation and angiogenesis. In this study, proinflammatory and proangiogenic attributes of PVA, PVP, HPMC, and CMC nanowafers were evaluated in the corneas after injury by RT-PCR analysis (Figure 3). The PVA nanowafers were nonstimulatory, and the expression levels of proinflammatory factors were almost equal to the OB control group, while the PVP, HPMC, and CMC nanowafers significantly upregulated the expression of

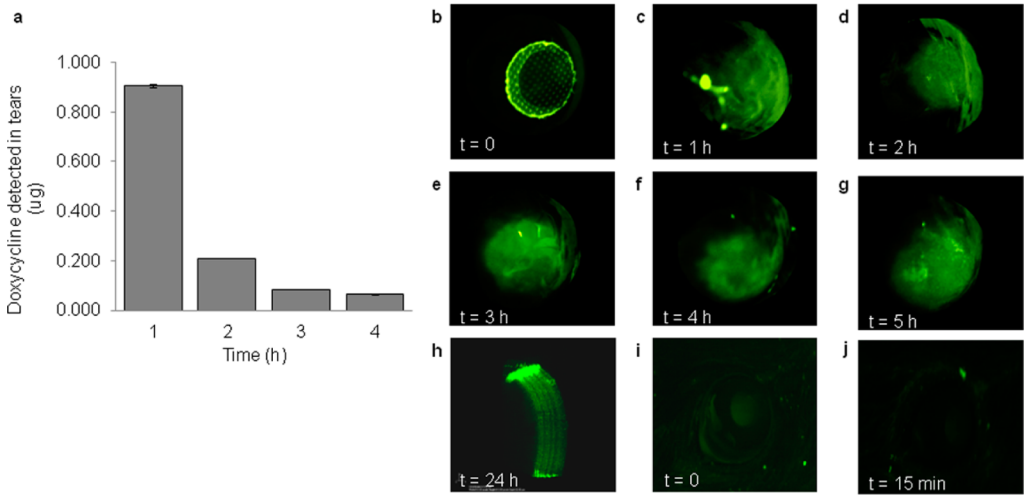

Figure 4. Nanowafer drug delivery enhances drug molecular transport into the cornea. (a) *In vivo* drug release from a doxycycline nanowafer placed on the cornea and measurement of the drug concentration in tears. (b–g) Fluorescence stereomicroscopic images of mouse cornea at regular time intervals demonstrating the doxycycline release from the nanowafer into the cornea. (h) Intravital confocal fluorescence image of the mouse eye showing the presence of doxycycline at 24 h. (i and j) Rapid clearance of doxycycline eye drops in 15 min in mice.

one or more inflammatory cytokines (IL-1α, IL-1β, and TNF-α) compared to the OB control group. The PVP, HPMC, and CMC nanowafers stimulated the expression levels of MMP-8, MMP-9, and TGF-β1, while the PVA nanowafers were nonstimulatory, and the expression levels of these factors were very close to the OB control group.

The polymer nanowafers were further investigated for their effect on the expression levels of proangiogenic vascular endothelial growth factor A (VEGF-A), tyrosine kinase receptors VEGF-R1 and VEGF-R2, and platelet-derived growth factor receptors (PDGFR-A and PDGFR-B). The PVA nanowafer has a nonstimulatory effect on the expression levels of these factors, and they remain very close to the OB control group. However, all other polymer nanowafers have upregulated VEGF-R1, VEGF-R2, and PDGFR-B expression levels. Taken together, these results indicate that PVA nanowafers are well tolerated by the ocular surface and do not stimulate the expression of proinflammatory and proangiogenic factors. To take advantage of these attributes, PVA was chosen for the fabrication of nanowafers. Furthermore, these results also indicate that the PVA nanowafers are well suited for the delivery of antiangiogenic small molecular tyrosine kinase receptor inhibitor (TKI) drugs to treat CNV.

Nanowafer Enhances Drug Diffusion into the Cornea. To demonstrate the ability of the nanowafers to release the drug for an extended period of time, PVA nanowafers loaded with doxycycline were fabricated. Doxycycline (antibiotic drug) was chosen for this study because of its green fluorescence, which allowed us to monitor the precorneal drug residence time and its subsequent diffusion into the cornea by real-time fluorescence imaging.[34] To monitor the drug concentration on the ocular surface as a measure of drug release from the nanowafer, tear samples were collected hourly for 5 h, and the doxycycline content was analyzed by HPLC.[35] After placement of a doxycycline nanowafer on the cornea, the drug concentration in the tears slowly decreased with time, and after 4 h, no detectable doxycycline concentration was present (Figure 4a). To monitor the drug diffusion into the mouse cornea after the instillation of a doxycycline nanowafer, it was subjected to fluorescence imaging at hourly intervals under general anesthesia. The corneas were green fluorescent even after 5 h when viewed under a stereomicroscope with 488 nm illumination, indicating the presence of drug in the cornea (Figure 4b–g). The corneas exhibited a strong green fluorescence even after 24 h, when subjected to intravital laser scanning confocal imaging, indicating the presence of doxycycline in the corneal tissue (Figure 4h). To compare the efficacy of the doxycycline delivery by nanowafer with topical eye drop treatment, another group of mice were treated with doxycycline eye drops. Upon examination under a fluorescence microscope, the corneas did not exhibit a measurable green fluorescence, indicating the complete clearance of the drug within a few minutes (Figure 4i and j). Although, doxycycline concentration was undetectable in tears after 4 h, the fluorescence and intravital confocal imaging studies have confirmed the presence of the drug in the corneal tissue for up to 24 h. Taken together, this study clearly demonstrates the ability of the nanowafer to release doxycycline for an extended period of time, thus enhancing the precorneal drug residence time and subsequent diffusion of drug molecules into the cornea.

Tyrosine Kinase Receptor Inhibitor Drugs to Load into the Nanowafers. TKI drugs were selected as the most suitable candidates for loading into PVA nanowafers and

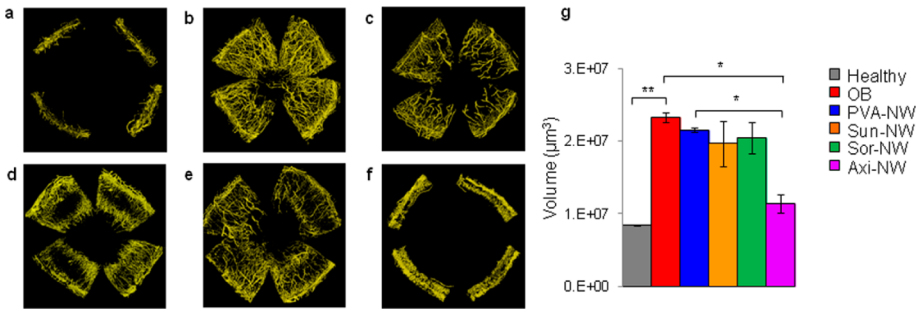

Figure 5. Selection of tyrosine kinase receptor inhibitor drugs. Screening of tyrosine kinase inhibitor drugs loaded nanowafers for their relative therapeutic efficacy in inhibiting corneal neovascularization after 10 days of treatment. Representative 3D reconstructed corneal images of fluorescence confocal microscopy: (a) healthy cornea (control); (b) untreated ocular burn (control); (c) blank PVA-NW; (d) Sora-NW; (e) Suni-NW; (f) Axi-NW. (g) Quantification of corneal neovascularization volume. $n = 3$ animals, *$P < 0.05$ *vs* OB control and $P < 0.05$ *vs* PVA-NW, **$P < 0.01$. All error bars represent standard deviation from the mean.

further evaluated for their relative therapeutic efficacy. The TKI drugs constitute a rapidly evolving class of low molecular weight antiangiogenic drugs that can selectively bind and inhibit the upregulation of tyrosine kinase receptors such as VEGFR1, VEGFR2, PDGFR-A, and PDGFR-B.[36] These drugs are very effective in suppression and regression of neovascularization.[37] Nanowafers containing sunitinib, sorafenib, and axitinib were fabricated for this study. These drugs were chosen, as they are already in clinical use as antiangiogenic therapeutics to treat late-stage renal carcinoma.[38−40]

To select the most suitable drug for the treatment of CNV, PVA nanowafers loaded with sunitinib (Sun-NW), sorafenib (Sor-NW), and axitinib (Axi-NW) were investigated for their relative therapeutic efficacy and compared with untreated OB group and PVA nanowafer (PVA-NW)-treated groups. For mouse experiments, each nanowafer was fabricated to be 2 mm in diameter to exactly cover the corneal surface and contained 5 μg of the drug. The nanowafers were instilled on the cornea immediately after the alkali burn. The mice were subjected to once a day nanowafer treatment for 10 days followed by a 5-day observation period. The CNV was monitored by slit-lamp imaging every other day. This study revealed an extensive neovascularization of the corneas in untreated OB and PVA-NW-treated control groups. The Sun-NW- and Sor-NW-treated groups also exhibited neovasculature. In all these groups, the new blood vessels proliferated from the limbal rim area to the center of the cornea. The Axi-NW-treated corneas were the clearest and had less CNV compared to the untreated OB control group, and the new blood vessels were closely restricted to the limbal area (Supplementary Figure S1). At the end of the treatment period, whole mount specimens of these corneas were prepared and treated with rat anti-mouse CD31 antibody and Alexa-Fluor 594-conjugated goat anti-rat secondary antibody to label vascular endothelium, and subjected to laser scanning confocal fluorescence imaging.[41] This study revealed that Sun-NW and Sora-NW were not very effective in suppressing the CNV. The Axi-NW treatment was the most effective, and the corneas appeared to be almost close to the healthy cornea with minimal CNV restricted to the limbal area (Figure 5a−f). The CNV volume was quantified for each group using the IMARIS program. The Axi-NW-treated group exhibited significantly less CNV compared to the untreated control and PVA-NW groups ($P < 0.05$). The Axi-NW is almost twice as effective as Sun-NW and Sor-NW in suppressing the CNV (Figure 5g). Taken together, these results demonstrated the pronounced therapeutic efficacy of the Axi-NW compared to the untreated control group and also the Sun-NW- and Sor-NW-treated mouse groups. On the basis of these results, Axi-NW was selected for further study.

To minimize the drug-related side effects, the maximum tolerated therapeutic dose was determined by conducting a drug escalation study. Administration of maximum tolerated dose is usually associated with maximum clinical benefit. For this study, nanowafers containing 10, 5, and 2.5 μg of axitinib (Axi-10-NW, Axi-5-NW, and Axi-2.5-NW) were fabricated and tested for their therapeutic efficacy in OB mice. Axi-5-NW and Axi-2.5-NW were the most efficacious compared to Axi-10-NW (Supplementary Figure S2). Both Axi-5-NW and Axi-2.5-NW exhibited almost the same efficacy, and the CNV volumes were significantly lower than the OB control group ($P < 0.01$). Slit-lamp examination revealed no changes in macroscopic appearance of the eyelids or the conjunctiva for 15 days during the Axi-5-NW and Axi-2.5-NW treatment and observation periods when compared with the control groups. There were no drug-related adverse effects of the Axi-5-NW and Axi-2.5-NW treatment. However, in the case of Axi-10-NW treatment, a few corneal perforations were observed after day 3. On the basis of this study, Axi-5-NW was selected as the maximum tolerated dose for comparing the efficacy of nanowafer and eye drop drug delivery methods.

Enhanced Therapeutic Efficacy of Axitinib Nanowafer. Because of the physiological barriers of the ocular surface,

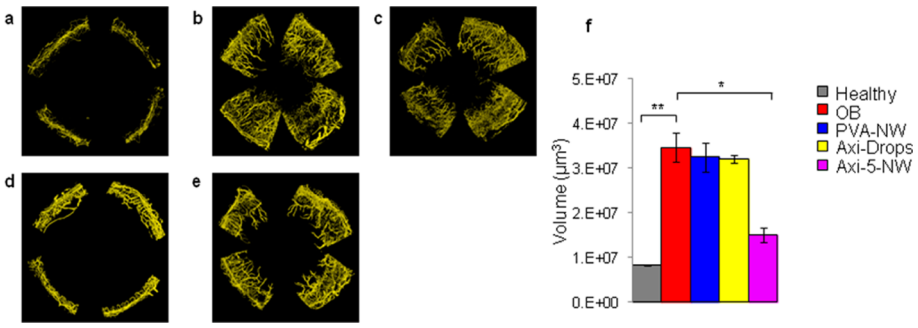

Figure 6. Axitinib nanowafer is more efficacious than the topical eye drop treatment. Representative 3D reconstructed corneal images revealing the enhanced therapeutic efficacy of Axi nanowafer compared to twice a day eye drop treatment. (a) Healthy cornea. (b) OB-induced cornea. (c) PVA-NW. (d) Axi-NW. (e) Twice a day Axi-eye drop (0.1%) treatment. (f) Quantification of corneal neovascularization volume. n = 3 animals, $^*P < 0.05$ *vs* OB control. All error bars represent standard deviation from the mean.

topical eye drops must be applied several times a day for a therapeutic effect, thus increasing the potential for toxic side effects. In this study, once a day Axi-5-NW treatment was compared with Axi eye drops (0.1%) administered twice a day for its therapeutic effect in inhibiting CNV in an OB mouse model. A circular Axi-5-NW was placed on the injured cornea under general anesthesia, daily for 10 days followed by 5 days of observation. On the 15th day, the corneas were collected, processed, and subjected to laser scanning fluorescence confocal microscopy.

The images of whole mount corneas clearly demonstrated a strong therapeutic effect of the Axi-5-NW treatment compared to the untreated OB control group (Figure 6a–e). The Axi-5-NW treatment has restricted the proliferation of blood vessels to the limbal area and very closely resembled the healthy uninjured cornea. However, the OB control, PVA-NW, and Axi eye drop treated corneas exhibited an extensive neovascularization. The new blood vessels were highly branched and extended from the limbal area toward the center of the cornea. In the case of Axi-5-NW treatment, the amount of drug delivered to the cornea was 5 μg per day, and for axitinib eye drop treatment it was 10 μg per day. Although, eye drop treated mice received twice the drug dosage as those treated with Axi-5-NW, still Axi-5-NW treatment was twice as efficacious as the eye drop treatment (Figure 6f). These results confirmed that the controlled drug release from Axi-5-NW is more effective in inhibiting CNV compared to the eye drop treatment even at a lower dosing frequency.

To further compare the efficacy of Axi-5-NW and Axi eye drops at the molecular level, expression levels of the drug target factors VEGF-A, VEGF-R1, VEGF-R2, PDGFR-A, PDGFR-B, TNF-α, bFGF, and TGF-β were measured, in addition to proinflammatory interleukins and proangiogenic matrix metalloproteinases. The Axi-NW was much more effective at suppressing Axi-target genes compared to the untreated OB and Axi-eye drop treatment (Figure 7). The Axi-5-NW also showed significant suppression of proinflammatory cytokine and proangiogenic MMP expression compared to OB alone and Axi-eye drops (Supplementary Figure S3). These results reaffirmed the enhanced efficacy of axitinib when delivered by a nanowafer once a day for 10 days compared to the twice a day topical eye drop treatment for the same period of time.

Axitinib Nanowafer Improves Corneal Wound Healing. The effect of Axi-5-NW on the corneal wound healing process was studied by corneal fluorescein staining. This study revealed that the corneal wound healing was unaffected by the Axi-5-NW treatment, and a normal healing pattern was observed. The rate of epithelial closure of the corneal surface was almost the same in both Axi-5-NW and Axi-eye drop treated groups, and complete corneal surface recovery was observed by the ninth day. However, the OB control and PVA-NW-treated groups demonstrated a slightly slower recovery, and complete healing was observed by the 11th day (Figure 8). These results confirmed that axitinib is nontoxic and did not affect the epithelial recovery of the OB-induced corneas, unlike other antiproliferative agents such as mitomycin C and 5-fluorouracil, which are prone to retarding the corneal epithelial recovery.[41]

CONCLUSIONS

Ocular drug delivery systems aim to deliver the pharmacologic agent at the desired therapeutic concentration to the target ocular tissue without damaging the healthy tissue. In the treatment of ocular disease, however, this aim becomes more challenging because of the protective ocular surface barriers and highly sensitive ocular tissues. The challenge is to delicately circumvent these protective ocular surface barriers and deliver the drug to the target site (cornea or conjunctiva) without causing permanent tissue damage. Despite sustained efforts, the development and optimization of new nano drug delivery systems have been very slow. To improve the therapeutic efficacy of ophthalmic drugs, the drug delivery system

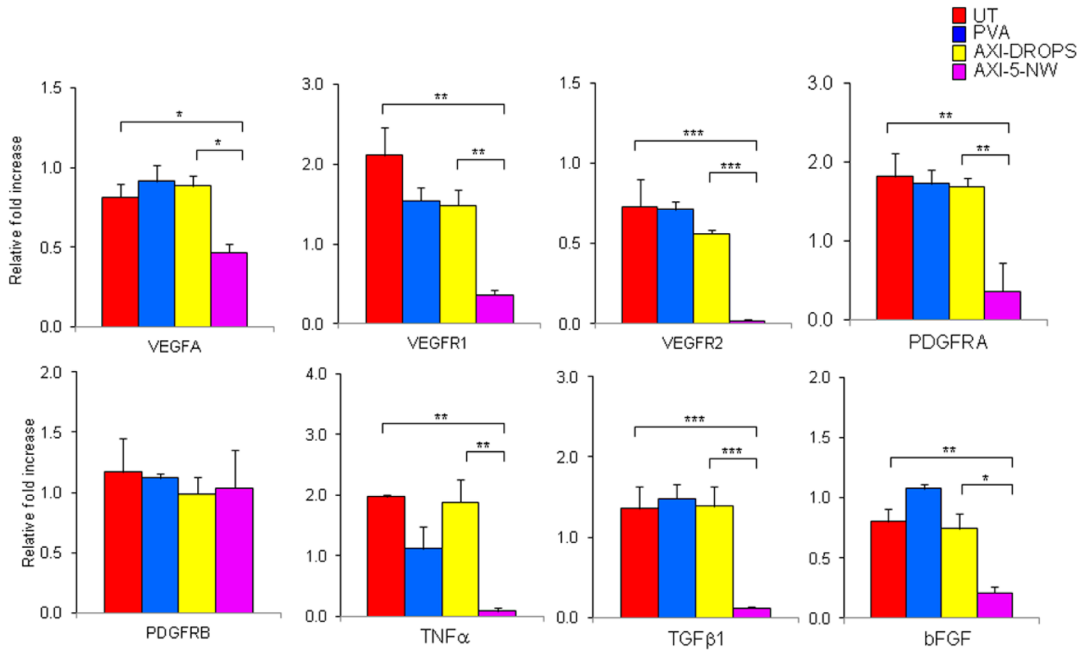

Figure 7. Enhanced therapeutic effect of axitinib nanowafer. RT-PCR analysis revealing the strong suppression of the expression levels of drug target genes by nanowafer compared to twice a day topical axitinib eye drop treatment. $n = 3$ (5 animals per group). *$P < 0.05$, **$P < 0.01$, ***$P < 0.001$. All error bars represent standard deviation from the mean.

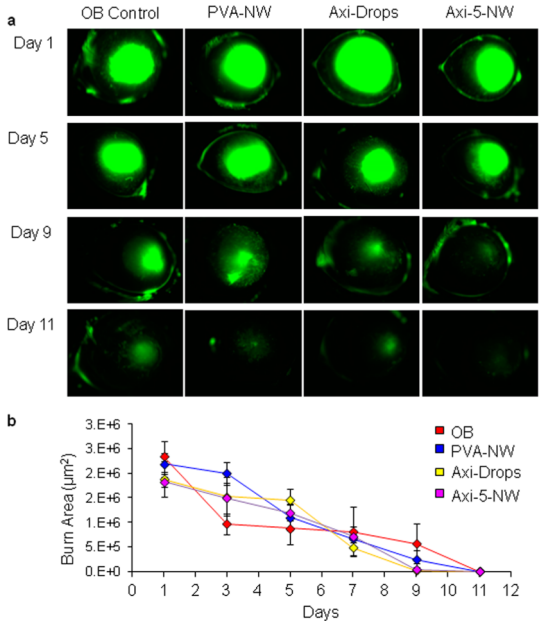

Figure 8. Axitinib nanowafer treatment improves the corneal wound healing after ocular burn injury. (a) Fluorescence images. (b) Plot demonstrating corneal surface healing as a measure fluorescence intensity. $n = 3$ animals. All error bars represent standard deviation from the mean.

should be able to release the drug in a controlled fashion, increase drug residence time on the ocular surface, improve the bioavailability of the drug, and improve the local tolerability of the drug. Also, the issue of patient compliance must be seriously considered in ocular drug delivery. For example, if a drug must be given 4−8 times a day for a week when treating a chronic disease, it is very unlikely to be given in a timely fashion. Therefore, development of a controlled release ocular drug delivery system that can release the drug in therapeutically effective concentrations for a longer duration of time (from a day to a week) is highly desired.

This work presents a nanowafer drug delivery platform involving the seamless integration of nanofabrication and drug delivery technologies. A systematic screening of a series of polymers confirmed that PVA is a nonimmunostimulatory polymer that can be used in the fabrication of ocular drug delivery nanowafers, wherein PVA and the drug axitinib work synergistically. The laser scanning confocal imaging and RT-PCR studies have quantitatively demonstrated the enhanced therapeutic efficacy of the nanowafer in terms of inhibiting neovascularization and improved suppression of proinflammatory and proangiogenic factors in an ocular burn induced mouse model. The nanowafer has demonstrated an enhanced efficacy compared to topically applied eye drop treatment. This study also demonstrated that the enhanced therapeutic efficacy is due to the increased drug residence time on the ocular surface, which subsequently diffused into the ocular tissue for therapeutic action. The additive effects of negligible inflammatory potential, mucoadhesivity, controlled drug release, and the therapeutic potential of the drug support the development of a broadly applicable synergistic nanowafer drug delivery system. Furthermore, the nanowafer, at the end of the stipulated drug release time, will dissolve and fade away. The simplicity and efficiency of the nanowafer drug

delivery system provides a new and novel modality for the noninvasive drug administration to the ocular surface. The nanowafer drug delivery system can deliver a wide range of drugs regardless of molecular weight or chemical properties. Development of a nanowafer drug delivery system that can be readily instilled on the ocular surface by the patient's fingertip without any clinical procedure will be not only very convenient but also most desirable for treating eye injuries, infections, chronic dry eye, glaucoma, and other ocular inflammatory conditions. Since, the polymers and drugs used in the development of the nanowafer are already in clinical use, it can be rapidly translated to the clinic for human trials.

MATERIALS AND METHODS

All animals were treated in accordance with the Association of Research in Vision and Ophthalmology (ARVO) Statement for the Use of Animals in Ophthalmic and Vision Research, and the protocols were approved by the Baylor College of Medicine Institutional Animal Care and Use Committee.

Nanowafer Fabrication. Silicon wafers having wells of 500 nm diameter and 500 nm depth were fabricated by e-beam lithography and dry reactive ion etching following a previously published procedure.[23,24] By using the silicon wafer as a master template, poly(dimethylsiloxane) imprints were fabricated. A clear PVA solution (5% w/v) was prepared by dissolving PVA (5 g) in 100 mL of a water/ethanol mixture (4:6) on a stirring hot plate at 70 °C (RT Elite stirring hot plate, Fisher Scientific) until a clear homogeneous solution was formed. Thus, the prepared PVA solution (5 mL) was transferred with a pipet onto a 3 in. diameter PDMS template containing vertical posts and kept in an oven (Isotemp 500 Series Economy Lab Ovens, Fisher Scientific) at 60 °C for 30 min. This procedure resulted in the formation of PVA nanowafers having 500 nm wells. The 500 nm wells in the PVA nanowafer were filled with Axitinib/PVA solution. The Axitinib/PVA solution was prepared by dissolving Axitinib (100 mg in 250 μL of DMSO) in 750 μL of 5% PVA solution. Thus, the prepared Axitinib/PVA solution (200 μL) was transferred onto a PVA nanowafer (3 in. diameter), swiped with a razor blade to fill the wells, and left at room temperature to evaporate the solvent.[27] The drug-filled hydrogel templates were cut into 2 mm diameter discs with a paper punch. The drug content in 2 mm nanowafers was evaluated by HPLC. The nanowafers thus prepared were used for *in vivo* experiments in mice.

Doxy Nanowafer Instillation, Imaging, and Tear Collection. A nanowafer was placed on top of each cornea with a forceps while observing under a stereomicroscope followed by wetting with 5 μL of balanced salt solution (BSS). The mice were anesthetized by ketamine (100 mg/kg) and xylazine (10 mg/kg) injection. The nanowafers dissolved in approximately half an hour. Since doxycycline is a fluorescent drug, Doxy nanowafers were monitored hourly for 5 h *via* imaging in a stereoscopic zoom microscope (model SMZ 1500; Nikon, Melville, NY, USA), with a fluorescence excitation at 470 nm.

Tear fluid was collected at regular intervals by instilling 2 μL of BSS on the ocular surface. After a few seconds the tears were collected from the conjunctival sac close to the lacrimal punctum.[35] The tear fluid and isotonic solution were collected with a 1 μL volume glass capillary tube (Drummond Scientific, Broomhall, PA, USA) by capillary action from the interior tear meniscus in the lateral canthus. The tear washings from a group of 15 mice were pooled, centrifuged, and stored at −80 °C prior to HPLC analysis to determine the drug concentration.

Intravital Imaging of Doxy Nanowafers. Mice instilled with doxycycline nanowafers after 24 h were anesthetized with ketamine and xyalizine and imaged under a Nikon ECLIPSE intravital microscope (Nikon, Melville, NY, USA). Images were captured with a resolution of 1024 × 768 pixels with X10 Nikon objectives.

HPLC Analysis. HPLC experiments were performed on a Shimadzu Prominence HPLC system. The analytical column was a Kinetex 5uXB-C18 100A (150 mm × 4.6 mm) from Phenomenex. The system was equipped with autosampler, in-line degasser, and column oven set at room temperature. The mobile phase for doxycycline analysis was a mixture of 5% acetic acid (55%) and methanol (45%) (Sigma-Aldrich, St. Louis, MO, USA). Injection volume was 5 μL, the flow rate was 1.0 mL/min, and the pressure was lower than 2500 psi.

Determination of total drug content in a nanowafer: The total amount of a drug loaded in the nanowafer was determined by dissolving an accurately weighed nanowafer in 1 mL of PBS solution, followed by addition of 2 mL of ethanol. The precipitated polymer was removed by centrifugation. The clear solution was filtered through a 0.2 μm syringe filter, analyzed by UV-HPLC, and compared with the standard curve to quantify the total drug content in the nanowafer. This experiment was performed in triplicates.

Study of drug release kinetics of the nanowafers by HPLC analysis: Each sample was filtered through a 0.2 μm syringe filter and subjected to HPLC analysis. The UV detection wavelength for doxycycline was 274 nm. The drug concentration was calculated by comparing the peak area of standards and sample.

Ocular Burn Mouse Model and Nanowafer Treatment. Naive female C57BL/c mice 6 to 8 weeks of age (The Jackson Laboratory, Bar Harbor, ME, USA) were anesthetized with an intraperitoneal injection of the rodent combination anesthesia previously mentioned, combined with topical anesthesia of the right eyes by 0.5% proparacaine. Whatman filter paper (2.5 mm diameter) was briefly soaked in 1 N NaOH solution and then placed on the right corneas for 30 s and then rinsed with 20 mL of BSS. Mice corneas were monitored daily using a slit lamp microscope (model 30-99-49, Zeiss, Oberkochen, Germany) for 14 days, and images were recorded by an attached Nikon D40X digital camera. For treatment, each day a specific nanowafer was placed on top of the ocular burn cornea of an anesthetized mouse corresponding to the treatment group. All mice then received 5 μL of BSS on the ocular burn cornea, including control groups.

Corneal Fluorescein Staining. The extent of corneal wound closure was examined by corneal fluorescein staining. On days 1, 3, 5, 7, 9, and 11 after ocular burn, mice were anesthetized with an intraperitoneal injection of the above-mentioned rodent combination anesthesia. A 1 μL amount of fluorescein (0.1%) was instilled on the ocular burn corneas for 1 min, followed by rinsing with 1 mL of BSS. Images were recorded by a stereoscopic zoom microscope (model SMZ 1500; Nikon), with a fluorescence excitation at 470 nm.

Corneal Whole Mount Staining. Fourteen days after the ocular burn, eyes were enucleated for corneal whole mount staining with some modifications.[42] Briefly, corneas including limbal area were dissected from freshly enucleated eyes, and surrounding conjunctiva, Tenon capsule, uvea, and lens were carefully removed, followed by making four slits with a scalpel blade at 90°, 180°, 270°, and 360° to flatten out the corneas, then fixed in 4% (wt/vol) paraformaldehyde solution at room temperature for 1 h. Tissues were blocked with 10% goat serum and 0.5% Triton X-100 prepared in PBS for 1 h. Rat anti-mouse CD31 antibody (1:300) (BD Biosciences, San Jose, CA, USA) supplemented with 5% goat serum and 0.1% Triton X-100 was added to the tissues and allowed to incubate at 4 °C for 3 days. After a series of washing with PBS and blocking with the above-mentioned solution, the tissues were incubated with Alexa-Fluor 594-conjugated goat anti-rat secondary antibody (Jackson ImmunoResearch, West Grove, PA, USA) in a dark chamber for 1 h at room temperature. The tissues were then mounted on slides using Fluoromount G (Southern Biotech, Birmingham, AL, USA) containing DAPI (1:300) (Life Technologies, Grand Island, NY, USA).

Laser Confocal Fluorescence Imaging and 3D Representations of Whole-Mounted Corneas. Images of whole-mounted corneas were obtained by stitching individual Z-stack images (~11 × 11) acquired in a Nikon Eclipse Ni confocal microscope provided with a 20× objective (Plan APO20X-0.75/OFN25-DIC-N2 by Nikon) and a 561 nm laser (blood vessel detection, red). Each Z-stack was captured using nonresonant galvano scanners, 512 × 512 pixel size, unidirectional scan, 0.5 scan speed, 2.2 pixel dwell, 0.9 μm Z-space, and 19.2 μm pinhole size. Images were stitched by NIS Elements software, and some of them were deconvolved in the NIS Deconvolution module in order to improve the signal. Images were further processed with IMARIS 7.7.2 (Bitplane AG, Zurich, Switzerland) software for 3D representations and volume calculations. Confocal images were masked using the surpass mode, and the surface function set it up with 3.0 μm surface grain size and 10 μm for the diameter of the largest sphere parameters. The thresholds were adjusted manually for each image. Blood vessel volumes of the 3D representations were calculated using the Statistic function. Data in figures are shown as mean ± SEM of each treatment repeated in triplicates. Statistical significance of comparison of mean values was assessed by one-way-ANOVA followed by Tukey's test for multiple comparisons. Mean differences of the groups were considered significant at $^{*}P < 0.05$, $^{**}P < 0.01$, and $^{***}P < 0.001$.

Quantitative Reverse Transcription–Polymerase Chain Reaction. Mice were sacrificed 5 days after OB with different treatment. After enucleating, corneas were excised and dissected from surrounding conjunctiva and uvea. Pools of five corneas were prepared in triplicate for each treating group. RNA was extracted by a previously reported procedure with RNeasy MicroKit columns (Qiagen, Valencia, CA, USA).[43] Samples were treated with DNase (Qiagen) and stored at −80 °C. The first-strand cDNA was synthesized from 1.0 μg of RNA with Ready-To-Go You-Prime First-Strand Beads (GE Healthcare, Princeton, NJ, USA) and random hexamers (Applied Biosystems, Foster City, CA, USA). RT-PCR was performed using TaqMan Gene Expression Master Mix and Assays (Applied Biosystems). Specific primers from Applied Biosystems were used to quantify gene expression levels. The threshold cycle for each target mRNA was normalized to glyceraldehyde-3-phosphate dehydrogenase mRNA and averaged. Three groups of five-cornea pools were processed for each group.

Conflict of Interest: The authors declare no competing financial interest.

Supporting Information Available: Slit-lamp images of the ocular burn induced corneas demonstrating the therapeutic effect of the drug nanowafers on corneal neovascularization; drug escalation study to determine the maximum tolerated drug dose in the nanowafer; and the PCR data demonstrating the nonimmunogenic nature of the Axi nanowafer. This material is available free of charge *via* the Internet at http://pubs.acs.org.

Acknowledgment. This work was supported by a grant from the Department of Defense (Award No. 1W81XWH-13-1-0146).

REFERENCES AND NOTES

1. Eye health statistics at a glance. Compiled by American Academy of Ophthalmology. April 2011. http://www.aao.org/newsroom/upload/Eye-Health-Statistics-April-2011.pdf.
2. Azar, D. T. Corneal Angiogenic Privilege: Angiogenic and Antiangiogenic Factors in Corneal Avascularity, Vasculogenesis, and Wound Healing. *Trans. Am. Ophthalmol. Soc.* **2006**, *104*, 264–302.
3. Urtti, A. Challenges and Obstacles of Ocular Pharmacokinetics and Drug Delivery. *Adv. Drug Delivery Rev.* **2006**, *58*, 1131–1135.
4. Novack, G. D. Ophthalmic Drug Delivery: Development and Regulatory Considerations. *Clin. Pharmacol. Ther.* **2009**, *85*, 539–543.
5. Kim, Y. C.; Chiang, B.; Wu, X.; Prausnitz, M. R. Ocular Delivery of Macromolecules. *J. Controlled Release* **2014**, *190*, 172–181.
6. Mannermaa, E.; Vellonen, K.-S.; Urtti, A. Drug Transport in Corneal Epithelium and Blood–Retina Barrier: Emerging Role of Transporters in Ocular Pharmacokinetics. *Adv. Drug Delivery Rev.* **2006**, *58*, 1136–1163.
7. Salminen, L. Review: Systemic Absorption of Topically Applied Ocular Drugs in Humans. *J. Ocul. Pharmacol.* **1990**, *6*, 243–249.
8. Baudouin, C. Side Effects of Antiglaucomatous Drugs on the Ocular Surface. *Curr. Opin. Ophthalmol.* **1996**, *7*, 80–86.
9. Topalkara, A. C.; Guler, C.; Arici, D. S.; Arici, M. K. Adverse Effects of Topical Antiglaucoma Drugs on the Ocular Surface. *Clin. Exp. Ophthalmol.* **2000**, *28*, 113–117.
10. Hoffart, L.; Matonti, F.; Conrath, J.; Daniel, L.; Ridings, B.; Masson, G. S.; Chavane, F. Inhibition of Corneal Neovascularization after Alkali Burn: Comparison of Different Doses of Bevacizumab in Monotherapy or Associated with Dexamethasone. *Clin. Exp. Ophthalmol.* **2010**, *38*, 346–352.
11. Mello, G. R.; Pizzolatti, M. L.; Wasilewski, D.; Santhiago, M. R.; Budel, V.; Moreira, H. The Effect of Subconjunctival Bevacizumab on Corneal Neovascularization, Inflammation and Re-epithelization in a Rabbit Model. *Clinics* **2011**, *66*, 1443–1449.
12. Diebold, Y.; Calonge, M. Applications of Nanoparticles in Ophthalmology. *Prog. Retina Eye Res.* **2010**, *29*, 596–609.
13. Gershkovich, P.; Wasan, K. M.; Barta, C. A. A Review of the Application of Lipid-Based Systems in Systemic, Dermal, Transdermal, and Ocular Drug Delivery. *Crit. Rev. Ther. Drug* **2008**, *25*, 545–584.
14. Choy, Y. B.; Park, J.-H.; McCarey, B. E.; Edelhauser, H. F.; Prausnitz, M. R. Mucoadhesive Microdiscs Engineered for Ophthalmic Drug Delivery: Effect of Particle Geometry and Formulation on Preocular Residence Time. *Invest. Ophthalmol. Vis. Sci.* **2008**, *49*, 4808–4815.
15. Chang, E.; McClellan, A. J.; Farley, W. J.; Li, D.-Q.; Pflugfelder, S. C.; De Paiva, C. Biodegradable PLGA-Based Drug Delivery Systems for Modulating Ocular Surface Disease under Experimental Murine Dry Eye. *J. Clin. Exp. Ophthalmol.* **2011**, *2*, 191.
16. He, C.; Kim, S. W.; Lee, D. S. *In Situ* Gelling Stimuli-Sensitive Block Copolymer Hydrogels for Drug Delivery. *J. Controlled Release* **2008**, *127*, 189–207.
17. Gulsen, D.; Chauhan, A. Ophthalmic Drug Delivery through Contact Lenses. *Invest. Ophthalmol. Vis. Sci.* **2004**, *45*, 2342–2347.
18. Singh, K.; Nair, A. B.; Kumar, A.; Kumria, R. Novel Approaches in Formulation and Drug Delivery using Contact Lenses. *J. Basic Clin. Pharm.* **2011**, *2*, 87–101.
19. Shin, Y. J.; Hyon, J. Y.; Choi, W. S.; Yi, K.; Chung, E.-S.; Chung, T.-Y.; Wee, W. R. Chemical Injury-Induced Corneal Opacity and Neovascularization Reduced by Rapamycin *via* TGF-β1/ERK Pathways Regulation. *Invest. Ophthalmol. Vis. Sci.* **2013**, *54*, 4452–4458.
20. Ludwig, A. The Use of Mucoadhesive Polymers in Ocular Drug Delivery. *Adv. Drug Delivery Rev.* **2005**, *57*, 1595–1639.
21. Moshirfar, M.; Pierson, K.; Hanamaikai, K.; Santiago-Caban, L.; Muthappan, V.; Passi, S. F. Artificial Tears Potpourri: A Literature Review. *Clin. Ophthalmol.* **2014**, *8*, 1419–1433.
22. Aragona, P.; Spinella, R.; Rania, L.; Postorino, E.; Sommario, M. S.; Roszkowska, A. M.; Puzzolo, D. Safety and Efficacy of 0.1% Clobetasone butyrate Eyedrops in the Treatment of Dry Eye in Sjögren Syndrome. *Eur. J. Ophthalmol.* **2013**, *23*, 368–376.
23. Acharya, G.; Shin, C. S.; McDermott, M.; Mishra, H.; Park, H.; Kwon, I. C.; Park, K. The Hydrogel Template Method for Fabrication of Homogeneous Nano/Micro Particles. *J. Controlled Release* **2010**, *141*, 314–319.
24. Acharya, G.; Shin, C. S.; Vedantham, K.; McDermott, M.; Rish, T.; Hansen, K.; Fu, Y.; Park, K. A Study of Drug Release from Homogeneous PLGA Microstructures. *J. Controlled Release* **2010**, *146*, 201–206.
25. Streilein, J. W. Ocular Immune Privilege: The Eye Takes a Dim but Practical View of Immunity and Inflammation. *J. Leukoc. Biol.* **2003**, *74*, 179–185.
26. Sivak, J. M.; Ostriker, A. C.; Woolfenden, A.; Demirs, J.; Cepeda, R.; Long, D.; Anderson, K.; Jaffee, B. Pharmacologic

Uncoupling of Angiogenesis and Inflammation During Initiation of Pathological Corneal Neovascularization. *J. Biol. Chem.* **2011**, *286*, 44965–44975.
27. Dobrovolskaia, M. A.; Mcneil, S. E. Immunological Properties of Engineered Nanomaerials. *Nat. Nanotechnol.* **2007**, *2*, 469–478.
28. Zolinik, B. S.; Gonzalez-Fernandez, A.; Sadrieh, N.; Dobrovolskaia, M. A. Nanoparticles and the Immune System. *Endocrinology* **2010**, *151*, 458–465.
29. Smith, D. M.; Simon, J. K.; Baker, J. R., Jr. Applications of Nanotechnology for Immunology. *Nat. Rev. Immunol.* **2013**, *13*, 592–605.
30. Barrientos, S.; Stojadinovic, O.; Golinko, M. S.; Brem, H.; Tomic-Canic, M. Growth Factors and Cytokines in Wound Healing. *Wound Rep. Reg.* **2008**, *16*, 585–601.
31. Qazi, Y.; Maddula, S.; Ambati, B. K. Mediators of Ocular Angiogenesis. *J. Genet.* **2009**, *88*, 495–515.
32. Ellenberg, D.; Azar, D. T.; Hallak, J. A.; Tobaigy, F.; Han, K. Y.; Jain, S.; Zhou, Z.; Chang, J.-H. Novel Aspects of Corneal Angiogenic and Lymphangiogenic Privilege. *Prog. Retinal Eye Res.* **2010**, *29*, 208–248.
33. Maddula, S.; Davis, D. K.; Maddula, S.; Burrow, M. K.; Ambati, B. K. Horizons in Therapy for Corneal Angiogenesis. *Ophthalmology* **2011**, *118*, 591–599.
34. Liss, R. H.; Norman, J. C. Visualization of Doxycycline in Lung Tissue and Sinus Secretions by Fluorescent Techniques. *Chemotherapy* **1975**, *21* (Suppl 1), 27–35.
35. Corrales, R. M.; Villarreal, A.; Farley, W.; Stern, M. E.; Li, D.-Q.; Pflugfelder, S. C. Strain-Related Cytokine Profiles on the Murine Ocular Surface in Response to Desiccating Stress. *Cornea* **2007**, *26*, 579–584.
36. Shawver, L. K.; Slamon, D.; Ullrich, A. Smart Drugs: Tyrosine Kinase Inhibitors in Cancer Therapy. *Cancer Cell* **2002**, *1*, 117–123.
37. Ribatti, D. Tyrosine Kinase Inhibitors as Antiangiogenic Drugs in Multiple Myeloma. *Pharmaceuticals* **2010**, *3*, 1225–1231.
38. Motzer, R. J.; Hutson, T. E.; Tomczak, P.; Michaelson, M. D.; Bukowski, R. M.; Rixe, O.; Oudard, S.; Negrier, S.; Szczylik, C.; Kim, S. T.; *et al*. Sunitinib *versus* Interferon *alfa* in Metastatic Renal Cell Carcinoma. *N. Engl. J. Med.* **2007**, *356*, 115–124.
39. Escudier, B.; Eisen, T.; Stadler, W. M.; Szczylik, C.; Oudard, S.; Siebels, M.; Negrier, S.; Chevreau, C.; Solska, E.; Desai, A. A.; *et al*. Sorafenib in Advanced Clear-Cell Renal-Cell Carcinoma. *N. Engl. J. Med.* **2007**, *356*, 125–134.
40. Gross-Goupil, M.; Francois, L.; Quivy, A.; Ravaud, A. Axitinib: A Review of its Safety and Efficacy in the Treatment of Adults with Advanced Renal Cell Carcinoma. *Clin. Med. Insights Oncol.* **2013**, *7*, 269–277.
41. Ando, H.; Ido, T.; Kawai, Y.; Yamamoto, T.; Kitazawa, Y. Inhibition of Corneal Epithelial Wound Healing: A Comparative Study of Mitomycin C and 5-Fluorouracil. *Ophthalmology* **1992**, *99*, 1809–1814.
42. Cao, R.; Lim, S.; Ji, H.; Zhang, Y.; Yang, Y.; Honek, J.; Hedlund, E.-M.; Cao, Y. Mouse Corneal Lymphangiogenesis Model. *Nat. Protoc.* **2011**, *6*, 817–826.
43. Yuan, X.; Mitchell, B. M.; Wilhelmus, K. R. Expression of Matrix Metalloproteinases during Experimental Candida albicans keratitis. *Invest. Ophthalmol. Vis. Sci.* **2009**, *50*, 737–742.

Appendix 2: Journal publication

Coursey et al, Dexamethasone nanowafer as an effective therapy for dry eye disease, *J. Control Release*. **213**, 168–174 (2015).

Journal of Controlled Release 213 (2015) 168–174

Contents lists available at ScienceDirect

Journal of Controlled Release

journal homepage: www.elsevier.com/locate/jconrel

Dexamethasone nanowafer as an effective therapy for dry eye disease

Terry G. Coursey [1], Johanna Tukler Henriksson [1], Daniela C. Marcano, Crystal S. Shin, Lucas C. Isenhart, Faheem Ahmed, Cintia S. De Paiva, Stephen C. Pflugfelder, Ghanashyam Acharya *

Ocular Surface Center, Department of Ophthalmology, Baylor College of Medicine, Houston, TX 77030, United States

ARTICLE INFO

Article history:
Received 9 April 2015
Received in revised form 16 June 2015
Accepted 3 July 2015
Available online 13 July 2015

Keywords:
Nanowafer
Drug delivery
Dry eye
Cornea
Dexamethasone
Inflammation

ABSTRACT

Dry eye disease is a major public health problem that affects millions of people worldwide. It is presently treated with artificial tear and anti-inflammatory eye drops that are generally administered several times a day and may have limited therapeutic efficacy. To improve convenience and efficacy, a dexamethasone (Dex) loaded nanowafer (Dex-NW) has been developed that can release the drug on the ocular surface for a longer duration of time than drops, during which it slowly dissolves. The Dex-NW was fabricated using carboxymethyl cellulose polymer and contains arrays of 500 nm square drug reservoirs filled with Dex. The in vivo efficacy of the Dex-NW was evaluated using an experimental mouse dry eye model. These studies demonstrated that once a day Dex-NW treatment on alternate days during a five-day treatment period was able to restore a healthy ocular surface and corneal barrier function with comparable efficacy to twice a day topically applied dexamethasone eye drop treatment. The Dex-NW was also very effective in down regulating expression of inflammatory cytokines (TNF-α, and IFN-γ), chemokines (CXCL-10 and CCL-5), and MMP-3, that are stimulated by dry eye. Despite less frequent dosing, the Dex-NW has comparable therapeutic efficacy to topically applied Dex eye drops in experimental mouse dry eye model, and these results provide a strong rationale for translation to human clinical trials for dry eye.

1. Introduction

Dry eye is one of the most common eye diseases that affects approximately 30–40 million people in the United States alone and represents a major public health problem [1,2]. It is accompanied by eye irritation, blurred vision, light sensitivity, and ocular surface epithelial disease [3,4]. Also, it is one of the primary causes for clinical visits and approximately 30% of patients report symptoms of mild or chronic dry eye disease [5–7]. The causative factors include inflammation, hormonal imbalance, and aging. In addition, dry eye is a common complication of LASIK surgery [8,9]. A steady growth in computer screen-related visually demanding tasks and contact lens use can exacerbate dry eye [3,10]. Many of these causative factors adversely impact one or more components of the lacrimal functional unit including the ocular surface, lacrimal glands, meibomian glands, and the interconnecting neural network [11,12]. Mild dry eye is primarily treated with artificial tear drops that hydrate and lubricate the eye, do not have any pharmacologic activity, and provide only temporary relief [13,14]. Chronic dry eye is associated with inflammation that often responds to topically applied corticosteroids and cyclosporine-A eye drops [15–17]. Because of the rapid clearance, eye drops must be administered several times in a day resulting in a high-and-low drug concentration profile and potentially toxic side effects [18,19]. Also, frequent dosing is inconvenient and can cause discomfort that can compromise compliance. To address these issues, several new strategies have been developed [20]. Recently, nanoparticle formulations have been used in ocular drug delivery [21–24]. The rapid clearance of these formulations from the eye contributed to their limited drug efficacy. As another advancement, drug soaked contact lenses were developed [25–27]. These contact lenses released the drug very rapidly. Despite these methodological advances, controlled delivery of drugs in therapeutically effective concentration to tissues in the anterior segment of the eye, such as cornea and conjunctiva, is still very inefficient. These limitations have lead to a call for the development of a novel nanowafer therapeutic with extended release attributes and enhanced efficacy to treat dry eye disease.

The nanowafer is a tiny disc-like or rectangular membrane that contains drug loaded nano-reservoirs (Fig. 1). The nanowafer can be readily applied on the eye by the patient's finger tip without any clinical procedure (Fig. 1). Although, instillation of drug solution or nanoparticle suspension as topical eye drop formulation is the simplest mode of ocular drug delivery, application of a nanowafer on the eye is as easy as applying a contact lens. The nanowafer, after its instillation on the ocular surface, can release the drug for a longer duration of time than eye drops, thus improving its therapeutic efficacy. During the course of the drug release, the nanowafer slowly dissolves. In this study, hydrogel-forming carboxymethyl cellulose (CMC) polymer was chosen for the nanowafer fabrication because of its water solubility, mucoadhesiveness, and use as an active ingredient in artificial tear eye drops [28,29]. The mucoadhesive

* Corresponding author.
E-mail address: gacharya@bcm.edu (G. Acharya).
[1] These authors contributed equally.

http://dx.doi.org/10.1016/j.jconrel.2015.07.007
0168-3659/

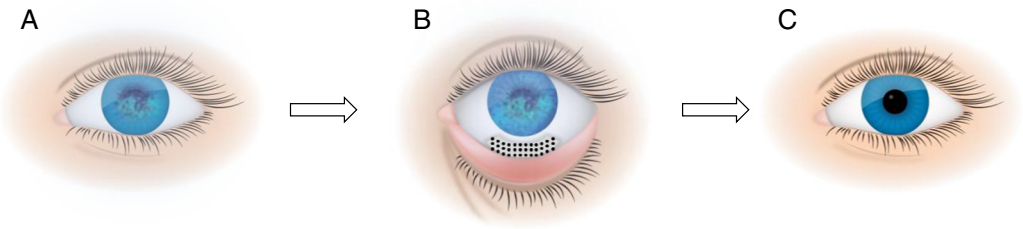

Fig. 1. Schematic of the nanowafer drug delivery to treat dry eye disease. (A) dry eye; (B) instillation of a nanowafer on the conjunctiva; and (C) restoration of a healthy cornea.

property of CMC facilitates quick adhesion and retention of the nanowafer on the ocular surface to withstand reflex tearing and blinking without being displaced. Furthermore, CMC stimulates re-epithelialization of the cornea through its binding to the matrix proteins [30]. The nanowafer contains arrays of nano-reservoirs that are filled with a glucocorticosteroid dexamethasone (Dex). Dex was chosen to fill the nanowafers because of its potent anti-inflammatory properties and has well documented efficacy for treating ocular inflammation [31]. It inhibits the production of inflammatory cytokines, chemokines, and decreases the synthesis of matrix metalloproteinase MMP-3, in addition to other factors [32]. Dex has been successfully used to treat dry eye related corneal epithelial diseases [33].

2. Materials and methods

2.1. Materials

Sodium carboxymethyl cellulose (CMC, MW 90,000) and HPLC solvents (acetonitrile) were obtained from Sigma Aldrich. USP grade dexamethasone sodium phosphate (Dex) was obtained from Spectrum Chemicals. PCR reagents and Oregon Green Dextran (72 KDa) were purchased from Life Technologies.

2.2. Animals

All animals were treated in accordance with the Association of Research in Vision and Ophthalmology (ARVO) Statement for the Use of Animals in Ophthalmic and Vision Research, and the protocols were approved by the Baylor College of Medicine Institutional Animal Care and Use Committee. Female C57/BL6 mice (6–8 weeks old) were purchased from the Jackson Laboratory.

2.3. Nanowafer fabrication

The nanowafers were fabricated according to a previously published procedure with slight modifications [34–36]. A clear CMC solution (4% w/v, 12 mL) was transferred with a pipette onto a polydimethylsiloxane (PDMS) imprint (3″ diameter) containing square posts (of 500 nm × 500 nm, 500 nm high) placed on a flat glass plate and left to dry at room temperature. Thus formed CMC nanowafer was carefully peeled away from the PDMS imprint. The concentration of the polymer solution can be varied to obtain the required thickness of the nanowafer. The CMC nanowafer obtained was ~3″ diameter, ~75 μm thick, and has arrays of wells (500 nm × 500 nm, 500 nm deep).

The CMC wafers were filled with Dex by transferring a thick solution of dexamethasone-CMC with micropipet onto the nanowafer followed by gently swiping with a Teflon swiper. A similar procedure was used for filling the CMC wafers with fluorescein (a green fluorescent dye). The drug or dye filled wells are open on one side of the nanowafer. The open face of the nanowafer was placed in direct contact with the ocular surface, so that the drug molecules can directly diffuse into the ocular tissue. The drug/dye filled nanowafers were punched into 2 mm diameter discs and used in the in vitro and in vivo experiments. Each 2 mm diameter nanowafer contained 5.027×10^5 wells.

2.4. In vitro drug release study

Accurately weighed Dex-NWs were placed inside dialysis tubes (MWCO 2000). Each loaded dialysis tube was placed inside a 5 mL Eppendorf tube containing phosphate buffered saline solution (PBS, pH 7.4) and constantly shaken at 37 °C. Aliquots were obtained at different time points and analyzed using a Shimadzu Prominence UV–HPLC system with a Kinetex 5uXB-C18 100A (150 mm × 4.6 mm) column from Phenomenex. Fresh PBS was added to replace the aliquot extracted. Each sample was filtered through a 0.2 μm syringe filter, and drug concentration was calculated by comparing the peak area of standards and sample detected at 240 nm. The UV–HPLC system was equipped with autosampler, in line degasser, and column oven set at room temperature. The mobile phase for Dex analysis was a mixture of 0.1 M monosodium phosphate (90%) at pH 4.6 and acetonitrile (10%). Injection volume was 5 μL, the flow rate was 0.8 mL/min, and the pressure was lower than 2500 psi. The total drug content in the nanowafer was determined by dissolving an accurately weighed nanowafer in 1 mL PBS solution and 2 mL of ethanol to precipitate the polymer. The suspension was centrifuged to remove the polymer. The clear solution was filtered through a 0.2 μm syringe filter followed by UV–HPLC analysis. The total drug content in the nanowafer was quantified by comparing with the standard curve. This experiment was performed in triplicates.

2.5. Dex-NW instillation and tear collection

Female C57/BL6 mice were anesthetized with an intraperitoneal injection of ketamine (100 mg/kg) and xylazine (10 mg/kg). The mice were treated with either one Dex-NW containing 10 μg of Dex placed on inferior bulbar conjunctiva or 2 μL eye drops (containing 10 μg of Dex in 2 μL of 0.1% CMC solution). Tear fluid was collected at regular intervals. 2 μL of balanced salt solution (BSS) was instilled on the ocular surface, after a few seconds, the tears, mixed with the isotonic solution, were collected from the conjunctival sac close to the lateral canthus with a 1 μL volume glass capillary tube (Drummond Scientific). The tear washings from a group of 15 mice were pooled, centrifuged, and stored at −80 °C prior to drug quantification. UV–HPLC analysis was performed following the same parameters established for the in vitro experiments except, using 10 μL as the injection volume.

2.6. Experimental mouse dry eye model

Desiccating stress (DS) was used to induce experimental dry eye in female C57/BL6 mice, six to eight weeks of age, by subcutaneous injection of 0.5 mg/0.2 mL scopolamine hydrobromide (Sigma Aldrich) into alternating hindquarters administered four times a day (8:30 a.m., 11 a.m., 1 p.m. and 4:30 p.m.) to inhibit tear secretion, exposure to an air draft, and <30% ambient humidity. Mice were euthanized after five days of desiccating stress (DS) treatment [37]. A group of age- and gender-matched mice that were housed in normal environmental conditions were used as non-stressed (NS) controls.

2.7. Evaluation of corneal smoothness

Reflected images of a white ring from the fiber-optic ring illuminator of the stereoscopic zoom microscope (SMZ 1500; Nikon) were obtained immediately after euthanasia. This ring light is firmly attached and surrounds the bottom of the microscope objective. Because the illumination path is nearly coincident with the optical axis of the microscope, the viewing area is evenly illuminated and nearly shadowless. The projected ring light will reflect off a wet surface and the regularity of the reflected ring depends on the smoothness of the ocular surface [38–40].

2.8. Corneal barrier function measurement

On the morning of the fifth day of DS, corneal staining was measured by Oregon Green Dextran (OGD). 0.5 μL of OGD was instilled on the cornea of both eyes and the mouse was left in the dark for 1 min before euthanization. The eyes were then washed with 2 mL of BSS. Excess liquid was blotted off the eye with tissue paper and digital images were captured and the mean fluorescence intensity within a 2 mm central corneal ring was measured with NIS Elements (Nikon). The data are presented as mean ± SEM of fluorescence gray levels from three independent experiments using 5 mice per group per experiment [38].

2.9. RNA isolation and real time RT-PCR

The corneal epithelium was scraped off with a scalpel and the tissue was collected for PCR analysis. Total RNA from corneal epithelium was isolated using a QIAGEN RNeasy Plus Micro RNA isolation kit (Qiagen) following the manufacturer's protocol. After isolation, the concentration of RNA was measured and cDNA was synthesized using the Ready-To-Go™ You-Prime First-Strand kit (GE Healthcare). Real time PCR was performed using specific Taqman probes for MMP-3 ((*Mmp3*) (Mm00440295_m1)), CCL-5 ((Ccl5) (Mm00445235-m1)), CXCL-10 (Cxcl10) (Mm01302427_m1), TNF-α ((*Tnfa*) (OriGene MP217748)), and IFN-γ ((*Ifng*) (Mm00801778_m1)) genes (Taqman Universal PCR Master Mix AmpErase UNG) in a commercial thermocycling system (StepOnePlus™ Real-Time PCR System, Applied Biosystems) according to the manufacturer's recommendations. The results were analyzed by the comparative threshold cycle method and normalized by beta 2 microglobulin (B2M) as the control.

2.10. Statistical analysis

Prism 6.0 software (GraphPad Software Inc.) was used for statistical analysis. One-way analysis of variance (ANOVA) was used to determine overall differences among groups, followed by a post-hoc test (Tukey's post hoc). An unpaired *t*-test is used to evaluate statistical differences between 2 experimental groups. The statistical significance was considered to be $P \leq 0.05$ and data are presented as mean ± SEM.

3. Results and discussion

In this article, we describe the development of a nanowafer therapeutic and demonstrate its in vivo efficacy in an experimental mouse dry eye model (dry eye mice) [37,38]. The nanowafers were fabricated

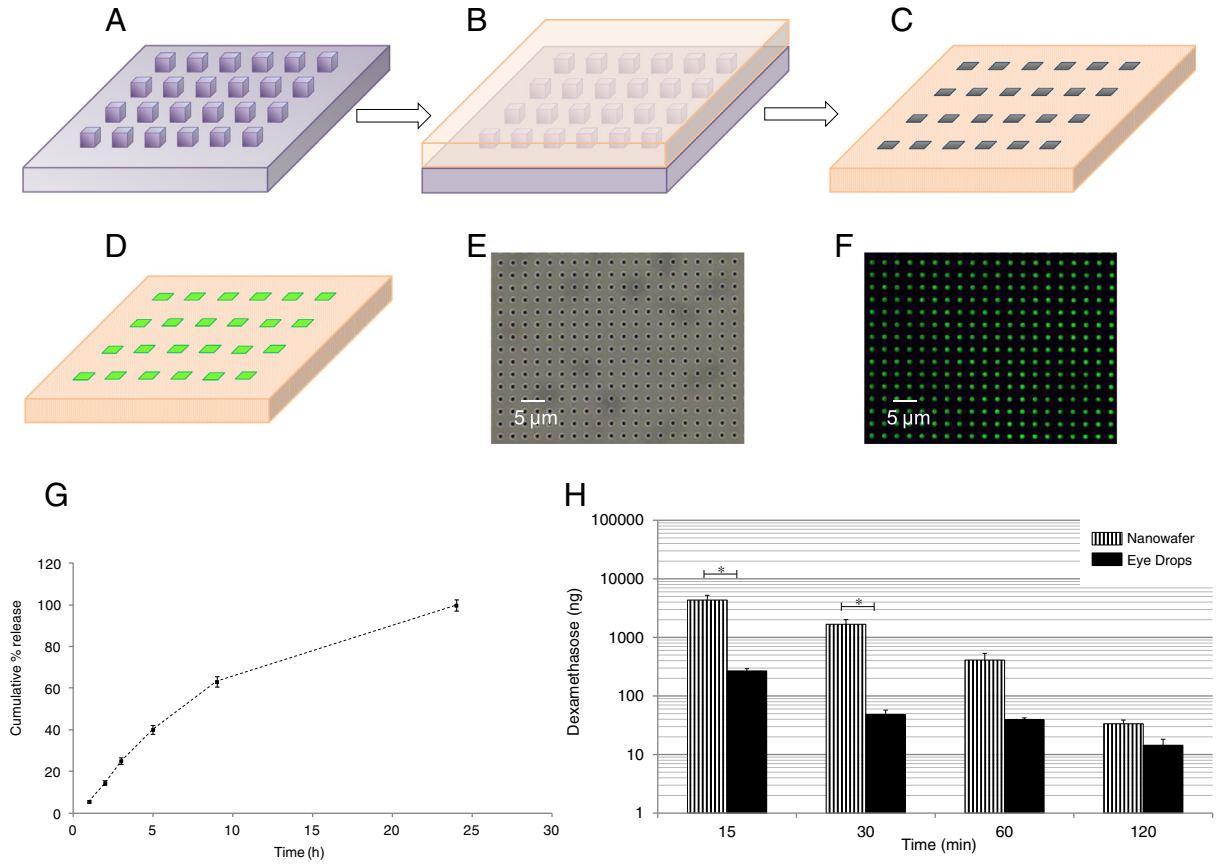

Fig. 2. Nanowafer fabrication and the drug release from Dex nanowafer. Fabrication of nanowafer by hydrogel template strategy: (A) a PDMS template containing vertical posts; (B) preparation of a CMC imprint of the PDMS template; (C) a CMC nanowafer; (D) a CMC nanowafer filled with drug/dye; (E) bright field image of a CMC nanowafer; (F) fluorescence image of a CMC nanowafer filled with fluorescein. Dex release from a nanowafer: (G) In vitro drug release profile; and (H) Dex concentration measured in tear samples collected from eyes treated with Dex-NW or Dex eye drops. *$P < 0.05$.

by hydrogel template strategy [34–36]. A schematic of the nanowafer fabrication procedure has been presented in Fig. 2A–F. Carboxymethyl cellulose (CMC) was chosen for the nanowafer fabrication because of its water solubility, mucoadhesiveness, and use as a constituent in artificial tear eye drops [28–30]. The nanowafer contains arrays of wells that were filled with a glucocorticosteroid dexamethasone (Dex, MW = 392 g/mol). For conducting in vivo studies in dry eye mice, 2 mm diameter nanowafers were fabricated to be placed on the conjunctiva.

The Dex loaded nanowafers (Dex-NW) were examined for their in vitro drug release kinetics by HPLC. The total Dex content in the Dex-NW was 10 μg. The initial release after 5 h was ~40% and the drug release continued for 24 h (Fig. 2G). To assess the drug release from the Dex-NW after its instillation on the conjunctiva, tear samples were collected at hourly intervals and analyzed for Dex concentration by HPLC. This study revealed the presence of Dex in tear samples for up to 2 h at significantly greater concentrations than eyes treated with Dex eye drops containing the same amount (10 μg in 2 μl) of the drug (Fig. 2H). Also, in the case of Dex release from the nanowafer, more drug was present in the first hour tear samples compared to the second hour samples. Because of the ocular surface barriers, such as reflex tearing and tight epithelial junctions, the drug diffusion into the cornea is very slow in the beginning, hence more drug was present in the first hour tear samples. However, with longer drug residence time provided by the nanowafer, more drug penetrates into the cornea. This results in a decrease in drug concentration in the tear samples collected at later time points.

To study the efficacy of the nanowafer in improving the drug molecular residence time on the ocular surface and its subsequent diffusion into it, fluorescein (a green fluorescent dye, MW = 332 g/mol) loaded nanowafers (Flo-NW) were fabricated. The Flo-NWs were instilled on the corneas of healthy mice and were examined by fluorescence imaging at every hour for 5 h. The ocular surface was initially non-fluorescent (Fig. 3A). After the placement of a nanowafer, the fluorescein molecules were slowly released on the cornea and green fluorescence was observed. Since, the fluorescein released from the nanowafer is in direct contact with the cornea, most of the drug will be able to penetrate into it. After 4 h, the green fluorescence of the cornea started to fade because of the diffusion of fluorescein molecules into the anterior chamber and its clearance by tear secretion (Fig. 3B–G). Once the fluorescein molecules pass through the cornea and reach the aqueous humor in the anterior chamber, they are cleared through the trabecular meshwork. In comparison, eyes treated with fluorescein eye drops were non-fluorescent after 5 min, indicating its rapid clearance from the ocular surface (Fig. 3H–L). Also, after instillation of the fluorescein drops on the eye, within a few minutes, most of it is concentrated on the eye lids, indicating its clearance from the ocular surface, compared to the nanowafer drug release, wherein only a small amount of fluorescein concentrated around the eyelids and most of it in the eye. This study has qualitatively demonstrated the ability of nanowafer to release the drug for a few hours thus improving the drug residence time on the cornea.

The in vivo efficacy of Dex-NW was evaluated in dry eye mice. A Dex-NW was placed on the inferior bulbar conjunctiva of a mouse (on days 1 and 3) that was subjected to desiccating stress for five days with no topical treatment. The efficacy of the Dex-NW was evaluated by corneal smoothness, corneal barrier function, and expression of pro-inflammatory cytokines, chemokines, and MMPs and compared with control CMC-NW (without Dex) treated and untreated dry eye mouse groups.

Chronic dry eye disease can desiccate the ocular surface and create corneal epithelial erosions that alter corneal smoothness and

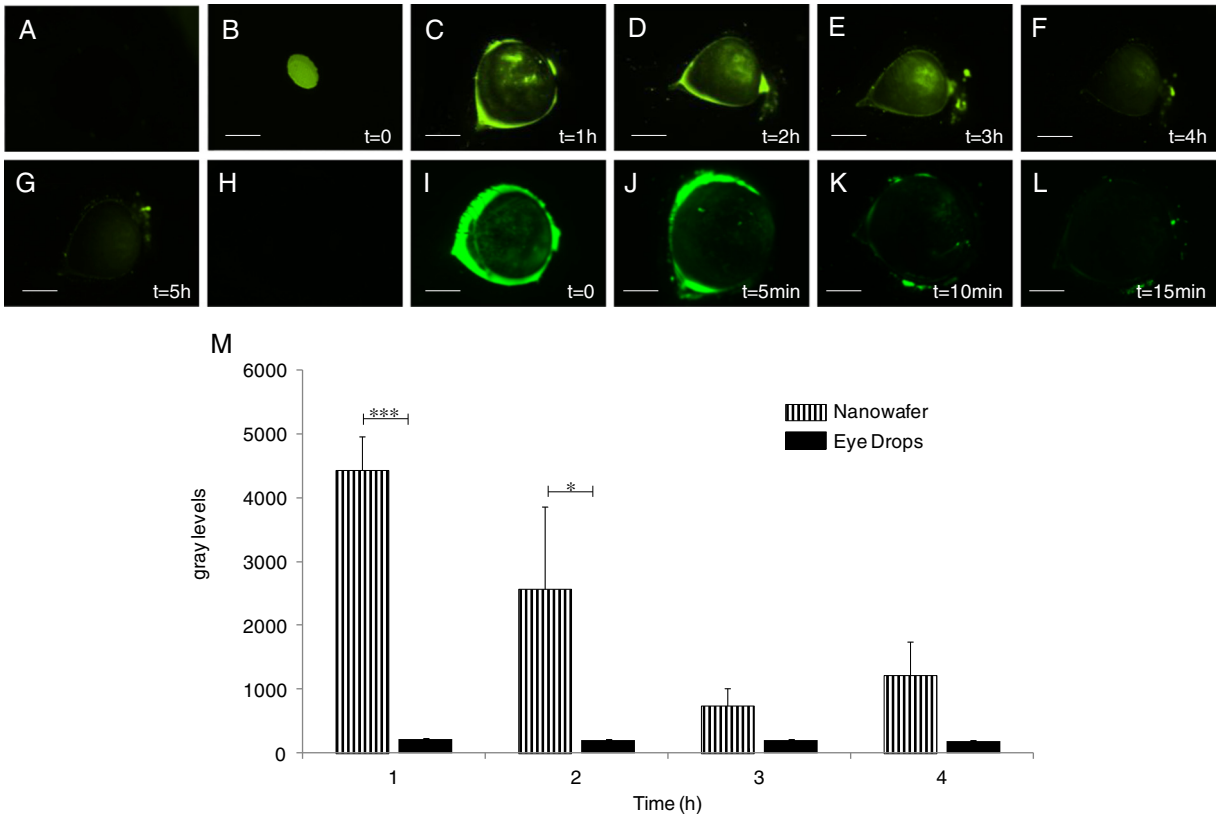

Fig. 3. Nanowafer improves the drug residence time on the cornea. (A) Fluorescence micrograph of the eye prior to fluorescein nanowafer (Flo-NW) instillation; (B–G) fluorescence micrographs depicting the presence of fluorescein dye at the specified time points in the corneal tissue after Flo-NW instillation; (H) fluorescence micrograph of the eye prior to fluorescein eye drops instillation; (I–L) rapid clearance of fluorescein eye drops within 5 min. (M) A plot depicting the fluorescence intensities (n = 3).*P < 0.05, ***P < 0.001. All error bars represent standard error of the mean. Scale bar: 1 mm.

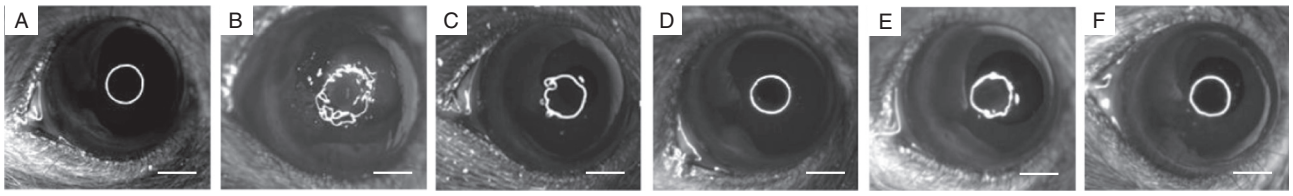

Fig. 4. Maintenance of a smooth corneal surface by Dex-NW treatment observed by the reflection of a ring of light in mice. (A) Healthy eye; (B) Desiccating stress induced dry eye; (C) CMC-eye drops; (D) Dex-eye drops; (E) CMC-NW; and (F) Dex-NW. Scale bar: 1 mm.

permeability [38–40]. Accordingly, corneal smoothness was monitored as a study parameter for the evaluation of nanowafer efficacy. The regularity of a white-light ring reflecting off the mouse cornea was used to evaluate corneal smoothness. A regular circular ring is reflected off the smooth normal corneal surface. In dry eye mice treated with control CMC nanowafers, the reflected rings were very irregular, while regular and uniform ring reflections were observed from eyes treated with Dex-NW, indicating maintenance of a smooth normal corneal surface (Fig. 4). Improved corneal smoothness over control affirms the efficacy of Dex-NW. These results indicate that the drug release from the nanowafer is effective in restoring or maintaining a healthy corneal surface that is subjected to desiccation.

To study the therapeutic effect of Dex-NW on maintaining a healthy corneal surface in mice exposed to DS, corneal epithelial barrier function was measured by staining the cornea with green fluorescent Oregon Green Dextran (OGD, 70 kDa). Corneal epithelial disruptions created due to the damage or loss of epithelial cells was visualized with the dye, where fluorescence intensity positively correlates with the degree of disruption in corneal barrier function [38]. For the corneal epithelial barrier function measurement, OGD was delivered as topical eye drops. Because the mice are exposed to DS, the corneas develop epithelial disruptions due to the damage or loss of epithelial cells. The corneal surface is no longer smooth with tight epithelial junctions. Upon instillation of OGD eye drops on these corneas, the OGD molecules will rapidly (<1 min) penetrate into the corneal tissue through the epithelial disruptions compared to healthy and drug treated corneas. Because of the short duration of the eye drops on the cornea (1 min) and the low blink rate of mouse, most of the eye drop stays on the ocular surface and does not get washed away.

Compared to a healthy eye, the dry eye mice absorbed more OGD. This study revealed that the corneal uptake of OGD significantly increased after five days in dry eye mice (Fig. 5). In contrast, treatment with Dex-NW or Dex drops maintained corneal epithelial barrier function. Treatment of dry eye mice with Dex eye drops (0.1%, 2 μL) administered twice a day for five days or instillation of Dex-NW on the first and third days during five-days of experimental dry eye maintained OGD staining at baseline levels. No difference in efficacy was observed between the Dex-NW and Dex drops treated groups, despite the lower dosing frequency for the Dex-NW. These results confirm the ability of the nanowafer to deliver Dex in therapeutic concentrations to the ocular tissue. Interestingly, CMC eye drops appear to be slightly more effective, although not significant, compared to the CMC nanowafer in maintaining the corneal barrier function (Fig. 5G). This could be because of the ability of the CMC polymer molecules in eye drop formulation delivered twice daily to quickly bind to the corneal epithelium thus filling some of the corneal epithelial disruptions caused by the desiccating stress, compared to the CMC nanowafer which was applied only twice during the 5 day treatment period [30]. Also, when an eye drop is instilled on the ocular surface, it will have some wetting/moisturizing effect on the surface regardless of whether it has any effective ingredients (vehicle effect). The nanowafer on the other hand did not produce as much vehicle effect as it was instilled only twice during the treatment period (on days 1 and 3).

Dry eye is a multifactorial disease. It activates an innate immune response in the cornea and conjunctiva that ultimately affects the corneal epithelium by producing chemokines and cytokines. Chemokines CXCL-9, -10, -11 attract T helper cells (type 1) which produce IFN-γ, while other chemokines, such as CCL5 attract innate immune cells [41]. Important immune mediators in the conjunctiva also include cytokines IFN-γ and TNF-α [42,43]. In particular, IFN-γ is known to cause conjunctival goblet cell loss and apoptosis of the ocular surface epithelium [44–47]. The gene expression of these molecules was evaluated due to their importance in the pathogenesis of dry eye. Matrix metalloproteinase MMP-9 and its physiological activator MMP-3 have been found to increase in the ocular surface epithelium of both human and experimental dry eye [48–51]. The MMPs break down a variety of substrates, including components of the corneal epithelial basement membrane and tight junction proteins that maintain corneal epithelial barrier function. MMPs have also been detected in the tear fluid of both dry eye patients and dry eye mice [39].

Inhibition of inflammatory cytokine and MMP expression confirms the efficacy of Dex-NW. Instillation of Dex-NW on the first and third days effectively inhibited expression of inflammatory cytokine and MMP production in the corneal epithelium compared to CMC-NW (control). The slight anti-inflammatory effect of CMC nanowafer is possibly due to the ability of CMC polymer molecules to bind to the corneal epithelium and protect it against the pro-inflammatory effects of the DS and modulate the healing process [30]. The efficacy of the Dex-NW (administered on first and the third days) was equal to twice a day topical administration of Dex eye drops for the five-day treatment period

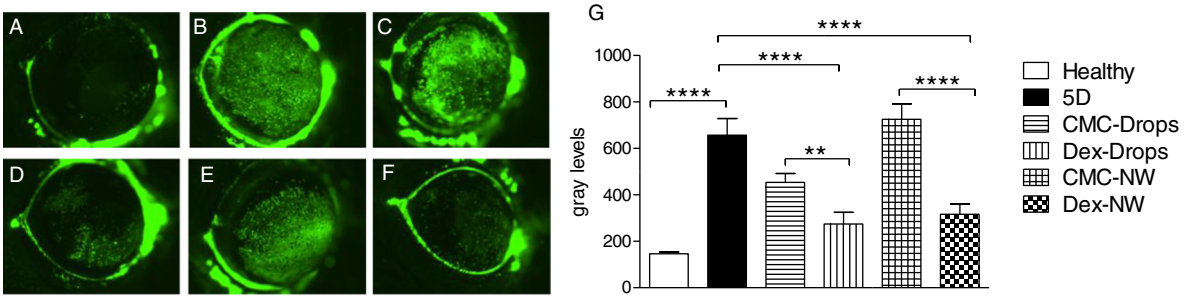

Fig. 5. Measurement of corneal epithelial barrier function. (A) Healthy eye; (B) subjected to five days of desiccating stress (5D); (C) CMC drops; (D) Dex drops; (E) CMC-NW; (F) Dex-NW; and (G) a plot depicting the fluorescence intensities.**P < 0.05, ****P < 0.0001. All error bars represent standard error of the mean.

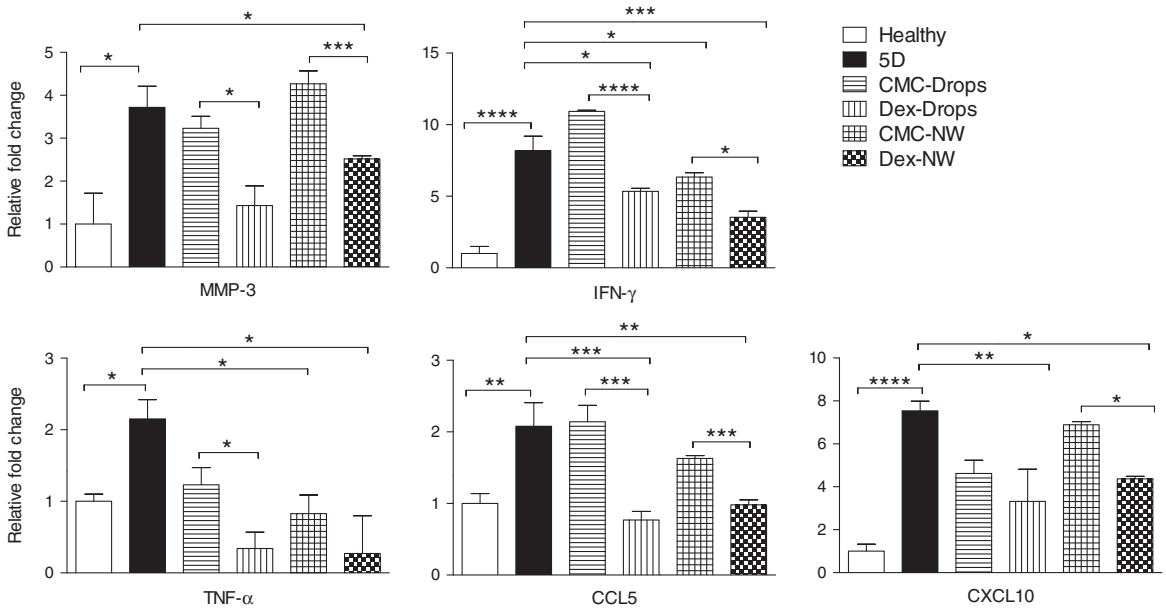

Fig. 6. RT-PCR analysis revealing down regulation of drug target genes by Dex-NW in the corneal epithelium after 5 days of desiccating stress is comparable to that of twice a day topical Dex eye drop treatment. *P < 0.05, **P < 0.01, ***P < 0.001, and ****P < 0.0001. All error bars represent standard error of the mean.

(Fig. 6). Both Dex-NW and Dex eye drop treatment inhibited the production of MMP-3, CCL-5, CXCL-10, TNF-α, and IFN-γ. Overall, the Dex-NW was effective in inhibiting inflammatory cytokine expression at the same level achieved with twice a day topically administered Dex eye drops.

4. Conclusions

Despite advances in the therapy of dry eye disease over the past two decades, challenges still remain in delivering therapeutic levels of anti-inflammatory drugs at a convenient dosing schedule and optimum tissue concentrations. This study evaluated the nanowafer drug delivery system to deliver Dex to the ocular surface. The Dex-NW was able to enhance diffusion of a corticosteroid into the cornea and maintain a smooth, healthy corneal surface with intact barrier function in mice with experimentally induced dry eye. In addition, the Dex-NW was effective in suppressing expression of inflammatory mediators associated with dryness of the cornea. The Dex-NW treatment was well tolerated on the mouse eye. Administration of Dex-NW only twice during the five-day treatment had equivalent efficacy to twice a day topical administration of Dex eye drops during same treatment period. The less frequent dosing schedule of the Dex-NW will improve convenience and enhance treatment compliance among dry eye patients. Furthermore, release of dexamethasone from the nanowafer can be adjusted to the minimal effective concentration to minimize the drug related toxicity of corticosteroids that can cause glaucoma and cataract at higher concentration. These results confirm the therapeutic efficacy and translational potential of the nanowafer drug delivery system to treat dry eye disease. Upon further development, Dex-NW can provide a simple and effective treatment with a more convenient dosing schedule than eye drops for dry eye disease.

Acknowledgments

This work was supported by the Department of Defense (Award No. 1W81XWH-13-1-0146), Research to Prevent Blindness (New York, NY), Oshman Foundation (Houston, TX), William Stamps Farish Fund (Houston, TX), and Hamill Foundation (Houston, TX).

References

[1] M.A. Lemp, B.D. Sullivan, L.A. Crews, Biomarkers in dry eye disease, Eur. Ophthalmic Rev. 6 (2012) 157–163.
[2] A. Tomlinson, Epidemiology of dry eye disease, in: P.A. Asbell, M.A. Lemp (Eds.), Dry Eye Disease: The Clinician's Guide to Diagnosis and Treatment, Thieme Medical Publishers, Inc., New York 2006, pp. 1–15.
[3] J.L. Gayton, Etiology, prevalence, and treatment of dry eye disease, Clin. Ophthalmol. 3 (2009) 405–412.
[4] R. Latkany, Dry eyes: etiology and management, Curr. Opin. Ophthalmol. 19 (2008) 287–291.
[5] P.D. O'Brien, L.M. Collum, Dry eye: diagnosis and current treatment strategies, Curr. Allergy Asthma Rep. 4 (2004) 314–319.
[6] D.A. Schaumberg, D.A. Sullivan, J.E. Buring, M.R. Dana, Prevalence of dry eye syndrome among US women, Am J. Ophthalmol. 136 (2003) 318–326.
[7] M.A. Lemp, Advances in understanding and managing dry eye disease, Am J. Ophthalmol. 146 (2008) 350–356.
[8] The epidemiology of dry eye disease. Report of the epidemiology subcommittee of the international dry eye work shop, Ocul. Surf. 5 (2007) 93–107.
[9] A.J. Bron, Diagnosis of dry eye, Surv. Ophthalmol. 45 (Suppl. 2) (2001) S221–S226.
[10] M. Uchino, Y. Uchino, M. Dogru, M. Kawashima, N. Yokoi, A. Komuro, Y. Sonomura, H. Kato, S. Kinoshita, D.A. Schaumberg, K. Tsubota, Dry eye disease and work productivity loss in visual display users: the Osaka study, Am J. Ophthalmol. 157 (2014) 294–300.
[11] S.C. Pflugfelder, M.E. Stern, R. Beuerman, The problem, in: S.C. Pflugfelder, M.E. Stern, R. Beuerman (Eds.), Dry Eye and the Ocular Surface, Marcel Dekker, New York 2004, pp. 1–10.
[12] The definition and classification of dry eye disease: report of the definition and classification subcommittee of the international dry eye work shop, Ocul. Surf. 5 (2007) 75–92.
[13] P.A. Simmons, J.G. Vehige, Clinical performance of a mid-viscosity artificial tear for dry eye treatment, Cornea 26 (2007) 294–302.
[14] D. Schmidl, L. Schmetterer, K.J. Witkowska, A. Unterhuber, V. Aranha Dos Santos, S. Kaya, J. Nepp, C. Baar, P. Rosner, R.M. Werkmeister, G. Garhofer, Tear film thickness after treatment with artificial tears in patients with moderate dry eye disease, Cornea 34 (2015) 421–426.
[15] S.C. Pflugfelder, Anti-inflammatory therapy of dry eye, Am J. Ophthalmol. 137 (2004) 337–342.
[16] A.M. Avunduk, M.C. Avunduk, E.D. Varnell, H.E. Kaufman, The comparison of efficacies of topical corticosteroids and nonsteroidal anti-inflammatory drops on dry eye patients: a clinical and immunocytochemical study, Am J. Ophthalmol. 136 (2003) 593–602.
[17] N. Kara, H. Altinkaynak, Y. Goker, K. Yuksel, Y. Yildirim, Evaluation of corneal morphologic and functional parameters after use of topical cyclosporine-a 0.05% in dry eye, J. Ocul. Pharmacol. Ther. 28 (2012) 593–597.
[18] C. Baudouin, Side effects of antiglaucomatous drugs on the ocular surface, Curr. Opin. Ophthalmol. 7 (1996) 80–86.
[19] M.K. Arici, D.S. Arici, A. Topalkara, C. Guler, Adverse effects of topical antiglaucoma drugs on the ocular surface, Clin. Exp. Ophthalmol. 28 (2000) 113–117.
[20] Y.C. Kim, B. Chiang, X. Wu, M.R. Prausnitz, Ocular delivery of macromolecules, J. Control. Release 190 (2014) 172–181.
[21] P. Aksungur, M. Demirbilek, E.B. Denkbas, J. Vandervoort, A. Ludwig, N. Unlu, Development and characterization of cyclosporine A loaded nanoparticles for ocular drug

delivery: cellular toxicity, uptake, and kinetic studies, J. Control. Release 151 (2011) 286–294.
[22] M. Shah, M.C. Edman, S.R. Janga, P. Shi, J. Dhandhukia, S. Liu, S.G. Louie, K. Rodgers, J.A. Mackay, S.F. Hamm-Alvarez, A rapamycin-binding protein polymer nanoparticle shows potent therapeutic activity in suppressing autoimmune dacryoadenitis in a mouse model of Sjogren's syndrome, J. Control. Release 171 (2013) 269–279.
[23] Y. Diebold, M. Calonge, Applications of nanoparticles in ophthalmology, Prog. Retin. Eye Res. 29 (2010) 596–609.
[24] Y.B. Choy, J.H. Park, B.E. McCarey, H.F. Edelhauser, M.R. Prausnitz, Mucoadhesive microdiscs engineered for ophthalmic drug delivery: effect of particle geometry and formulation on preocular residence time, Invest. Ophthalmol. Vis. Sci. 49 (2008) 4808–4815.
[25] I.M. Carvalho, C.S. Marques, R.S. Oliveira, P.B. Coelho, P.C. Costa, D.C. Ferreira, Sustained drug release by contact lenses for glaucoma treatment — a review, J. Control. Release 202 (2015) 76–82.
[26] K. Singh, A.B. Nair, A. Kumar, R. Kumria, Novel approaches in formulation and drug delivery using contact lenses, J. Basic Clin. Pharm. 2 (2011) 87–101.
[27] R. Garhwal, S.F. Shady, E.J. Ellis, J.Y. Ellis, C.D. Leahy, S.P. McCarthy, K.S. Crawford, P. Gaines, Sustained ocular delivery of ciprofloxacin using nanospheres and conventional contact lens materials, Invest. Ophthalmol. Vis. Sci. 53 (2012) 1341–1352.
[28] M. Moshirfar, K. Pierson, K. Hanamaikai, L. Santiago-Caban, V. Muthappan, S.F. Passi, Artificial tears potpourri: a literature review, Clin. Ophthalmol. 8 (2014) 1419–1433.
[29] A. Ludwig, Mucoadhesive polymers in ocular drug delivery, Adv. Drug Deliv. Rev. 57 (2005) 1595–1639.
[30] Q. Garrett, P.A. Simmons, S. Xu, J. Vehige, Z. Zhao, K. Ehrmann, M. Willcox, Carboxy methyl cellulose binds to human corneal epithelial cells and is a modulator of corneal epithelial wound healing, Invest. Ophthalmol. Vis. Sci. 48 (2007) 1559–1567.
[31] T.J. Nagelhout, D.A. Gamache, L. Roberts, M.T. Brady, J.M. Yanni, Preservation of tear film integrity and inhibition of corneal injury by dexamethasone in a rabbit model of lacrimal gland inflammation-induced dry eye, J. Ocul. Pharmacol. Ther. 21 (2005) 139–148.
[32] A.R. Djalilian, C.N. Nagineni, S.P. Mahesh, J.A. Smith, R.B. Nussenblatt, J.J. Hooks, Inhibition of inflammatory cytokine production in human corneal cells by dexamethasone, but not cyclosporin, Cornea 25 (2006) 709–714.
[33] M.A. Patane, A. Cohen, S. From, G. Torkildsen, D. Welch, G.W. Ousler III, Ocular iontophoresis of EGP-437 (dexamethasone phosphate) in dry eye patients: results of a randomized clinical trial, Clin. Ophthalmol. 5 (2011) 633–643.
[34] X. Yuan, D.C. Marcano, C.S. Shin, X. Hua, L.C. Isenhart, S.C. Pflugfelder, G. Acharya, Ocular drug delivery nanowafer with enhanced therapeutic efficacy, ACS Nano 9 (2015) 1749–1758.
[35] G. Acharya, C.S. Shin, K. Vedantham, M. McDermott, T. Rish, K. Hansen, Y. Fu, K. Park, A study of drug release from homogeneous PLGA microstructures, J. Control. Release 146 (2010) 201–206.
[36] G. Acharya, C.S. Shin, M. McDermott, H. Mishra, H. Park, I.C. Kwon, K. Park, The hydrogel template method for fabrication of homogeneous nano/microparticles, J. Control. Release 141 (2010) 314–319.
[37] D. Dursun, M. Wang, D. Monroy, D.Q. Li, B.L. Lokeshwar, M.E. Stern, S.C. Pflugfelder, A mouse model of keratoconjunctivitis sicca, Invest. Ophthalmol. Vis. Sci. 43 (2002) 632–638.
[38] C.S. De Paiva, R.M. Corrales, A.L. Villarreal, W. Farley, D.-Q. Li, M.E. Stern, S.C. Pflugfelder, Apical corneal barrier disruption in experimental murine dry eye is abrogated by methylprednisolone and doxycycline, Invest. Ophthalmol. Vis. Sci. 47 (2006) 2847–2856.
[39] R.M. Corrales, M.E. Stern, C.S. De Paiva, J. Welch, D.-Q. Li, S.C. Pflugfelder, Dessicating stress stimulates expression of matrix metalloproteinase by the corneal epithelium, Invest. Ophthalmol. Vis. Sci. 47 (2006) 3293–3302.
[40] C.S. De Paiva, S.B. Pangelinan, E. Chang, K.-C. Yoon, W.J. Farley, D.-Q. Li, S.C. Pflugfelder, Essential role for c-Jun N-terminal kinase 2 in corneal epithelial response to desiccating stress, Arch. Ophthalmol. 127 (2009) 1625–1631.
[41] R.M. Corrales, M.E. Stern, C.S. de Paiva, J. Welch, D.Q. Li, S.C. Pflugfelder, Desiccating stress stimulates expression of matrix metalloproteinases by the corneal epithelium, Invest. Ophthalmol. Vis. Sci. 47 (2006) 3293–3302.
[42] K. Yoon, C.S. Park, I.C. You, H.J. Choi, K.H. Lee, S.K. Im, H.Y. Park, S.C. Pflugfelder, Expression of CXCL9, -10, -11, and CXCR3 in the tear film and ocular surface of patients with dry eye syndrome, Invest. Ophthalmol. Vis. Sci. 51 (2010) 643–650.
[43] D.T. Jones, D. Monroy, Z. Ji, S.S. Atherton, S.C. Pflugfelder, Sjogren's syndrome: cytokine and Epstein-Barr viral gene expression within the conjunctival epithelium, Invest. Ophthalmol. Vis. Sci. 35 (1994) 3493–3504.
[44] S.C. Pflugfelder, D. Jones, Z. Ji, A. Afonso, D. Monroy, Altered cytokine balance in the tear fluid and conjunctiva of patients with Sjogren's syndrome keratoconjunctivitis sicca, Curr. Eye Res. 19 (1999) 201–211.
[45] X. Zhang, W. Chen, C.S. de Paiva, R.M. Corrales, E.A. Volpe, A.J. McClellan, W.J. Farley, D.Q. Li, S.C. Pflugfelder, Interferon-γ exacerbates dry eye induced apoptosis in conjunctiva via dual apoptotic pathways, Invest. Ophthalmol. Vis. Sci. 52 (2011) 6279–6285.
[46] X. Zhang, C.S. de Paiva, Z. Su, E.A. Volpe, D.Q. Li, S.C. Pflugfelder, Topical interferon-γ neutralization prevents conjunctival goblet cell loss in experimental murine dry eye, Exp. Eye Res. 118 (2014) 117–124.
[47] C.S. de Paiva, A.L. Villarreal, R.M. Corrales, H.T. Rahman, V.Y. Chang, J.W. Farley, M.E. Stern, J.Y. Niederkorn, D.Q. Li, S.C. Pflugfelder, IFN-γ promotes goblet cell loss in response to desiccating ocular stress, Invest. Ophthalmol. Vis. Sci. 47 (2006) (E-Abstract 5579).
[48] C.S. de Paiva, A.L. Villarreal, R.M. Corrales, H.T. Rahman, V.Y. Chang, W.J. Farley, M.E. Stern, J.Y. Niederkorn, D.Q. Li, S.C. Pflugfelder, Dry eye-induced conjunctival epithelial squamous metaplasia is modulated by interferon-γ, Invest. Ophthalmol. Vis. Sci. 48 (2007) 2553–2560.
[49] L. Sobrin, Z. Liu, D.C. Monroy, A. Solomon, M.G. Selzer, B.L. Lokeshwar, S.C. Pflugfelder, Regulation of MMP-9 activity in human tear fluid and corneal epithelial culture supernatant, Invest. Ophthalmol. Vis. Sci. 41 (2000) 1703–1709.
[50] S.C. Pflugfelder, W. Farley, L. Luo, L.Z. Chen, C.S. de Paiva, L.C. Olmos, D.Q. Li, M.E. Fini, Matrix metalloproteinase-9 knockout confers resistance to corneal epithelial barrier disruption in experimental dry eye, Am. J. Pathol. 166 (2005) 61–71.
[51] C.S. de Paiva, R.M. Corrales, A.L. Villarreal, W.J. Farley, D.Q. Li, M.E. Stern, S.C. Pflugfelder, Corticosteroid and doxycycline suppress MMP-9 and inflammatory cytokine expression, MAPK activation in the corneal epithelium in experimental dry eye, Exp. Eye Res. 83 (2006) 526–535.

Appendix 3: Journal publication

Marcano et al. Synergistic cysteamine delivery nanowafer as an efficacious treatment modality for corneal cystinosis. *Mol Pharm*. **13**:3468-3477 (2016).

molecular pharmaceutics

Article

pubs.acs.org/molecularpharmaceutics

Synergistic Cysteamine Delivery Nanowafer as an Efficacious Treatment Modality for Corneal Cystinosis

Daniela C. Marcano,[†] Crystal S. Shin,[†] Briana Lee,[‡] Lucas C. Isenhart,[†] Xing Liu,[§] Feng Li,[§] James V. Jester,[‡] Stephen C. Pflugfelder,[†] Jennifer Simpson,*[,‡] and Ghanashyam Acharya*[,†]

[†]Department of Ophthalmology, Baylor College of Medicine, Houston, Texas 77054, United States

[‡]Department of Ophthalmology, University of California, Irvine, California 92697, United States

[§]Metabolomics Core Facility, Baylor College of Medicine, Houston, Texas 77054, United States

Supporting Information

ABSTRACT: A synergy between the polymer biomaterial and drug plays an important role in enhancing the therapeutic efficacy, improving the drug stability, and minimizing the local immune responses in the development of drug delivery systems. Particularly, in the case of ocular drug delivery, the need for the development of synergistic drug delivery system becomes more pronounced because of the wet ocular mucosal surface and highly innervated cornea, which elicit a strong inflammatory response to the instilled drug formulations. This article presents the development of a synergistic cysteamine delivery nanowafer to treat corneal cystinosis. Corneal cystinosis is a rare metabolic disease that causes the accumulation of cystine crystals in the cornea resulting in corneal opacity and loss of vision. It is treated with topical cysteamine (Cys) eye drops that need to be instilled 6−12 times a day throughout the patient's life, which causes side effects such as eye pain, redness, and ocular inflammation. As a result, compliance and treatment outcomes are severely compromised. To surmount these issues, we have developed a clinically translatable Cys nanowafer (Cys-NW) that can be simply applied on the eye with a fingertip. During the course of the drug release, Cys-NW slowly dissolves and fades away. The *in vivo* studies in cystinosin knockout mice demonstrated twice the therapeutic efficacy of Cys-NW containing 10 μg of Cys administered once a day, compared to 44 μg of Cys as topical eye drops administered twice a day. Furthermore, Cys-NW stabilizes Cys for up to four months at room temperature compared to topical Cys eye drops that need to be frozen or refrigerated and still remain active for only 1 week. The Cys-NW, because of its enhanced therapeutic efficacy, safety profile, and extended drug stability at room temperature, can be rapidly translated to the clinic for human trials.

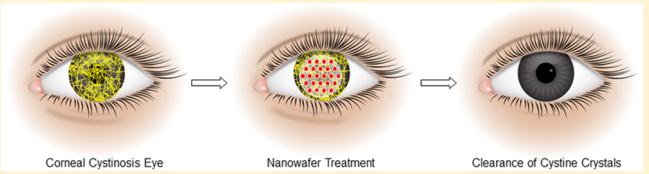

KEYWORDS: *Nanowafer, drug delivery, corneal cystinosis, cysteamine*

INTRODUCTION

Polymer biomaterials play an important role in the development of drug delivery systems, implants, and matrixes for tissue repair and regeneration.[1−3] In particular, a synergy between the polymer biomaterial and the drug will enhance the therapeutic efficacy of the drug delivery system in disease treatment.[4] In ocular drug delivery, because of the wet mucosal surface and highly innervated cornea eye is very sensitive and the ocular surface generates a rapid and strong inflammatory response to the foreign materials invasion.[5,6] Hence, choosing the right polymer and drug combination that elicit negligible immunological and inflammatory responses is crucial for the development of synergistic drug delivery systems.[7−9] In this article, we describe the development of a cysteamine delivery nanowafer (Cys-NW) to treat corneal cystinosis in a cystinosin knockout mouse model ($Ctns^{-/-}$). In Cys-NW, the drug and the polymer are in synergy to induce minimal inflammatory responses, improve drug stability, and enhance the therapeutic efficacy.

Corneal cystinosis is a rare metabolic disease that causes cystine to accumulate in cells because of the defective transport across the lysosomal membrane into the cytoplasm.[10,11] Thus, accumulated cystine, a disulfide amino acid, crystallizes in the cornea.[12] It begins in infancy, and by the time the patient reaches 6−8 years of age, the symptoms begin to appear, such as corneal lesions, ocular inflammation, and photophobia, which affect the patient's quality of life to such an extent that a slight glimmer of sunlight can be debilitating. In later stages, it manifests into corneal opacification, erosion, keratitis, and eventual blindness.[13]

Presently, corneal cystinosis is treated with topical cysteamine hydrochloride (Cys) eye drops.[14−19] The oral formulation of Cys cannot reach the cornea because of its lack of vasculature, and has negligible therapeutic effect on dissolving the corneal crystals.[20] Cys is a highly water-soluble small molecular drug. It cleaves the disulfide bond in cystine to form a lysine-like cysteine−cysteamine mixed disulfide, which will be cleared from the tissue.[21−23] Topical Cystaran

Received: June 1, 2016
Revised: August 25, 2016
Accepted: August 29, 2016

DOI: 10.1021/acs.molpharmaceut.6b00488
Mol. Pharmaceutics XXXX, XXX, XXX−XXX

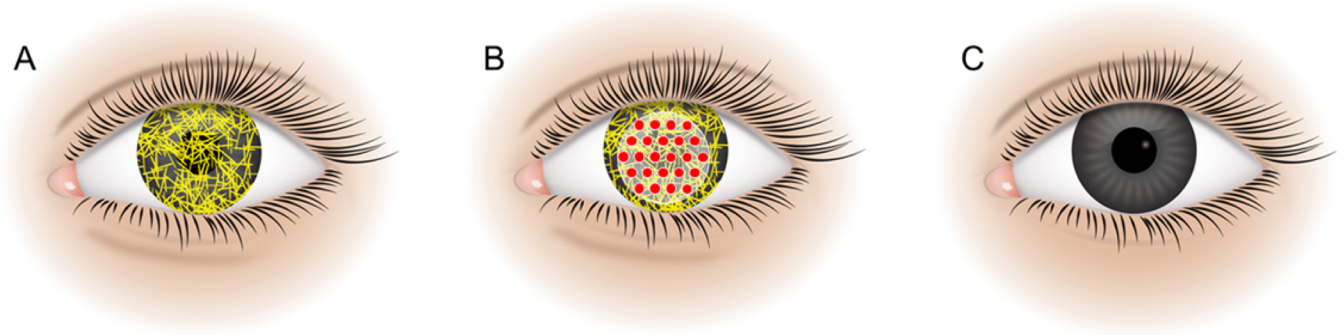

Figure 1. Cys delivery nanowafer as an efficacious treatment modality for corneal cystinosis. A schematic diagram depicting (A) a corneal cystinosis eye, (B) placement of a Cys-NW on the eye, and (C) clearance of corneal crystals after nanowafer treatment.

ophthalmic solution is the only medication approved by FDA for the treatment of corneal cystinosis.[24] Eye drops are rapidly cleared from the ocular surface due to reflex tearing, constant blinking, and nasolacrimal drainage, and have only a short contact time on the eye. Typically, less than 5% of the drug can penetrate through the ocular epithelium.[25,26] Hence, it is very difficult to maintain a therapeutically effective concentration of Cys in the eye for sufficient time to dissolve the cystine crystals. As a consequence, Cys eye drops need to be administered every hour while awake or at least 6−12 times in a day to be therapeutically effective, which is both inconvenient and impractical for school-going children and working adults.[27,28] Because of the continuous and prolonged usage of Cys eye drops, patients develop inflammation and ulcers in the eyes. The pungent smell of cysteamine also contributes to non-compliance and severely compromised treatment outcomes. Another major issue with topical Cys eye drops is its rapid oxidation in aqueous solutions to form a therapeutically inactive disulfide cystamine.[29,30] Hence, eye drop bottles need to be stored frozen. Once a bottle is opened, the drug is effective for only 1 week, after which it must be discarded.[31] This results in a high cost of treatment. To surmount these issues, we have developed a cysteamine nanowafer (Cys-NW) for the efficacious treatment of corneal cystinosis (Figure 1).

EXPERIMENTAL SECTION

Materials for Nanowafer Fabrication and Drug Release Studies. Poly(vinyl alcohol) (MW 146,000, 87−89% hydrolyzed), cysteamine hydrochloride, HPLC grade methanol, and red fluorescent quantum dots (6 nm) were obtained from Sigma-Aldrich, St. Louis, MO. Slide-A-Lyzer/mini dialysis units (MWCO 2000) were obtained from Pierce Biotechnology (Rockford, IL).

In Vivo Studies. All the experimental protocols involving mice were approved by the Institutional Animal Care and Use Committee prior to the initiation of this study. Healthy female C57BL/6 (8−10 weeks old) mice were used for tear collection and quantum dot (QD) diffusion experiments. Both genders of cystinosin knockout mice with C57BL/6 background ($Ctns^{-/-}$) were used for drug delivery experiments. Mice were randomly assigned to each experimental group.

Nanowafer Fabrication. Cys-NW was fabricated via hydrogel template strategy.[32−35] Briefly, a silicon wafer containing arrays of square wells (500 nm × 500 nm and 500 nm deep) was fabricated by e-beam lithography and was used to prepare poly(dimethylsiloxane) (PDMS) imprints containing vertical posts that were 500 nm × 500 nm and 500 nm in height. Poly(vinyl alcohol) (5 g in 100 mL water, 5% w/v) was poured onto the PDMS imprint and placed in an oven at 70 °C for 30 min to form a PVA wafer containing arrays of wells. These wells were filled with a thick solution of Cys (Sigma-Aldrich, St. Louis, MO) and PVA. Cys (10 mg) was dissolved in 1 mL of PVA solution (5%) and used for filling the nanowafers. The Cys-PVA solution (200 μL) was transferred with a pipet onto a dry PVA wafer containing nanoreservoirs facing up (previously peeled from the PDMS template). Then, the thick solution was swiped swiftly across the wafer using a razor blade to fill the nanoreservoirs and remove the excess solution. The filled Cys-NWs were vacuum-dried at room temperature for the solvent to evaporate. Thus, formed Cys-NW was punched into 2 mm circular disks with a paper punch. These 2 mm diameter Cys-NWs were used for the in vitro drug release, drug stability experiments, and for the *in vivo* studies in mice. Red fluorescent quantum dots (6 nm) were loaded into nanowafers to fabricate the QD-NW. These nanowafers were used for the study of quantum dot diffusion in the mouse cornea experiments.

Analysis of in Vitro Cys Stability in the Nanowafers. Cys stability studies were performed by placing Cys-NW of 2 mm diameter in separate plastic Petri dishes and sealed with parafilm. These Petri dishes were stored at room temperature for 10, 12, 14, 16, and 32 weeks at room temperature. Samples were dissolved in a mixture of methanol/water (50:50), centrifuged, and analyzed by liquid chromatography tandem mass spectrometry (Agilent 6490 Triple Quadruple LC−MS/MS system), equipped with a XDB C-18 column (50 mm × 4.6 mm, Agilent). A mixture of methanol/water (50:50) with 0.1% formic acid was used as the mobile phase with flow rate of 0.3 mL/min. The system was operated in a positive mode with electrospray ionization. Data acquisition in MRM mode and data quantification were performed with the corresponding Agilent MassHunter software. The MRM transition for Cys (monomer) was 78/61 and 153/108 for cystamine (dimer). Standards for calibration curves were always freshly prepared. Data was expressed as mean ± SEM.

Analysis of in Vitro Cys Release Studies. Cys-NWs (2 mm of diameter) were added to dialysis tubes provided with sterile water and transferred into a 5 mL size Eppendorf tubes containing also sterile water. The vials were constantly shaken (140 shakes/min, Brinkmann OrbiMix 1010 coupled with Incubator 1000, BioSurplus) at 37 °C. At different time points (1, 2, 3, 6, and 9 h), aliquots of 100 μL were taken out, and fresh water was used to replace the extracted aliquot volume. Samples were centrifuged (1000 rpm) for 10 s and stored at

DOI: 10.1021/acs.molpharmaceut.6b00488
Mol. Pharmaceutics XXXX, XXX, XXX−XXX

−80 °C until analyzed by mass spectrometry. Cys was measured using liquid chromatogram-tandem mass spectrometry (LC−MS/MS, 6490 QQQ Agilent). The samples were reconstituted in 100 μL of water/methanol (v/v 50:50), followed by centrifugation (RCF 15,000) for 15 min. The resulting supernatants were transferred to sample vials, and 5 μL was injected for analysis. The separation was achieved using a 50 mm × 4.6 mm XDB C-18 column (Agilent, Santa Clara, CA). The flow rate of the mobile phase was 0.3 mL/min with 50:50 methanol/water containing 0.1% formic acid. LC−MS/MS was operated in a positive mode with electrospray ionization. The data were acquired using Agilent MassHunter data acquisition software (Agilent) in the multiple reaction monitoring (MRM) mode. The quantification was performed by Agilent Mass Hunter quantitative analysis software. The MRM transition for Cys was 78/61. Standards for calibration curves were always freshly prepared. Results were reported as the mean ± SEM of quadruplicates.

Cys-NW Instillation and Measurement of Cys Concentration in Tear Samples. Healthy female C57/BL6 mice were anesthetized with ketamine (100 mg/kg) and xylazine (10 mg/kg) by intraperitoneal injection, followed by the placement of a Cys-NW on the cornea. After mice were awake, tear fluid was collected hourly for 4 h.[36] Briefly, 2 μL of sterile water was instilled on the ocular surface, and after a few seconds, the tear washings were collected from the eye with a 1 μL volume glass capillary tube (Drummond Scientific, Broomhall, PA). The tear washings from a group of 50 mice were pooled, centrifuged, and stored at −80 °C prior to drug evaluation. In this experiment, sterile water, rather than a sterile balanced salt solution (BSS), was used, due to the interference of salt ions during mass spectrometry detection. Cys concentration was measured using LC−MS/MS as described previously. The MRM transition for Cys was 78/61. Standards for calibration curves were always freshly prepared. Results were reported as the mean ± SEM of triplicates.

Confocal Laser Scanning Microscopy of QD Diffusion in the Cornea. Healthy female C57/BL6 mice were anesthetized with ketamine (100 mg/kg) and xylazine (10 mg/kg) by intraperitoneal injection. A QD-NW was placed on the cornea. At 4, 12, 24, and 48 h after the QD-NW instillation, mice were sacrificed and eyes were excised. Eye tissues were embedded in optimal cutting temperature compound prior to flash freezing in liquid nitrogen. Frozen tissues were sectioned at 10 μm thickness with a cryostat (HM505E; Micron International GmbH, Waldorf, Germany). Sections were fixed with 4% paraformaldehyde (Electron Microscopy Sciences, Hatfield, PA) for 10 min at room temperature and rinsed with phosphate buffered saline. Then sections were mounted with Fluoromount G (Southern Biotech, Birmingham, AL, USA) containing DAPI (1:300) prior to fluorescence imaging. Fluorescence images were obtained using a confocal laser scanning microscope (Eclipse Ni-E; Nikon, Melville, NY) with a 100× oil immersion objective (numerical aperture, 1.45; working distance, 1.3 mm). Obtained images were processed by NIS Elements software (Nikon, Melville, NY).

In Vivo Confocal Microscopic Analysis of Corneal Cystine Crystal Volume. Corneal crystal volume in cystinosis mice was determined as previously reported.[37,38] Briefly, in vivo corneal cystine crystal content was imaged by using a tandem scanning confocal microscope (TSCM; Tandem Scanning Corporation, Reston, VA) with a 24× surface-contact objective (numerical aperture, 0.6; working distance, 1.5 mm), encoder mike controller (Oriel 18011; Oriel, Stratford, CT) for focal plane control, and a low light level camera (MTI VE-1000; Dage MTI, Michigan City, IN). One drop of preservative-free, Refresh Tears (Allergan, Irvine, CA) was placed on the tip of the objective as a coupling gel. All camera settings were kept constant throughout the experiment. For each eye, three to five through-focus data sets were obtained from select central and peripheral corneal locations, including epithelium, stroma, and endothelium. To quantify the cystine crystal content in the cornea, several sets of through-focus images (3D images, *z*-stacking) were analyzed by Metamorph Image Processing Software (Molecular Devices). Initially, the stromal regions were extracted from the through-focus data set and then thresholded using the threshold subroutine to include all high intensity pixels representing light scattering from the cystine crystals. Threshold regions were set to include pixels intensity from 100 to 255. Pixels within the threshold region were then counted using the Measure subroutine for all planes in the image stack to record the crystal volume. To calculate a percent of crystal volume index (CVI), the crystal volume was divided by the extracted stromal volume multiplied by 100.

Drug Escalation Study and in Vivo Efficacy of Cys-NW by Crystal Volume Measurements. A drug escalation study was conducted in 7 month old $Ctns^{-/-}$ mice, divided into 5 groups, with 5 animals per group. For this experiment, Cys-NWs containing a series of concentrations of Cys for this study were fabricated, i.e., Cys40-NW, Cys15-NW, Cys10-NW, and Cys5-NW (containing 40, 15, 10, and 5 μg of Cys, respectively). Mice were treated daily with the corresponding Cys-NW for 1 week. In addition, a blank PVA-NW was used as a control. The nanowafer was placed on only the right cornea. All mice were subjected to slit-lamp examination for corneal opacities. Because doses that showed questionable opacity levels were not used for the in vivo confocal microscopy experiments, the doses selected for crystal analysis were Cys5-NW and Cys10-NW.

$Ctns^{-/-}$ mice were divided into two groups of five animals each. One group was treated on the right eye with Cys5-NW, and the other group with one Cys10-NW per day for 27 days. Baseline corneal cystine crystal volume was quantified using in vivo confocal microscopy prior to the application of the nanowafers. At the end of the treatment period, the corneal crystal volume was remeasured under exactly the same image capture parameters. Cys10-NW were selected for the in vivo efficacy evaluation experiments.

Again, $Ctns^{-/-}$ mice were divided into two groups of five animals each. The first group was treated with 5 μL of 0.44% Cys solution twice a day, while the second group was treated with one Cys10-NW per day for 30 days.

Measurement of Cystine Concentration in Corneas by Mass Spectrometry. $Ctns^{-/-}$ mice (7 months old) were treated with Cys eye drops, PVA-NW, and Cys-NW for 30 days. Eye drop treatment (5 μL of 0.44% cysteamine solution) was performed twice a day. PVA-NW and Cys-NW treatments were applied once a day. An untreated set of animals was used as control. After the treatment period, mice were euthanized by cervical dislocation under anesthesia, and the eyes were enucleated and preserved in dextran solution (1%) at 4 °C. Corneas were then extracted, cleaned, and perforated with 2 mm biopsy punch, obtaining the central area of the cornea. Three corneas per sample (n = 7) were used. They were ultrasonicated in 100 μL of 0.1 N HCl, and the cystine was extracted using 400 μL of acetonitrile. Samples were

DOI: 10.1021/acs.molpharmaceut.6b00488
Mol. Pharmaceutics XXXX, XXX, XXX−XXX

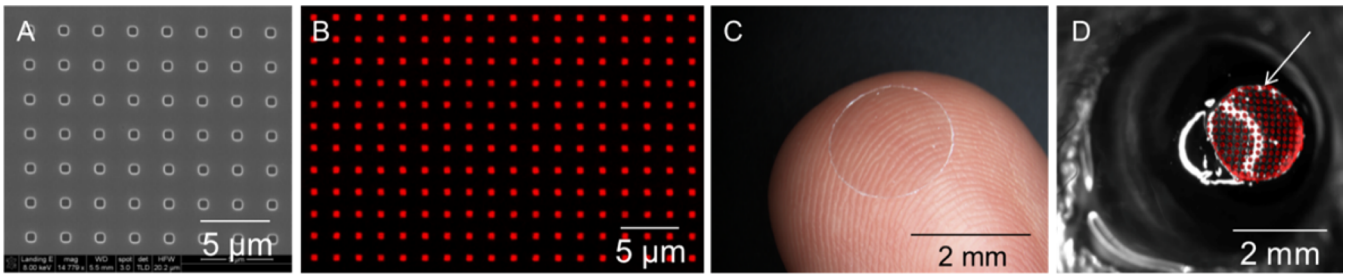

Figure 2. Ocular drug delivery nanowafer. (A) A scanning electron micrograph (SEM) presenting an unfilled nanowafer. (B) Fluorescence image of a red quantum dot-filled nanowafer. (C) Cys-NW on a fingertip demonstrating its transparency. (D) Nanowafer applied on a mouse eye.

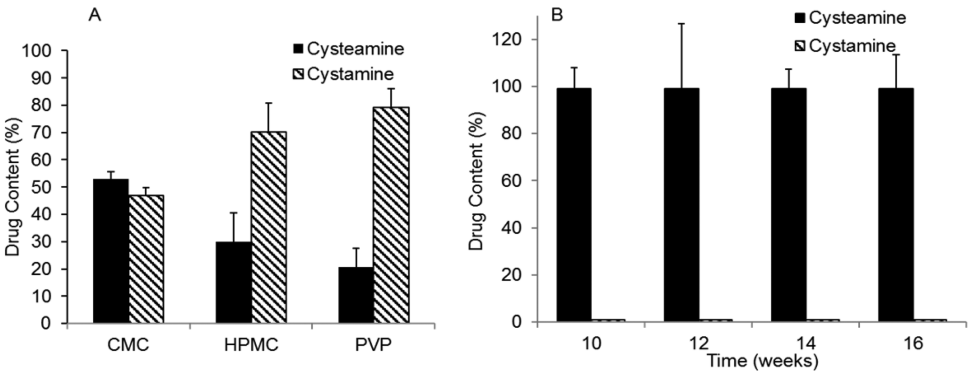

Figure 3. Cys-NW prevents the formation of therapeutically inactive cystamine and improves the drug stability. (A) A plot depicting the rapid deterioration of Cys (monomer) in CMC, HPMC, and PVP nanowafers within 2 weeks. (B) Cys is stable for up to 4 months in PVA nanowafer. Data is expressed as mean ± SEM.

concentrated using a pump dry system, reconstituted in methanol/water (50:50), and analyzed by LC−MS/MS. The multiple reaction monitoring (MRM) transition for cystine was 241/152. Data was expressed as mean ± SEM. Statistical analyses were performed using repeated measures one-way ANOVA with Tukey's multiple comparison post-tests (GraphPad Software, Inc.).

Evaluation of Safety Profile of Cys-NW on Human Corneal Explant Culture. Human corneoscleral tissues, which were not suitable for clinical use, from donors 23−64 years, were obtained from the Lions Eye Bank of Texas (Houston, TX, USA). Human tissues were handled according to the tenets of the Declaration of Helsinki.

Human corneal explant was cultured and maintained using a previously described method with a modification.[39] Briefly, corneoscleral tissues were rinsed with Hank's balanced solution containing gentamicin (50 μg/mL) and amphotericin B (1.25 μg/mL). Once excess sclera tissue was removed, the remaining tissue was cut into equal pieces (approximately 2 × 2 mm^2) using a surgical scalpel. Each explant tissue with epithelium side up was transferred into an 8-well chamber slide. The explants were cultured in Supplemental Hormonal Epithelial Medium (DMEM/F12, 1:1) containing EGF (5 ng/mL), insulin (5 μg/mL), transferrin (5 μg/mL), sodium selenite (5 ng/mL), hydrocortisone (0.5 μg/mL), cholera toxin A (30 ng/mL), 0.5% DMSO, gentamicin (50 μg/mL), and amphotericin B (1.25 μg/mL) and 5% FBS and were maintained at 37 °C with 5% CO_2 and 95% humidity. The culture media were exchanged every 3 days for 14 days.

After 14 days, explant tissues were removed and PVA-NW, Cys eye drop, and Cys-NW were placed in each well; then the culture was maintained at 37 °C with 5% CO_2 and 95% humidity for 24 h. Each well was gently rinsed with PBS and incubated with Hoechst 33342 (10 μg/mL) for 7 min at 37 °C and counterstained with propidium iodide (PI; 2.5 μg/mL). Fluorescence images were obtained using an inverted fluorescence microscope (Nikon Eclipse Ti), and images were analyzed using software IMARIS (Bitplane AG, Zurich, Switzerland) for quantification of stained cells. Cells stained with PI indicated dead cells, and total cell numbers equaled to cells stained with Hoechst 33342. The number of live cells was calculated by subtracting dead cell counts from the total number of cells.

RESULTS

In this study, we present the development of a Cys-NW, wherein the drug carrying polymer and the drug work synergistically to provide an augmented therapeutic effect compared to conventional eye drop therapy.

Cys-NW Fabrication. The Cys-NWs were fabricated via a slightly modified hydrogel template strategy (Figure S1). In this study, poly(vinyl alcohol) (PVA), polyvinylpyrrolidone (PVP), hypromellose (HPMC), and carboxymethyl cellulose (CMC) nanowafers loaded with Cys were fabricated. These polymers were selected for their water solubility, biocompatibility, transparency, and mucoadhesive properties so as to readily adhere to the wet mucosal surface and conform to the curvature of the eye.[40] Aqueous solutions of these polymers are currently in clinical use as artificial tears, and therefore nanowafers fabricated with these polymers can function both as a drug delivery system and also as lubricant.[41] The polymer wafer containing square wells (500 nm × 500 nm and 500 nm depth, with 2 μm spacing) were filled with a thick solution of drug/polymer mixture and punched with a 2 mm paper punch to obtain circular Cys-NW of 2 mm diameter and 80 μm thick circular discs. The nanowafer is a tiny transparent circular disc

DOI: 10.1021/acs.molpharmaceut.6b00488
Mol. Pharmaceutics XXXX, XXX, XXX−XXX

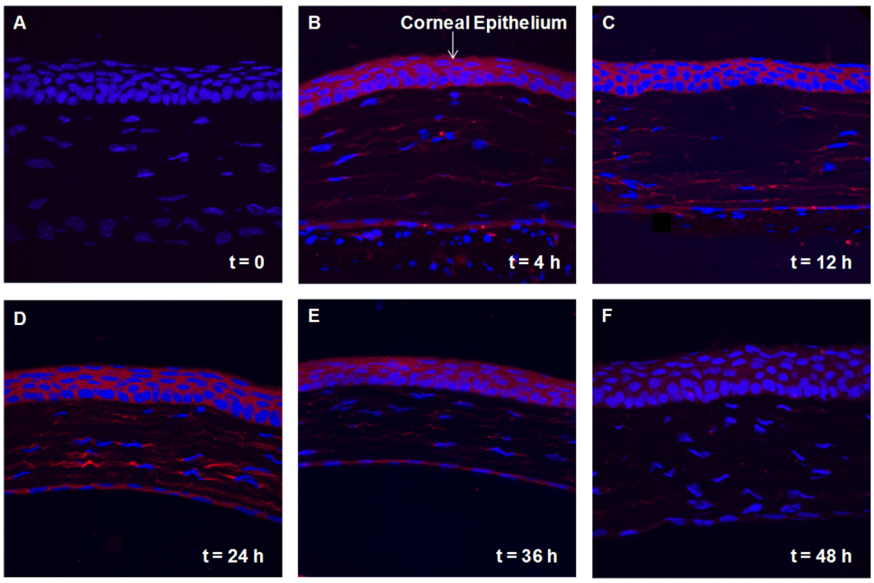

Figure 4. Nanowafer drug delivery enhances the drug diffusion into the cornea. Confocal laser scanning microscopic images of untreated cornea (A) and QD-NW treated corneal sections obtained at regular time intervals demonstrating the QD diffusion and retention in the corneas for up to 48 h (B–F).

that can be applied on the ocular surface with a fingertip and can withstand constant blinking without being displaced (Figure 2). It contains arrays of drug-loaded nanoreservoirs from which the drug will be released in a tightly controlled fashion for an extended period of time. The slow drug release from the nanowafer increases the drug residence time on the ocular surface and its subsequent absorption into the surrounding ocular tissue. At the end of the stipulated period of drug release, the nanowafer will dissolve and fade away.

The Cys-NWs are highly transparent. The refractive index of a Cys-NW is very close to that of a soft contact lens. Also, when a Cys-NW is placed on a fingertip, the fingerprint lines are very clearly visible through the nanowafer (Figure 2C). Hence, nanowafer application on the cornea will not affect the normal vision.

Analysis of Cys-NW Stability. Cys is chemically unstable in eye drop formulation and rapidly oxidizes to its therapeutically inactive dimer cystamine. Hence, the stability of Cys was evaluated in the nanowafer at room temperature. In this study, Cys-NWs fabricated with CMC, HPMC, PVP, and PVA were evaluated. After fabrication, all the nanowafers were stored at room temperature (25 °C). The Cys-NWs were analyzed for pure Cys and its dimer cystamine concentrations by mass spectrometry. Experiment was run in triplicates. This study revealed that, within 2 weeks Cys in CMC, HPMC, and PVP, nanowafers began to dimerize to therapeutically inactive cystamine. As can be seen in Figure 3A, ∼45% of cystamine was formed in CMC nanowafers, while up to 80% of cystamine was formed in HPMC and PVP nanowafers. In the case of PVA nanowafers, Cys is stable and in therapeutically effective form for up to four months when stored at room temperature (Figure 3B), compared to the eye drop formulation in which Cys is stable only for 1 week even under refrigerated conditions.[31] This is possibly because of the ion pairing of Cys with the polymers. In the case of PVA nanowafer, because of the neutral PVA, the Cys molecules are protected in the polymer matrix from dimerization to therapeutically inactive cystamine, thus enhancing its stability. However, Cys slowly started to oxidize after 6 months to its dimer (Figure S2).

Nanowafer Improves Cys Retention Time in the Eye. The mouse cornea is ∼3.2 mm in diameter, and for the in vivo experiments in mice, nanowafers of 2 mm diameter and 80 μm thick were fabricated, so as to exactly fit within the cornea.[42] Since, the nanowafers are fabricated with a mucoadhesive polymer, they readily adhere to the corneal surface. Cys-NW is very soft and stretchable in dry state. The nanowafer, upon application, readily adheres and conforms to the curvature of the cornea. Also, after application of a Cys-NW on the mouse cornea, 5 μL of balanced salt solution (BSS) was added to wet the cornea and further improve the nanowafer adhesion. During the application of the cysteamine nanowafer, no pressure or bending is required. Furthermore, PVA nanowafer is known to elicit negligible inflammatory responses when applied on the eye.[32] The nanowafer was applied on the mouse cornea with forceps followed by the instillation of 5 μL of BSS to wet the surface (Figure 2D).

The in vitro Cys release from the Cys-NW was monitored by mass spectrometry. During the first hour ∼35% Cys was released, and it continued for 6 h under sink conditions (Figure S3). To measure the Cys concentration in the tear washings, Cys-NW were applied on the corneas of healthy mice, and the tear samples were collected at hourly time intervals. Tear samples from Cys-NW treated eyes contained measurable levels of Cys for up to 2 h and was not detectable in the third hour tear samples (Figure S3). However, in the case of topically applied Cys eye drops, Cys was not detected even in the first hour tear samples, indicating its rapid clearance from the ocular surface. PVA is a water-soluble nondegradable polymer. During the course of the drug release the Cys-NW completely dissolves. The drug release from the Cys-NW is a combination of both diffusion and dissolution. No degradation process is required to release the drug. This study reaffirms that the drug molecules do not get sufficient time to diffuse into the ocular tissue because of the rapid clearance of topically applied eye drops due to reflex tearing, blinking, and nasolacrimal drainage. This limits the bioavailability of the drug and results in a compromised therapeutic effect. The nanowafer, upon placement on the eye, slowly releases Cys, thus increasing the drug

DOI: 10.1021/acs.molpharmaceut.6b00488
Mol. Pharmaceutics XXXX, XXX, XXX–XXX

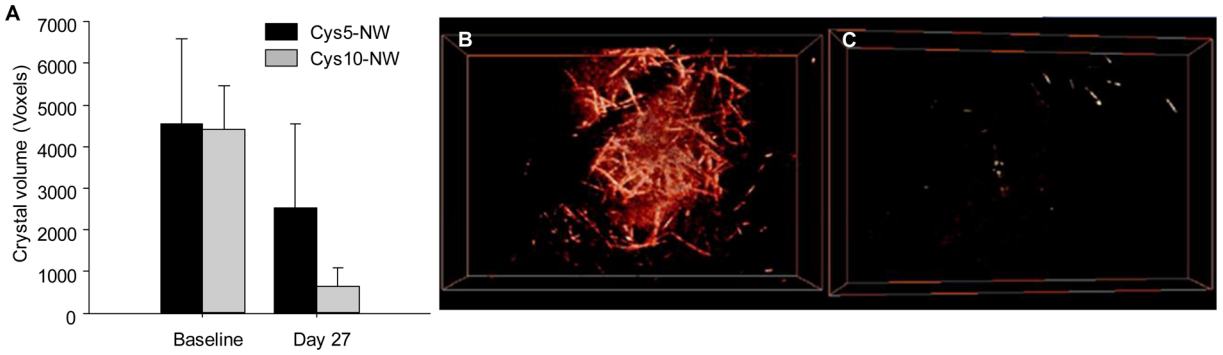

Figure 5. Determination of therapeutically most effective Cys concentration in the nanowafer. (A) A plot depicting the efficacies of Cys5-NW and Cys10-NW on dissolving corneal cystine crystal volume. (B,C) Confocal images of cystine crystal volume change in Cys10-NW treated corneas before and 27 days after Cys-NW therapy.

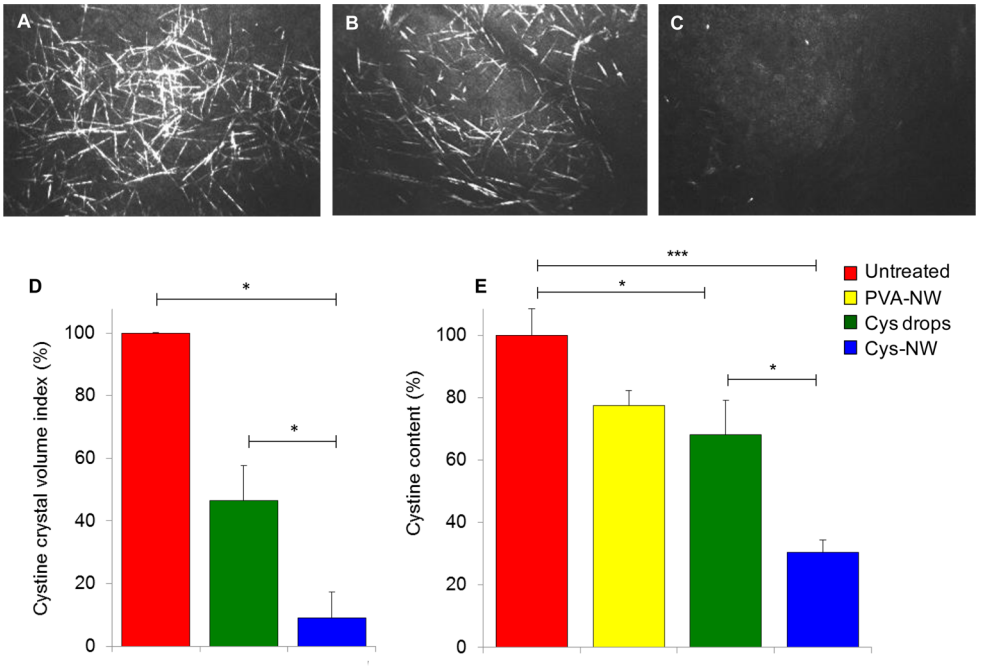

Figure 6. Cys-NW is more efficacious than topical Cys eye drop treatment. Representative laser confocal images of (A) untreated cystinosis cornea, (B) twice a day topical Cys eye drops treated cornea, and (C) once a day Cys-NW treated cornea. (D) A plot depicting the total cystine crystal content in the corneas quantified by laser confocal image analysis (mean ± SD). (E) A plot depicting the total cystine mass content in the corneas quantified by mass spectrometry (mean ± SEM).

residence time on the ocular surface and its subsequent diffusion into the ocular tissue. This increased drug diffusion improves the bioavailability of Cys and enhances its therapeutic efficacy in dissolving the corneal cystine crystals. Furthermore, the desired drug content in Cys-NW and drug release profiles can be modulated by fabricating nanowafers containing drug reservoirs of requisite dimensions. During the course of the drug release, the nanowafer slowly dissolves and eventually disappears. To demonstrate the dissolution and disappearance of the nanowafer with time after its instillation on the ocular surface, a fluorescein loaded nanowafer was placed on the mouse cornea. Bright field microscopy revealed that the nanowafer began to disappear after 1 h of its instillation on the cornea. However, fluorescence microscopy revealed the presence of fluorescein loaded nanowafer on the cornea for up to 4 h. The nanowafer was completely dissolved in 4−5 h and cleared from the ocular surface due to constant blinking (Figure S4). Furthermore, because the nanowafer was fabricated using PVA, which is also in use as artificial tear eye drops, the nanowafer provides lubrication and relief during its dissolution.

To evaluate the ability of a nanowafer to increase the drug molecular residence time on the cornea and its subsequent diffusion into the corneal tissue, a red QD-NW was fabricated and tested on a healthy mouse cornea. Because Cys is nonfluorescent, it cannot be monitored by fluorescence microscopy. Hence, a QD-NW was fabricated to monitor QD diffusion and residence times in the cornea by fluorescence microscopy. The QD-NW were fabricated using hydrophobic CdSe/ZnS core−shell-type quantum dots stabilized with octadecylamine ligands. The fluorescence emission wavelength of the QD-NW is λ_{em} 580 nm. Although, this is not an exact replication of Cys diffusion into the cornea, this study provides evidence for the drug diffusion into the cornea. Upon placement of the QD-NW on the mouse cornea, the QDs began to diffuse into the corneal tissue, and it was observed for up to 48 h (Figure 4). At this point, the fluorescence intensity

DOI: 10.1021/acs.molpharmaceut.6b00488
Mol. Pharmaceutics XXXX, XXX, XXX−XXX

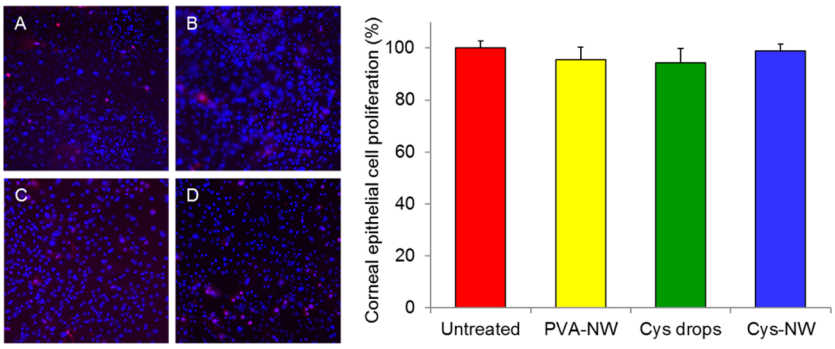

Figure 7. Safety profile of Cys-NW on human corneal explant epithelial cell cultures. Fluorescence micrographs of human corneal epithelial cells after live−dead cell assay: (A) untreated, (B) PVA-NW treated, (C) Cys-eye drop treated, and (D) Cys-NW treated human corneal epithelial cells. (E) A plot depicting the percentage of live human corneal epithelial cells after the treatments.

of the QDs in the corneal tissue began decreasing as the QDs diffuse through the cornea and reach the aqueous humor in the anterior chamber and cleared through the trabecular meshwork.

Determination of Therapeutically Most Effective Dose. Drug escalation studies were conducted to determine the maximum tolerated dose and to minimize the drug related acute toxicity. Administration of maximum tolerated dose is usually associated with maximum clinical benefit. Maximum tolerated drug dose was determined by monitoring corneal opacity in mice. Cys-NWs containing a series of concentrations of Cys for this study were fabricated, i.e., Cys40-NW, Cys15-NW, Cys10-NW, and Cys5-NW (containing 40, 15, 10, and 5 μg of Cys, respectively), and a blank PVA-NW was used as control. Maximum tolerated dose was evaluated in cystinosin knockout mice ($Ctns^{-/-}$ mice). In these mice, the cystine crystals begin to appear at 3 months of age in the corneal endothelium, and the crystal content progressively increases up to 7 months, followed by corneal scarring, thus mimicking the clinical disease progression seen in humans.[43] The $Ctns^{-/-}$ mice (7 months old) were divided into 5 groups, treated with the corresponding Cys-NW for 1 week, and examined using slit lamps imaging at the end of the treatment period. Slit lamp examination revealed no visible corneal opacities in mouse groups treated with PVA-NW, Cys5-NW, and Cys10-NW. In the case of Cys15-NW and Cys40-NW treated mouse groups, the eyes began to develop slight corneal opacification, and the experiments were discontinued. Based on these results, Cys10-NW and Cys5-NW were selected for the determination of therapeutically most effective dose.

The therapeutically most effective concentration of Cys-NW was evaluated in $Ctns^{-/-}$ mouse model by measuring the reduction in the corneal cystine crystal volume. In this study, $Ctns^{-/-}$ mice were divided into two groups. Baseline corneal cystine crystal volume was quantified using in vivo confocal microscopy in the right eye of each animal prior to the application of Cys-NW.[37,38] A Cys-NW was placed on the right eye every day for 27 days. At the end of the treatment period, the corneal crystal volume was remeasured under exactly the same image capture parameters. Cys10-NW was more effective in dissolving the corneal cystine crystals compared to Cys5-NW (Figure 5).

Cys-NW Is More Efficacious than Topical Cys Eye Drop Treatment. To determine the in vivo efficacy of Cys10-NW in comparison to topical Cys eye drop formulation (0.44%), two groups of $Ctns^{-/-}$ mice (three per group) were treated separately with Cys-NW (10 μg of Cys, once a day) and Cys eye drops (5 μL, 22 μg) twice a day for 30 days. At the end of this period, the cystine crystal content in the corneas was estimated by laser confocal image analysis.[33,34] These studies revealed that, compared to the baseline corneal cystine crystal volume, twice a day Cys eye drop treatment reduced the crystal volume by 55%, while the once a day Cys-NW treatment reduced the crystal volume by 90%, confirming that the Cys-NW treatment is significantly more efficacious than Cys eye drop treatment (Figure 6A-D).

At this point, although the Cys-NW is very effective in dissolving cystine crystals, the confocal microscopic analysis was able to quantify only up to the submicron sized cystine crystals and not the molecular cystine content present in the corneal epithelium. Therefore, the efficacy of the nanowafer was also evaluated by measuring the amount of cystine present in cystinosis mice corneas using mass spectrometry.

This study revealed that once a day Cys10-NW treatment for 30 days reduced the corneal cystine mass by 65%, while twice a day administration of Cys eye drops during the same treatment period resulted in a decrease in corneal cystine content by 34%, compared to the untreated control group (Figure 6E). Furthermore, the amount of Cys delivered per day by the nanowafer was 10 μg, while the twice a day Cys eye drop treatment delivered 44 μg. These results reaffirmed the enhanced efficacy of Cys10-NW with half the drug dosage compared to the topical Cys eye drop treatment, as observed in confocal microscopic analysis. The blank PVA wafer (control) was able to dissolve a small amount of the corneal cystine crystals. A possible reason could be, since the PVA wafer is in close contact with the cornea, some cystine crystals must have been dissolved by PVA due to hydrotropic effect.[44]

The enhanced efficacy of Cys-NW in dissolving cystine crystals is mainly because of the increased drug residence time on the cornea, which enabled the Cys molecules to diffuse into the corneal epithelium. Once the Cys molecules penetrate into the cornea, they react with cystine molecules to form cysteine-cysteamine mixed disulfide, which will be cleared from the cornea. Topically applied eye drops will be rapidly cleared from the ocular surface due to blinking and have a very short contact time on the ocular surface. As a consequence, the drug absorption is severely limited by the ocular surface barriers resulting in extremely low bioavailability. For this reason, topical Cys eye drops must be administered several times in a day to achieve a measurable therapeutic effect.

Safety Profile of Cys-NW on Human Corneal Explant Epithelial Cultures. The safety of Cys-NW was examined on human corneal explant epithelial cells. In this study, human corneal explants were cultured in a 12-well plate to promote the

DOI: 10.1021/acs.molpharmaceut.6b00488
Mol. Pharmaceutics XXXX, XXX, XXX−XXX

proliferation of corneal epithelial cells.[39] Monolayers of human corneal epithelial cells formed in the wells were separately treated with PVA-NW, Cys eye drops, and Cys-NW, respectively, followed by live−dead cell assay. In this study, no significant cell death was observed with Cys eye drops and Cys-NW treatments, when compared to the untreated human corneal cell monolayers (Figure 7). This study revealed that Cys-NW is as safe as Cys eye drops on human corneal explant epithelial cell cultures.

DISCUSSION

The ultimate goal of this work was to develop a nanowafer therapeutic that can efficiently deliver Cys for an extended period of time and enhance the therapeutic efficacy. A cystinosis patient has to instill the Cys eye drops on the eyes at least 6−12 times in a day for several years.[27] This is very inconvenient and also unlikely that it will be applied in a timely manner every day, resulting in patient noncompliance and compromised therapeutic efficacy. Furthermore, considering the fact that the cystinosis patients are generally school going children and young adults, noncompliance to Cys eye drop treatment and drug related side effects become more significant.

The results of this study confirm that Cys-NW is more efficacious than the topical eye drop formulations. This study also demonstrated that the enhanced efficacy of Cys-NW is due to the longer residence time of the drug molecules on the eye, which enabled their diffusion into the ocular surface epithelium, unlike eye drops, which will be cleared from the ocular surface within a few minutes due to reflex tearing and rapid blinking. The nanowafer readily adheres to the ocular surface and can withstand constant blinking without being displaced. The nanowafer will completely dissolve in 4−5 h and cleared from the ocular surface due to constant blinking. Hence, there will be no accumulation of the polymer on the eye. Drug release from the nanowafer can be controlled by choosing the right drug reservoir dimension and drug loading concentration. Thus, the drug release from the nanowafer can be programmed to have prolonged drug efficacy to suit patient's requirements. For the in vivo mouse study, 2 mm diameter nanowafers were fabricated; however for human applications, a larger nanowafer (of 8 mm diameter) will be fabricated that can be applied on the eye with a fingertip.

The nanowafer drug delivery system presents several advantages compared to the conventional ophthalmic solutions applied as topical eye drops and drug delivery contact lenses. Nanowafers are designed for controlled release ocular drug delivery applications. The nanowafers are easy to fabricate, more efficacious at a lower dosing frequency, provide a sustained drug availability in the eye, and protect the drug from deterioration. The nanowafer can release the drug in a therapeutically effective concentration and at the end of the stipulated period of drug release, the nanowafer will dissolve and fade away, i.e., "self-clearing" and does not need to be removed. Because the drug molecules slowly diffuse from the polymer matrix of the nanowafer, they are protected from degradation and rapid release. The nanowafers are fabricated with polymers that are currently in clinical use as artificial tear eye drops, and therefore, the nanowafers can function both as a drug delivery system and also as lubricant. The nanowafer therapeutic can provide mechanical barrier to protect the eye from desiccation. These attributes of the nanowafer will improve patient comfort and compliance to treatment. Since, the polymers and drugs used in the nanowafer fabrication are already in clinical use, the nanowafer can be rapidly translated to the clinic for human use.

The Cys-NW was fabricated using PVA, which is in clinical use as artificial tears. Also, PVA is noninflammatory and nontoxic on the ocular surface even after prolonged usage.[45,46] Therefore, as a nanowafer, PVA can function both as a drug delivery system and also as a lubricant on the ocular surface. Furthermore, PVA nanowafer is known to elicit negligible inflammatory responses when applied on the eye.[32] Because of its enhanced therapeutic efficacy, safety profile, and extended stability at room temperature, Cys-NW is a major advancement in the treatment and management of corneal cystinosis.

The enhanced therapeutic efficacy and translational potential of Cys-NW in comparison to topical Cys eye drop treatment has been demonstrated in treating corneal cystinosis in $Ctns^{-/-}$ mouse model. This study may not exactly represent the clinical situations, and whether Cys-NW can be effective in humans requires further investigation. Although, Cys and PVA are independently in clinical use as ophthalmic solutions, the efficacy of Cys and PVA as a nanowafer therapeutic needs to be thoroughly evaluated in human clinical trials. The nanowafer drug delivery system holds promise for future research not only in exploring its broad applicability in treating other ocular surface diseases but also in translational medicine.

CONCLUSIONS

This study has demonstrated the enhanced therapeutic efficacy and translational potential of Cys-NW in comparison to topical Cys eye drops in treating corneal cystinosis in $Ctns^{-/-}$ mouse model. For human use, the Cys-NW can be applied on the eye with a fingertip like a contact lens, and it will remain in the eye to deliver the drug for a longer duration of time, thus enhancing the drug residence time, bioavailability, therapeutic efficacy, and treatment compliance. The nanowafer is self-clearing, i.e., during the course of the drug release it will dissolve and eventually disappear. The human corneal explant epithelial culture studies have revealed negligible cytotoxic effects of Cys-NW. Furthermore, the nanowafer prevents oxidation of Cys to its therapeutically inactive disulfide form cystamine, thus enhancing its stability and shelf life at room temperature. The nanowafer drug delivery system is broadly applicable and holds promise for future research in treating other eye diseases, such as dry eye, ocular infections, eye injuries, and glaucoma.

ASSOCIATED CONTENT

Supporting Information

The Supporting Information is available free of charge on the ACS Publications website at DOI: 10.1021/acs.molpharmaceut.6b00488.

Schematic of the nanowafer fabrication, stability of Cys-NW, and the drug residence time on the ocular surface (PDF)

AUTHOR INFORMATION

Corresponding Authors

*E-mail: jens@uci.edu. Phone: 949-824-4122. Fax: 949-824-4015.

*E-mail: gacharya@bcm.edu. Phone: 713-798-7701. Fax: 713-798-1457.

DOI: 10.1021/acs.molpharmaceut.6b00488
Mol. Pharmaceutics XXXX, XXX, XXX−XXX

Author Contributions

The manuscript was written through contributions of all authors. All authors have given approval to the final version of the manuscript.

Notes

The authors declare no competing financial interest.

■ ACKNOWLEDGMENTS

The authors gratefully acknowledge the Alkek Center for Molecular Discovery−Metabolomics core facility for the mass spectrometry analysis. Funding: Cystinosis Research Foundation, Irvine, CA (Award No. CRF-53944, CRFS-2014-008), Department of Defense (Award No. 1W81XWH-13-1-0146), Research to Prevent Blindness (New York, NY, USA), and Alkek Award for Experimental Therapeutics.

■ REFERENCES

(1) Hubbell, J. A.; Chilkoti, A. Nanomaterials for Drug Delivery. *Science* **2012**, *337*, 303−305.
(2) Kearney, C. J.; Mooney, D. J. Macroscale Delivery Systems for Molecular and Cellular Payloads. *Nat. Mater.* **2013**, *12*, 1004−1017.
(3) Seliktar, D. Designing Cell-Compatible Hydrogels for Biomedical Applications. *Science* **2013**, *336*, 1124−1128.
(4) Hubbell, J. A.; Langer, R. Translating Materials Design to the Clinic. *Nat. Mater.* **2013**, *12*, 963−966.
(5) Akpek, E. K.; Gottsch, J. D. Immune Defense at the Ocular Surface. *Eye* **2003**, *17*, 949−956.
(6) Forrester, J. V.; Xu, H. Good News−Bad News: The Yin and Yang of Immune Privilege in the Eye. *Front. Immunol.* **2012**, *3*, 338.
(7) Dobrovolskaia, M. A.; McNeil, S. E. Immunological Properties of Engineered Nanomaterials. *Nat. Nanotechnol.* **2007**, *2*, 469−478.
(8) Dobrovolskaia, M. A.; Germolec, D. R.; Weaver, J. L. Evaluation of Nanoparticle Immunotoxicity. *Nat. Nanotechnol.* **2009**, *4*, 411−414.
(9) Li, P.; Poon, Y. F.; Li, W.; Zhu, H.-Y.; Yeap, S. H.; Cao, Y.; Qi, X.; Zhou, C.; Lamrani, M.; Beuerman, R. W.; Kang, E.-T.; Mu, Y.; Li, C. M.; Chang, M. W.; Leong, S. S.; Chan-Park, M. B. A Polycationic Antimicrobial and Biocompatible Hydrogel with Microbe Membrane Suctioning Ability. *Nat. Mater.* **2011**, *10*, 149−156.
(10) Gahl, W. A.; Thoene, J.; Schneider, J. Cystinosis: A Disorder of Lysosomal Membrane Transport. In *Metabolic and Molecular Basis of Inherited Disease*; Scriver, C. J., Beaudet, A. L., Sly, W. S., Valle, D., Eds.; McGraw-Hill: New York, 2001; pp 5085−5108.
(11) Kalatzis, V.; Cherqui, S.; Antignac, C.; Gasnier, B. Cystinosin, the Protein Defective in Cystinosis, is a H+-Driven Lysosomal Cystine Transporter. *EMBO J.* **2001**, *20*, 5940−5949.
(12) Tsilou, E.; Zhou, M.; Gahl, W.; Sieving, P. C.; Chan, C. C. Ophthalmic Manifestations and Histopathology of Infantile Nephropathic Cystinosis: Report of a Case and Review of the Literature. *Surv. Ophthalmol.* **2007**, *52*, 97−105.
(13) Gahl, W. A.; Kuehl, E. M.; Iwata, F.; Lindblad, A.; Kaiser-Kupfer, M. I. Corneal Crystals in Nephropathic Cystinosis: Natural History and Treatment with Cysteamine Eyedrops. *Mol. Genet. Metab.* **2000**, *71*, 100−120.
(14) Shams, F.; Livingstone, I.; Oladiwura, D.; Ramaesh, K. Treatment of Corneal Cystine Crystal Accumulation in Patients with Cystinosis. *Clin. Ophthalmol.* **2014**, *8*, 2077−2084.
(15) Kaiser-Kupfer, M. I.; Fujikawa, L.; Kuwabara, T.; Jain, S.; Gahl, W. A. Removal of Corneal Crystals by Topical Cysteamine in Nephropathic Cystinosis. *N. Engl. J. Med.* **1987**, *316*, 775−779.
(16) Jones, N. P.; Postlewaite, J.; Noble, J. L. Clearance of Corneal Crystals in Nephropathic Cystinosis by Topical Cysteamine 0.5%. *Br. J. Ophthalmol.* **1991**, *75*, 311−312.
(17) Tsilou, E. T.; Thompson, D.; Lindblad, A. S.; Reed, G. F.; Rubin, B.; Gahl, W.; Thoene, J.; Del Monte, M.; Schneider, J. A.; Granet, D. B.; Kaiser-Kupfer, M. I. A Multi-Centered Randomized Double Masked Clinical Trial of a New Formulation of Topical Cysteamine for the Treatment of Corneal Cystine Crystals in Cystinosis. *Br. J. Ophthalmol.* **2003**, *87*, 28−31.
(18) Dufier, J. L. Evolution of Ocular Manifestations in Nephropathic Cystinosis: a Long Term Study of a Population Treated with Cysteamine. *J. Pediatr. Ophthalmol. Strabismus.* **2003**, *40*, 142−146.
(19) Kaiser-Kupfer, M. I.; Gazzo, M. A.; Datiles, M. B.; Caruso, R. C.; Kuehl, E. M.; Gahl, W. A. A Randomized Placebo-Controlled Trial of Cysteamine Eye Drops in Nephropathic Cystinosis. *Arch. Ophthalmol.* **1990**, *108*, 689−693.
(20) Cantani, A.; Giardini, O.; Cantani, A. C. Nephropathic Cystinosis: Ineffectiveness of Cysteamine Therapy for Ocular Changes. *Am. J. Ophthalmol.* **1983**, *9*, 713−714.
(21) Gahl, W. A.; Tietze, F.; Butler, J. D.; Schulman, J. D. Cysteamine Depletes Lysosomal Cystine by the Mechanism of Disulfide Interchange. *Biochem. J.* **1985**, *228*, 545−550.
(22) Pisoni, R. L.; Thoene, J. G.; Christensen, H. N. Detection and Characterization of Carrier-Mediated Cationic Amino Acid Transport in Lysosomes of Normal and Cystinotic Human Fibroblasts. *J. Biol. Chem.* **1985**, *260*, 4791−4798.
(23) Jezegou, A.; Llinares, E.; Anne, C.; Kieffer-Jaquinod, S.; O'Regan, S.; Aupetit, J.; Chabli, A.; Sagne, C.; Debacker, C.; Chadefaux-Vekemans, B.; Journet, A.; Andre, B.; Gasnier, B. Heptahelical protein PQLC2 is a Lysosomal Cationic Amino Acid Exporter Underlying the Action of Cysteamine in Cystinosis Therapy. *Proc. Natl. Acad. Sci. U. S. A.* **2012**, *109*, 20180−20181.
(24) Cystaran is the only FDA-Approved Ophthalmic Therapy for Corneal Crystals in Cystinosis Patients. http://www.cystaran.com.
(25) Novack, G. D. Ophthalmic Drug Delivery: Development and Regulatory Considerations. *Clin. Pharmacol. Ther.* **2009**, *85*, 539−543.
(26) Mannermaa, E.; Vellonen, K.-S.; Urtti, A. Drug Transport in Corneal Epithelium and Blood Retina Barrier: Emerging Role of Transporters in Ocular Pharmacokinetics. *Adv. Drug Delivery Rev.* **2006**, *58*, 1136−1163.
(27) Gahl, W. A.; Kuehl, E. M.; Iwata, F.; Lindblad, A.; Kaiser-Kupfer, M. I. Corneal Crystals in Nephropathic Cystinosis: Natural History and Treatment with Cysteamine Eyedrops. *Mol. Genet. Metab.* **2000**, *71*, 100−120.
(28) MacDonald, I. M.; Noel, L. P.; Mintsioulis, G.; Clarke, W. N. The Effect of Topical Cysteamine Drops on Reducing Crystal Formation within the Cornea of Patients Affected by Nephropathic Cystinosis. *J. Pediatr. Ophthalmol. Strabismus* **1990**, *27*, 272−274.
(29) Iwata, F.; Kuehl, E. M.; Reed, G.; McCain, L.; Gahl, W. A.; Kaiser-Kupfer, M. A Randomized Clinical Trial of Topical Cysteamine Disulfide (Cystamine) versus Free Thiol (Cysteamine) in the Treatment of Corneal Cystine Crystals in Cystinosis. *Mol. Genet. Metab.* **1998**, *64*, 237−242.
(30) Purkiss, R. Stability of Cysteamine Hydrochloride in Solution. *J. Clin. Pharm. Ther.* **1977**, *2*, 199−203.
(31) Cystaran (cysteamine ophthalmic solution) 0.44% Sterile, Prescribing Information: http://www.cystaran.com/Cystaran_PI.pdf.
(32) Yuan, X.; Marcano, D. C.; Shin, C. S.; Hua, X.; Isenhart, L. C.; Pflugfelder, S. C.; Acharya, G. Ocular Drug Delivery Nanowafer with Enhanced Therapeutic Efficacy. *ACS Nano* **2015**, *9*, 1749−1758.
(33) Coursey, T. G.; Henriksson, J. T.; Marcano, D. C.; Shin, C. S.; Isenhart, L. C.; Ahmed, F.; De Paiva, C. S.; Pflugfelder, S. C.; Acharya, G. Dexamethasone Nanowafer as an Effective Therapy for Dry Eye Disease. *J. Controlled Release* **2015**, *213*, 168−174.
(34) Acharya, G.; Shin, C. S.; Vedantham, K.; McDermott, M.; Rish, T.; Hansen, K.; Fu, Y.; Park, P. A Study of Drug Release from Homogeneous PLGA Microstructures. *J. Controlled Release* **2010**, *146*, 201−206.
(35) Acharya, G.; Shin, C. S.; McDermott, M.; Mishra, H.; Park, H.; Kwon, I. C.; Park, K. The Hydrogel Template Method for Fabrication of Homogeneous Nano/Microparticles. *J. Controlled Release* **2010**, *141*, 314−319.
(36) Corrales, R. M.; Villarreal, A.; Farley, W.; Stern, M. E.; Li, D. Q.; Pflugfelder, S. C. Strain-Related Cytokine Profiles on the Murine Ocular Surface in Response to Desiccating Stress. *Cornea* **2007**, *26*, 579−584.

DOI: 10.1021/acs.molpharmaceut.6b00488
Mol. Pharmaceutics XXXX, XXX, XXX−XXX

(37) Simpson, J.; Nien, C. J.; Flynn, K.; Jester, B.; Cherqui, S.; Jester, J. Quantitative in vivo and ex vivo Confocal Microscopy Analysis of Corneal Cystine Crystals in the Ctns−/− Knockout Mouse. *Mol. Vis.* **2011**, *17*, 2212−2220.
(38) Simpson, J. L.; Nien, C. J.; Flynn, K. J.; Jester, J. V. Evaluation of Topical Cysteamine Therapy in the CTNS−/− Knockout Mouse Using in vivo Confocal Microscopy. *Mol. Vis.* **2011**, *17*, 2649−2654.
(39) Li, D. Q.; Lokeshwar, B. L.; Solomon, A.; Monroy, D.; Ji, Z.; Pflugfelder, S. C. Regulation of MMP-9 Production by Human Corneal Epithelial Cells. *Exp. Eye Res.* **2001**, *73*, 449−59.
(40) Ludwig, A. The Use of Mucoadhesive Polymers in Ocular Drug Delivery. *Adv. Drug Delivery Rev.* **2005**, *57*, 1595−1639.
(41) Moshirfar, M.; Pierson, K.; Hanamaikai, K.; Santiago-Caban, L.; Muthappan, V.; Passi, S. F. Artificial Tears Potpourri: A Literature Review. *Clin. Ophthalmol.* **2014**, *8*, 1419−1433.
(42) Remtulla, S.; Hallett, P. E. A Schematic Eye for the Mouse, and Comparisons with the Rat. *Vision Res.* **1985**, *25*, 21−31.
(43) Kalatzis, V.; Serratrice, N.; Hippert, C.; Payet, O.; Arndt, C.; Cazevieille, C.; Maurice, T.; Hamel, C.; Malecaze, F.; Antignac, C.; Muller, A.; Kremer, E. J. The Ocular Anomalies in a Cystinosis Animal Model Mimic Disease Pathogenesis. *Pediatr. Res.* **2007**, *62*, 156−162.
(44) Lee, S. C.; Acharya, G.; Lee, J.; Park, K. Hydrotropic Polymers: Synthesis and Characterization of Polymers Containing Picolylnicotinamide Moieties. *Macromolecules* **2003**, *36*, 2248−2255.
(45) White, C. J.; Thomas, C. R.; Byrne, M. E. (2014). Bringing Comfort to the Masses: a Novel Evaluation of Comfort Agent Solution Properties. *Cont Lens Anterior Eye* **2014**, *37*, 81−91.
(46) Chauhan, N. P. S.; Pathak, A. K.; Bhanat, K.; Ameta, R.; Rawal, M. K.; Punjabi, P. B. Pharmaceutical Polymers. In *Encyclopedia of Biomedical Polymers and Polymeric Biomaterials*; Mishra, M., Ed.; Taylor and Francis: New York, 2015; pp 5929−5942.

DOI: 10.1021/acs.molpharmaceut.6b00488
Mol. Pharmaceutics XXXX, XXX, XXX−XXX

Appendix 4: Conference paper

Acharya et al, Nanowafer Drug Delivery to Treat Corneal Neovascularization. *Invest. Ophthalmol. Vis. Sci.* 2015; 56(7):5032

studies showed increased internalization of targeted micelles as compared to non-taregeted micelles.
Conclusions: Folic acid conjugated Vitmain E TPGS was successfully synthesized. Highly hydrophobic drugs like FA can be formulated into clear aqueous eye drops. Folic acid targeted micelles can be utilized to efficiently deliver drugs to retinal and other ocular tissues.
Commercial Relationships: Sujay J. Shah, None; **Sulabh Patel**, None; **Ashaben Patel**, None; **Ashim K. Mitra**, None
Support: NIH Grant 2 R01 EY010659-12A2

Program Number: 5031 **Poster Board Number:** C0008
Presentation Time: 3:45 PM–5:30 PM
Functionalized nanoparticle technology for enhanced drug delivery
Jai Parekh, David Freilich, Stephanie Youlios, Sima Parekh, Uday Kompella. EyeTrans Technologies, New York City, NY.
Purpose: Due to short residence time of eye drops, drug bioavailability to the eye surface is low, particularly for poorly soluble and poorly permeable drugs, necessitating frequent dosing in treating dry eye and glaucoma. Following intravitreal injections, target specific delivery is currently not feasible for macromolecule and small molecule drugs useful in treating wet age-related macular degeneration and other back of the eye diseases. To address these unmet needs our objective is to develop novel nanoparticle based technologies for topical and intraocular drug and gene delivery.
Methods: Small nanoparticles technologies capable of drug encapsulation and surface modification with hydrophilic cell recognizing components (functionalized nanoparticles) were designed to enhance mucus penetration as well as epithelial surface recognition and uptake. These technologies licensed by EyeTrans are under development for ocular drug delivery and therapy. The nanoparticle technologies utilize a drug carrier, a ligand on the particle surface to recognize cell surface, and other polymers to enhance delivery or stabilize the particle.
Results: This presentation will describe nanoparticle preparation and evidence to date indicating that surface functionalization enhances ocular surface tissue uptake as well as retinal pigment epithelial cell uptake of nanoparticles in ex vivo/in vitro studies. Further, it will describe evidence indicating that dosing with biodegradable functionalized nanoparticles enhances drug delivery to the tissues of the eye in an animal model.
Conclusions: Nanoparticle and drug delivery can be enhanced by using particle surface features that allow tissue recognition and uptake.
Commercial Relationships: Jai Parekh, EyeTrans Technologies (S); **David Freilich**, EyeTrans Technologies (S); **Stephanie Youlios**, None; **Sima Parekh**, None; **Uday Kompella**, EyeTrans Technologies (P), EyeTrans Technologies (S)

Program Number: 5032 **Poster Board Number:** C0009
Presentation Time: 3:45 PM–5:30 PM
Nanowafer Drug Delivery to Treat Corneal Neovascularization
Ghanashyam Acharya, Xiaoyong Yuan, Daniela Marcano, Crystal Shin, Xia Hua, Lucas Isenhart, Stephen C. Pflugfelder. Ophthalmology, Baylor College of Medicine, Houston, TX.
Purpose: Development of a controlled release nanowafer drug delivery system for treating corneal neovascularization.
Methods: The axitinib-nanowafers (Axi-NW) were fabricated *via* the hydrogel template strategy with a few modifications. The nanowafers thus prepared were tested in ocular burn induced murine model. The corneas were subjected to laser scanning confocal imaging and RT-PCR analysis of gene expression.
Results: The nanowafer is a tiny transparent circular disc containing arrays of drug loaded nanoreservoirs (**Figure 1**). The *in vivo* therapeutic efficacy of the nanowafer was demonstrated by treating corneal neovascularization (CNV) in a murine ocular burn (OB) model. In this study, once a day Axi-5-NW treatment was compared with Axi eye drops (0.1%) administered twice a day for its therapeutic effect in inhibiting CNV in OB mouse model. The Axi-5-NW treatment restricted the proliferation of blood vessels to the limbal area and treated eyes very closely resembled the healthy uninjured cornea. However, the OB controls - PVA-NW and Axi eye drop treated corneas exhibited extensive neovascularization (**Figure 2a-e**). In the case of Axi-5-NW treatment, the amount of drug delivered to the cornea was 5 μg per day, and for axitinib eye drop treatment it was 10 μg per day. Although, eye drop treated mice received twice the drug dosage as those treated with Axi-5-NW, still Axi-5-NW treatment was twice as efficacious as the eye drop treatment (**Figure 2f**). The RT-PCR study revealed that Axi-NW was very effective in downregulating the drug target genes VEGF-A, VEGF-R1, VEGF-R2, PDGFR-A, PDGFR-B, TNF-α, bFGF and TGF-β, compared to the untreated OB and Axi-eye drop treatment.
Conclusions: Once a day axitinib delivery by the nanowafer is more efficacious than the twice a day topical eye drop treatment.

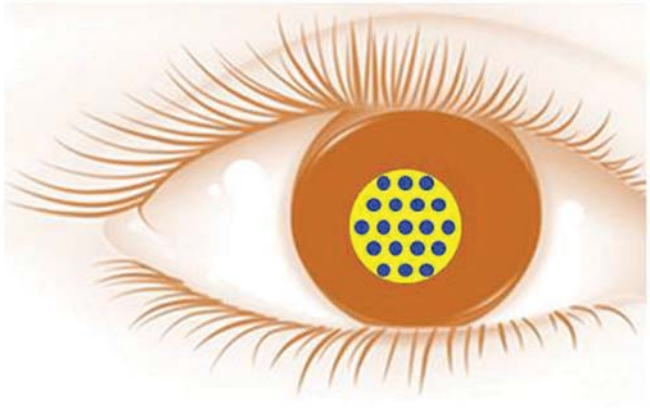

Figure 1. Schematic of the Ocular drug delivery nanowafer instilled on the cornea.

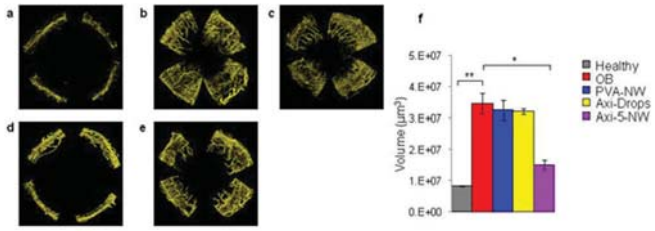

Figure 2. Axitinib-nanowafer is more efficacious than the topical eye drop treatment. Confocal fluorescence images revealing the enhanced therapeutic efficacy of Axi-nanowafer. **a**, Healthy cornea. **b**, OB induced cornea. **c**, PVA-NW. **d**, Axi-NW. **e**, Twice a day Axi-eye drop (0.1%) treatment. **f**, Quantification of corneal neovascularization volume. n = 3 animals,
* P<0.05 vs OB control. All error bars represent standard deviation from the mean.
Commercial Relationships: Ghanashyam Acharya, None; **Xiaoyong Yuan**, None; **Daniela Marcano**, None; **Crystal Shin**, None; **Xia Hua**, None; **Lucas Isenhart**, None; **Stephen C. Pflugfelder**, None

Appendix 5: Conference paper

Shin et al, Nanowafer Drug Delivery for Restoration of Healthy Ocular Surface in Dry Eye Condition. *Invest. Ophthalmol. Vis. Sci.* 2015; 56(7):321.

USA). A control group (4) was left untreated and received no eye drops, but was kept under the same conditions as the therapy groups. Clinical readouts were undertaken weekly (amount of tear fluid; corneal epithelial staining) in combination with a final preparation of conjunctival tissue for counting goblet cell density.
Results: Senescent mice showed a significantly higher increase in epithelial staining after 14 days of EDE and a significantly stronger reduction of tear production compared to young mice. Therapeutic treatment of mice with ScA/F4H5 showed a significantly earlier and stronger increase of tear production and an earlier decrease of epithelial damage following EDE compared to untreated controls, F4H5 alone and Restasis® in both age groups. Clinically senescent mice developed a more severe EDE and efficacy of F4H5/CsA was detected later (after 3 weeks of therapy) than in younger mice (after 1 week).
Conclusions: CsA in F4H5 is highly effective in reducing corneal staining and maintaining conjunctival goblet cells in EDE. Compared to Restasis®, F4H5/CsA was shown to be equally effective, but with a faster therapeutic response in this study. Based on these results first applications in humans are on the way that may lead to a new therapeutic option in treating dry eye disease.
Commercial Relationships: Uta Gehlsen, None; **Tobias Braun**, None; **Claus Cursiefen**, Allergan (C), Gene Signal (C), Novaliq (C); **Philipp Steven**, Novaliq (F)

Program Number: 320 **Poster Board Number:** C0205
Presentation Time: 8:30 AM–10:15 AM
Conjunctival Aquaporins Are Involved in the Resolution of Ocular Phenotype in a Rabbit Dry Eye Model
Dhruva Bhattacharya[1], Yuan Ning[2, 3], Fangkun Zhao[2, 3], Rongji Chen[1], Jinsong Zhang[2, 3], Mingwu Wang[1]. [1]Ophthalmology and Vision Science, University of Arizona College of Medicine, Tucson, AZ; [2]The Fourth Affiliated Hospital of China Medical University, Liaoning Province, China; [3]Eye Hospital of China Medical University, Liaoning Province, China.
Purpose: Longitudinal study of a rabbit dry eye model (over 4-months) found a spontaneous resolution of the dry eye phenotype. Mechanisms of tear fluid compensation in the absence of lacrimal gland were explored.
Methods: A rabbit dry eye model was created by bilateral resection of lacrimal gland (LG), Hardarian gland (HG) and nictitating membrane (NM). Ocular surface of these rabbits (N=8) were characterized by clinical tests (Schirmer tests, fluoroscein test, and rose Bengal staining). In parallel, conjunctival impression cytology (CIC) was done before excision (BE) and every month after excision (AE) over 4-months. Conjunctival molecular biomarkers was studied to supplement the clinical tests, including inflammatory cytokine genes (*interleukin 1*β*: IL-1*β, *tumor necrosis factor: TNF*-α) and *matrix metalloproteinase* (*MMP*-9), using Reverse Transcription-Quantitative-Polymerase Chain Reaction (RT-qPCR). To assess involvement of conjunctiva in restoration of ocular fluid balance, the following genes were assessed by RT-qPCR of CIC: cystic fibrosis trans-membrane conductance regulator: CFTR, sodium potassium chloride co-transporters: NKCC1, sodium potassium ATPase: NKA; epithelial sodium channels: ENaCα and water transporters: Aquaporins (AQP4, AQP5).
Results: Dry eye phenotype in this rabbit model was confirmed at 1-month AE by increased fluorescein ($P < 0.0001$), rose Bengal ($P < 0.0001$) staining, and elevated biomarker mRNAs (IL-1β, $P = 0.0027$; TNF-α, $P = 0.0045$; MMP-9, $P = 0.0295$). However, from 1-month on, fluorescein, rose Bengal staining and biomarkers reduced over time to near baseline (BE) at 4-months. Improvement of dry eye phenotype led to increased Schirmers test scores at 2 and 3-months ($P = 0.0009$) and reduced to baseline at 4-months AE. Conjunctival CFTR, NKA, NKCC1 and ENaCα did not show any up regulation over 4-months. AQP4 was up regulated in 2-months AE and declined to baseline at 4-months AE. AQP5 too was up regulated at 1-month AE and stayed up-regulated at 4-months AE.
Conclusions: In absence of LG, HG and NM a spontaneous resolution of dry eye phenotype was observed in our rabbit model. The conjunctival AQPs are possibly involved in a compensatory tear fluid balance at ocular surface. Similar role played by accessory lacrimal glands cannot be excluded.
Commercial Relationships: Dhruva Bhattacharya, None; **Yuan Ning**, None; **Fangkun Zhao**, None; **Rongji Chen**, None; **Jinsong Zhang**, None; **Mingwu Wang**, None

Program Number: 321 **Poster Board Number:** C0206
Presentation Time: 8:30 AM–10:15 AM
Nanowafer Drug Delivery for Restoration of Healthy Ocular Surface in Dry Eye Condition
Crystal Shin, Daniela Marcano, Johanna Henriksson, Ghanashyam Acharya, Stephen C. Pflugfelder. Ophthalmology, Baylor College of Medicine, Houston, TX.
Purpose: Dry eye is a steroid responsive ocular surface inflammatory disease. Therapeutic efficacy of dexamethasone treatment with a controlled release nanowafer (Dex-NW) or drops was compared in a murine desiccating stress model of dry eye.
Methods: Carboxymethyl cellulose (CMC) nanowafers and phospho dexamethasone loaded CMC nanowafers (Dex-NW) were fabricated by hydrogel template strategy. The in vivo efficacy of the Dex-NW was evaluated in the experimental dry eye induced mouse model by measuring corneal barrier function to 70kDa Oregon green dextran (OGD) and expression of inflammatory genes by RT-PCR.
Results: The nanowafer drug delivery system was designed for sustained controlled delivery of dexamethasone to ocular surface tissues (cornea/conjunctiva) in a controlled fashion and in vivo efficacy was demonstrated in a 5-day experimental dry eye induced mouse model. Corneal epithelial barrier disruption was measured by intensity of staining with fluorescent Oregon green conjugated dextran (OGD). Dex-NW placed on the bulbar conjunctiva on days 1 and 3 was equally effective as dexamethasone drops instilled twice a day eye for five days (Figure 1). RT-PCR analysis revealed that the down regulation of drug target genes IL-1α, IL-1β, TNF-α, IFN-δ, and MMP-3, and MMP-9 by Dex-NW treatment was comparable to twice a day topically administrated dexamethasone eye drop formulation (Figure 2). In both these studies, the dexamethasone delivered by the eye drop treatment was 20 μg compared to 5 μg of the drug delivered by the nanowafer during the same treatment period.
Conclusions: The Dex-NW was equally effective in suppressing dry eye induced corneal inflammation as conventional dexamethasone eye drops, even at a 4-fold lower drug concentration and alternate day dosing frequency.

Appendix 6: Conference paper

Shin et al. Anti-angiogenic polymer therapeutic for corneal neovascularization. Invest. Ophthalmol. Vis. Sci. 2016; 57:3516.

OPEN ACCESS

ARVO Annual Meeting Abstract | September 2016

Anti-Angiogenic Polymer Therapeutic for Corneal Neovascularization

Crystal Shin; Xiaoyong Yuan; Daniela Marcano; Lucas Isenhart; Ken Simmons; Stephen C Pflugfelder; Ghanashyam Acharya

— Author Affiliations & Notes

Crystal Shin
Ophthalmology, Baylor College of Medicine, Houston, Texas, United States

Xiaoyong Yuan
Ophthalmology, Baylor College of Medicine, Houston, Texas, United States

Daniela Marcano
Ophthalmology, Baylor College of Medicine, Houston, Texas, United States

Lucas Isenhart
Ophthalmology, Baylor College of Medicine, Houston, Texas, United States

Ken Simmons
Ophthalmology, Baylor College of Medicine, Houston, Texas, United States

Stephen C Pflugfelder
Ophthalmology, Baylor College of Medicine, Houston, Texas, United States

Ghanashyam Acharya
Ophthalmology, Baylor College of Medicine, Houston, Texas, United States

Footnotes

Commercial Relationships **Crystal Shin**, None; **Xiaoyong Yuan**, None; **Daniela Marcano**, None; **Lucas Isenhart**, None; **Ken Simmons**, None; **Stephen Pflugfelder**, None; **Ghanashyam Acharya**, None

Support Department of Defense 1W81XWH-13-1-0146

Investigative Ophthalmology & Visual Science September 2016, Vol.57, 3516. doi:

Abstract

Purpose : Currently corneal neovascularization is treated with topical formulations of anti-inflammatory or anti-VEGF drugs which can cause adverse side effects. The purpose of this study was to develop a non-invasive biopolymer therapeutic nanowafer to treat corneal neovascularization. The *in vivo* efficacy of the nanowafer was evaluated in a murine ocular burn model.

Methods : A sulfated polysaccharide, dextran sulfate (DS) nanowafers and an antiangiogenic drug, axitinib, loaded DS nanowafers were fabricated by hydrogel template strategy. The chemical burn induced mouse corneas were treated daily with the DS nanowafers, axitinib loaded DS (Axi-DS) nanowafers, DS eye drops to compare their therapeutic efficacies and to evaluate synergistic effect of DS. After treatments, mouse corneas were subjected to immunofluorescence imaging and RT-PCR analyses.

Results : Overall, the nanowafer treatment minimized corneal neovascularization when compared to untreated ocular burn corneas in murine models. Immunofluorescence images presented CD31 positive vasculature endothelium in corneas and showed the DS nanowafer treatment was as effective as Axi-DS nanowafer treatment in suppressing neovascularization. The RT-PCR analysis revealed that after five days of DS nanowafer treatment, gene expressions of proinflammatory cytokines (IL-1α and IL-1β) and angiogenic factors (VEGFA, VEGFR1, and VEGFR2) were downregulated (Figure 1). This result showed that DS nanowafer had anti-angiogenic effect on inhibiting corneal neovascularization.

Conclusions : This study demonstrated the anti-–angiogenic effect of a biopolymer, dextran sulfate, in a murine ocular burn model. In addition, an anti-angiogenic drug incorporated dextran sulfate nanowafer maximized their therapeutic efficacies.

This is an abstract that was submitted for the 2016 ARVO Annual Meeting,

held in Seattle, Wash., May 1-5, 2016.

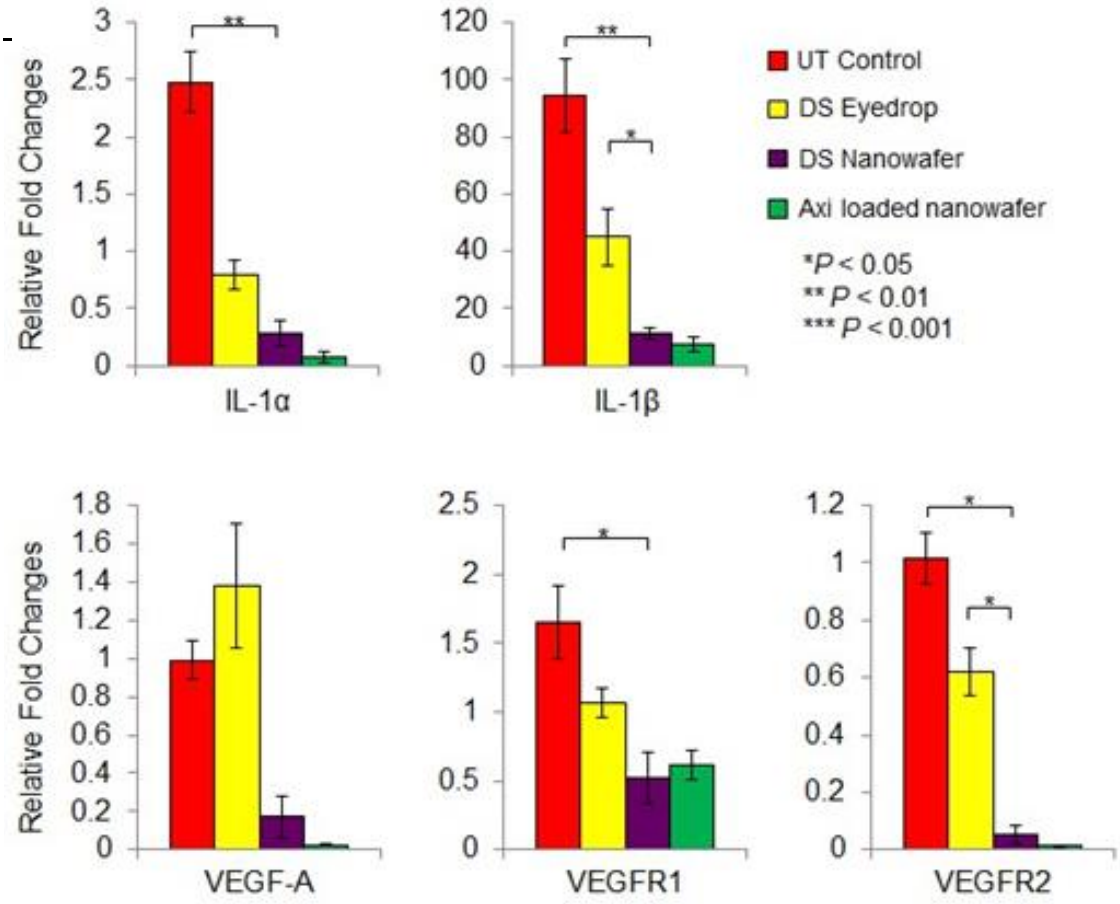

View Original Download Slide

Figure 1. RT-PCR analysis showing that downregulation of proinflammatory cytokines and angiogenic factors by nanowafer treatments

Appendix 7: Conference abstract

Marcano et al. Extended release cysteamine nanowafer as an efficacious treatment modality for corneal cystinosis. Controlled Release Society Meeting 2016, July 17-20, Seattle, WA.

2016 CRS Annual Meeting Presentations

July 17-20, 2016
Seattle, Washington

The CRS Annual Meeting presentation webcasts are available to CRS members. Non-member annual meeting attendees have access for one year following the annual meeting for viewing.

Presentation Categories

⊞ Comparative Pharmacokinetics in Preclinical Sciences

⊞ Delivery Technologies in Cosmetics, Personal Care, and Household Products

⊞ Delivery Technologies in Nutraceuticals, Food, and Oral Products

⊞ Encapsulation and Controlled Release for Industrial Applications

⊞ Industry Roundtable: Clinical Advances in Cancer Nanomedicines

⊞ Integration of Imaging and Drug Delivery

⊞ Local Drug Delivery

⊞ Manufacture, Characterization, Stability, and Regulatory Aspects

⊞ Mini Symposia: Developing Therapeutic Options for Combating Cancer: A “One Health” Challenge for Humans and Dogs”

⊞ New Processes, New Materials, New Products

⊟ Ocular Drug Delivery

11 **Silicon-Based Nanomaterials for Ocular Drug Delivery**
Presenter: Sailor, Michael. Authors: M. SAILOR (1), J. Wang (1), T. Kumeria (1), L. Cheng (1), H. Hou (1), W. Freeman (1)

(1) University of California, San Diego, U.S.A.

View Abstract | View Presentation

---

12 **Bridging Product Design and Performance for Bioequivalence: A Journey through the Eye**
Presenter: Xu, Xiaoming. Authors: X. XU (1)
(1) U.S. FDA, U.S.A.

View Abstract | View Presentation

---

13 **An Update on FDA's Research Program for Ophthalmic Generic Products**
Presenter: Choi, Stephanie. Authors: S. CHOI (1)
(1) FDA, U.S.A.

View Abstract | View Presentation

---

269 **Smart Wireless Contact Lens for Ocular Theranosis**
Presenter: Keum, Dohee. Authors: D. KEUM (1), S. Hahn (1)
(1) POSTECh, Korea

View Abstract | View Presentation

---

270 **Ultradeformable bilosomes for enhanced ocular delivery of terconazole: In vitro characterization and factorial analysis**
Presenter: Abdelbary, Aly. Authors: A. ABDELBARY (1), A. Al-mahallawi (1), W. Abd-Elsalam (1)
(1) Faculty of Pharmacy-Cairo University, Egypt

View Abstract

---

271 **Ultrasound-responsive nanobubbles for enhanced posterior eye delivery of therapeutics**
Presenter: Thakur, Sachin. Authors: S. THAKUR (1), H. Parekh (1), I. Rupenthal (2), E. Chen (2)
(1) School of Pharmacy, the University of Queensland, Australia; (2) Buchanan Ocular Therapeutics Unit, School of Medicine, the University of Auckland, New Zealand

View Abstract | View Presentation

---

272 **Extended Release Cysteamine Nanowafer as an Efficacious Treatment Modality for Corneal Cystinosis**
Presenter: Marcano, Daniela. Authors: D. MARCANO (1), C. Shin (1), B. Lee (2), L. Isenhart (1), F. Li (1), J. Jester (2), S. Pflugfelder (1), J. Simpson (2), G. Acharya (1)
(1) Baylor College of Medicine, U.S.A.; (2) University of California, U.S.A.

View Abstract

---

273 **Convective loading and release of latanoprost via a silicone hydrogel contact lens in vitro**
Presenter: Pitt, William. Authors: R. HORNE (1), W. Pitt (1), K. Judd (1)
(1) Brigham Young University, U.S.A.

View Abstract

---

274 **Retinylamine Modified Multifunctional Lipid DNA Delivery System for the Treatment of LCA2**
Presenter: Sun, Da. Authors: D. SUN (1), B. Sahu (2), S. Gao (2), A. Maeda (2), K. Palczewski (2), Z. Lu (2)
(1) Case Western Reserve University, U.S.A.; (2) Case Western Reserve Univserity, U.S.A.

View Abstract

---

275 **Potential Preclinical Approaches to Establish Bioequivalence of Ophthalmic Products**
Presenter: Bhyrapuneni, Gopinadh. Authors: G. BHYRAPUNENI (1), V. Benade (1), G. Ayyanki (1), V. Kamuju (1), S. Daripelli (1), R. Ponnamaneni (1), A. Manoharan (1), S. Irappanavar (1), N. Muddana (1), R. Nirogi (1)
(1) Suven Life Sciences Limited, India

View Abstract

---

276 **Flexible Formulating for Problem Therapeutics**
Presenter: Groves, Rhian. Authors: R. GROVES (1), P. Seaman (1)
(1) Midatech Pharma, United Kingdom

Extended Release Cysteamine Nanowafer as an Efficacious Treatment Modality for Corneal Cystinosis

Daniela C. Marcano[1], Crystal S. Shin[1], Briana Lee[3], Lucas Isenhart[1], Feng Li[2], James Jester[3], Stephen C. Pflugfelder[1], Jennifer Simpson[3], Ghanashyam Acharya[1].
[1]Department of Ophthalmology Baylor College of Medicine, Houston, TX, 77030, USA,
[2]Metabolomics Core Facility, Baylor College of Medicine, Houston, TX, 77030, USA,
[3]Department of Ophthalmology, University of California, Irvine, CA, 92697, USA
dmarcano@bcm.edu

Purpose: To demonstrate the enhanced efficacy of stability of cysteamine nanowafer compared to cysteamine eye drops for the dissolution of corneal cystine crystals in a cistinosin knock-out mouse ($CTNS^{-/-}$) model.

Methods: Nanowfers of 2 mm in diameter and 80 µm thick were fabricated by a modified hydrogel template strategy (1,2). The nanowafer contains arrays of cysteamine filled nanoreservoirs (500 nm diameter). In treatment group $CTNS^{-/-}$ mice (7 month old), cysteamine nanowafers were applied daily for 30 days. Another group $CTNS^{-/-}$ of mice were treated once a day with 5 µL of the cysteamine eye drop solution (0.44%). The therapeutic effect of the cysteamine-nanowafer was evaluated both by measuring the reduction in the corneal cystine crystal volume (3) and by quantifying the amount of cystine by mass spectrometry. The stability of the cysteamine in the drug-loaded nanowafers was assessed by determining the concentration of cysteamine and cystamine (oxidation product) in nanowafers that were prepared and stored for 10, 12, 14, and 16 weeks at room temperature.

Results: Cysteamine-nanowafers were stable for up to 4 months, and no formation of cystamine was observed during this period. Cystine quantification in corneas by mass spectrometry showed that the cysteamine-nanowafer reduced the corneal cystine content by 65% and the eye drops by 34%. Remarkably, the amount of cysteamine delivered per day by the nanowafer was 10 µg, while the twice a day cysteamine eye drop treatment delivered 22 µg. Cystine quantification by cystine crystal content in the corneas, estimated by laser confocal image analysis, showed that in comparison to the baseline corneal cystine crystal volume, eye drop treatment reduced the crystal volume by 55%, while the cysteamine-nanowafer treatment reduced the crystal volume by 90%.

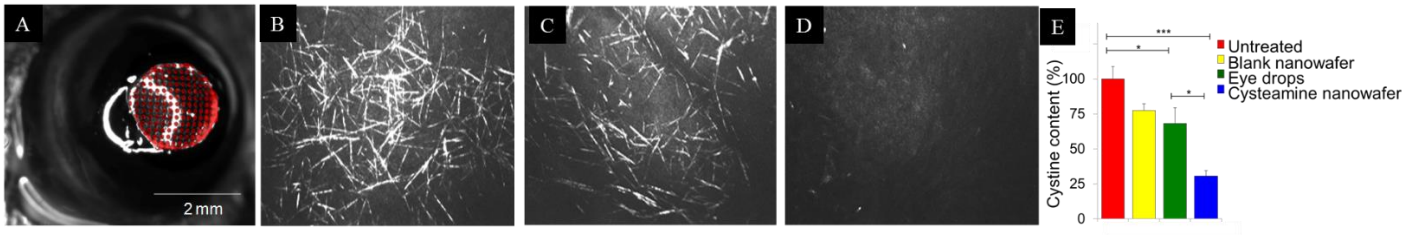

Figure 1. (A) Nanowafer applied on a mouse cornea. Laser confocal images of (B) cystinosis cornea, (C) eye drops treated cornea, (D) cysteamine-nanowafer treated cornea. (E) Quantification of corneal cystine crystals.

Conclusions: These studies revealed that cysteamine loaded in nanowafers was stable for up to 16 weeks when stored at room temperature, unlike the eye drop formulation, in which cysteamine is stable only for a week, even under refrigerated conditions. Reduction of the corneal crystals confirmed the efficacy of the loaded nanowafer.

Acknowledgements: We thank the Alkek Center for Molecular Discovery- metabolomics core facility for the mass spectrometry analysis. Funding: Cystinosis Research Foundation, Irvine, CA (Award No. CRF-53944, CRFS-2014-008), Department of Defense (Award No. 1W81XWH-13-1-0146).

References:

1. Yuan X., Marcano D.C., Shin C.S., Hua X., Isenhart L.C., Pflugfelder S.C., Acharya G. ACS Nano. (2015) 1749–1758.
2. Coursey T.G., Henriksson J.T., Marcano D.C., Shin C.S., Isenhart L.C., Ahmad F., De Paiva C.S., Pflugfelder S.C., Acharya G. J Control Release. (2015) 168-174.
3. Simpson J., Nien C. J., Flynn K., Jester B., Cherqui S., Jester J. Mol. Vis. (2011) 2212-2220.

Appendix 8: Conference abstract

Shin et al. Dextran sulfate wafer as an anti-angiogenic polymer therapeutic. Controlled Release Society Meeting 2016, July 17-20, Seattle, WA.

2016 CRS Annual Meeting Presentations

July 17-20, 2016
Seattle, Washington

The CRS Annual Meeting presentation webcasts are available to CRS members. Non-member annual meeting attendees have access for one year following the annual meeting for viewing.

Presentation Categories

⊞ Comparative Pharmacokinetics in Preclinical Sciences

⊞ Delivery Technologies in Cosmetics, Personal Care, and Household Products

⊞ Delivery Technologies in Nutraceuticals, Food, and Oral Products

⊞ Encapsulation and Controlled Release for Industrial Applications

⊞ Industry Roundtable: Clinical Advances in Cancer Nanomedicines

⊞ Integration of Imaging and Drug Delivery

⊞ Local Drug Delivery

⊞ Manufacture, Characterization, Stability, and Regulatory Aspects

⊞ Mini Symposia: Developing Therapeutic Options for Combating Cancer: A “One Health” Challenge for Humans and Dogs”

⊞ New Processes, New Materials, New Products

⊟ Ocular Drug Delivery

11 **Silicon-Based Nanomaterials for Ocular Drug Delivery**
Presenter: Sailor, Michael. Authors: M. SAILOR (1), J. Wang (1), T. Kumeria (1), L. Cheng (1), H. Hou (1), W. Freeman (1)

View Abstract

277 **OpsiSporin - Development of Controlled Release Cyclosporin for the treatment of posterior uveitis**
Presenter: Bamsey, Katherine. Authors: K. BAMSEY (1), P. Seaman (1), R. Groves (1)
(1) Midatech Pharma, United Kingdom

View Abstract | View Presentation

278 **Dextran Sulfate Wafer as an Anti-Angiogenic Polymer Therapeutic**
Presenter: Shin, Crystal. Authors: C. SHIN (1), X. Yuan (1), D. Marcano (1), L. Isenhart (1), K. Simmons (1), S. Pflugfelder (1), G. Acharya (1)
(1) Baylor College of Medicine, U.S.A.

View Abstract | View Presentation

279 **Composite Nanotherapeutics for Long Term Ocular Delivery of Macromolecules**
Presenter: Agrahari, Vibhuti. Authors: V. AGRAHARI (1), V. Agrahari (2), W. Hung (3), L. Christenson (3), A. Mitra (2)
(1) University of Missouri-Kanss City, U.S.A.; (2) University of Missouri Kansas City, U.S.A.; (3) University of Kansas Medical Center, U.S.A.

View Abstract

280 **Template Directed Chemical Polymerization of Electroactive Polypyrrole Particles Loaded With Dexamethasone**
Presenter: Uppalapati, Dedeepya. Authors: D. UPPALAPATI (1), M. Sharma (1), Z. Agrawe (1), B. Boyd (2), J. Travas-Sejdic (1), D. Svirskis (1)
(1) The University of Auckland, New Zealand; (2) Monash Univeristy, Australia

View Abstract

281 **Controlled Release of Avastin® from the Tethadur™ Biodegradable Matrix**
Presenter: Kelly, Catherine. Authors: C. KELLY (1), D. Nadarassan (1), K. Webb (1), Q. Shabir (1), H. O'Brien (1), C. Storey (1), A. Loni (1), L. Canham (1)
(1) PsiMedica, United Kingdom

View Abstract | View Presentation

Oligonucleotide Delivery: New Applications and Opportunities

14 **Engineering Cyclodextrin Nanoparticles for the Delivery of siRNA**
Presenter: Geall, Andrew. Authors: A. GEALL (1)
(1) Avidity NanoMedicines, U.S.A.

View Abstract

15 **Design of lipid nanoparticle delivery systems to enable therapeutic applications of siRNA and mRNA**
Presenter: Cullis, Pieter. Authors: P. CULLIS (1)
(1) University of BC, Canada

View Abstract | View Presentation

282 **Exploring MicroRNA Expression Profiles Related to Cell Death Pathways in Mouse Embryonic Fibroblast Cells Treated with Polyethylenimine**
Presenter: Kuo, Jung-hua. Authors: J. KUO (1), M. Jan (2), C. Lin (2)
(1) Department of Pharmacy, Chia Nan University of Pharmacy and Science, Taiwan; (2) Institute of Microbiology and Immunology, Chung Shan Medical University, Taiwan

View Abstract

283 **Dual-sensitive mixed-micelles for co-delivery of miRNA 34a and doxorubicin into tumor cells**
Presenter: Costa, Daniel. Authors: D. COSTA (1), G. Salzano (1), C. Sarisozen (1), E. Luther (1), P. Dhargalkar (1), G. Mattheolabakis (1), V. Torchilin (1)
(1) Northeastern University, U.S.A.

View Abstract

Dextran Sulfate Wafer as an Anti-Angiogenic Polymer Therapeutic

Crystal S. Shin, Xiaoyong Yuan, Daniela C. Marcano, Lucas C. Isenhart, Ken Simmons,
Stephen C. Pflugfelder, Ghanashyam Acharya
Department of Ophthalmology, Baylor College of Medicine, Houston, TX, 77030, USA
crystal.shin@bcm.edu

Purpose: Eye injuries, prolonged inflammation, infections, and chronic dry eye trigger corneal neovascularization (CNV) leading to impaired vision and blindness. Presently, eye injuries are treated with topical eye drop formulations of corticosteroid drugs: fluorometholone, prednisolone acetate, and dexamethasone which cause side effects, such as glaucoma, cataract formation, and temporary blurred vision, resulting in discomfort and poor patient compliance [1]. To surmount these issues, we have developed a dextran sulfate (DS) polymer wafer for the effective treatment of CNV with negligible side effects. In this study DS was chosen for wafer fabrication because of its demonstrated anti-angiogenic attributes [2].

Methods: The effect of dextran sulfate on cell proliferation was first evaluated *in vitro*. Dextran sulfate of different molecular weights, 500 kDa and 40 kDa were used to treat human mammary epithelial cell line (HMLE), human umbilical vein endothelial cell line (HUVEC), and murine endothelial cell line (2H11) and MTS assay was performed. DS (500 kDa) eye drop formulation was prepared and DS (500 kDa) wafers were fabricated by modified hydrogel template strategy [3]. The *in vivo* therapeutic efficacy of DS wafer was evaluated in ocular burn (OB) induced mouse model. The OB induced mice were treated daily with DS eye drops and DS wafer for 14 days. After treatments, mouse corneas were enucleated and incubated with a platelet endothelial cell adhesion molecule-1 marker, CD31, for immunofluorescence imaging.

Results: Our studies have demonstrated that cell proliferation in HMLE, HUVEC, and 2H11 cell lines was inhibited when cells were treated with DS; the higher concentration of 500 kDa DS was more effective in inhibiting proliferation in all cell lines (Fig 1). Therefore, high molecular weight DS was chosen for fabricating DS wafers for further animal studies. After 14 days of treatment, immunofluorescence imaging analysis showed that wafer treatments were effective in suppressing corneal neovascularization compared to untreated burned corneas and DS eye drop treated corneas (Fig 2). In untreated burned corneas, vascularization towards the center of the cornea was observed. The DS wafer treatment was more effective than the eye drop treatment in minimizing vascularization.

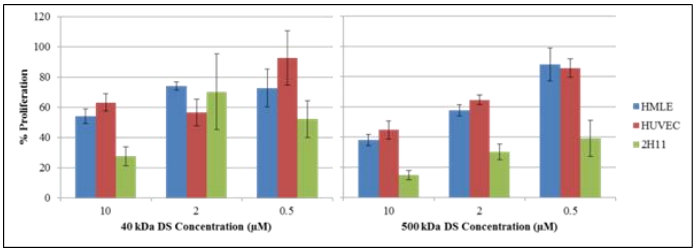

Figure 1. The effect of DS (40 kDa and 500 kDa) on cellular proliferation in HMLE, HUVEC, 2H11 cell lines.

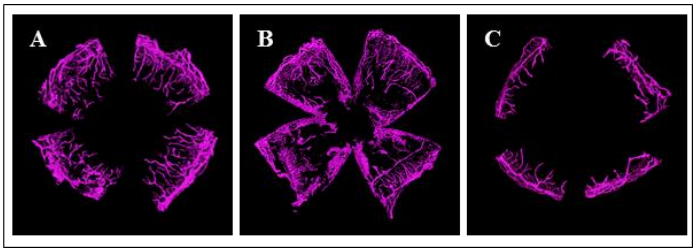

Figure 2. Representative immunofluorescence images of CD31 positive endothelial cells in mouse corneas: (A) untreated, (B) DS eye drop, and (C) DS wafer

Conclusions: This study demonstrated that DS wafer is more efficacious as an anti-angiogenic polymer therapeutic compared to topical DS eye drop treatment for treating CNV in ocular burn induced mouse model.

References:

1. Hos D., Saban D.R., Bock F., Regenfuss B., Onderka J., Masli S., Cursiefen C. Arch Ophthalmol. 2011 (129) 445-452.
2. Narazaki M., Segarra M., Tosato G. Blood. 2008 (111) 4126-4136.
3. Yuan X., Marcano D.C., Shin C.S., Hua X., Isenhart L.C., Pflugfelder S.C., Acharya G. ACS Nano. 2015 (9) 1749-1758.